The Molecular Basis of Histone Demethylation

John R. Horton, Molly Gale, Qin Yan, and Xiaodong Cheng

Abstract The methylation of lysine residues on histone tails--and their subsequent demethylation--is among some of the most important covalent post-translational modifications controlling gene expression. When gene expression goes awry, disease ensues and often this disease is some form of cancer. Thus, an understanding of histone tail modification in nucleosomes is critical in mankind's attempts to eradicate cancers. This chapter examines our present knowledge of the enzymes that demethylate the lysine residues on histone tails, known as KDMs. The substrate-binding specificities of KDMs are quite diverse. The determinants of their specificity goes beyond just the amino acids involved in recognition and catalysis as observed in KDM crystal structures of their catalytic domains but extend to interactions of their many domains to each other and with other proteins in multicomponent complexes. These aspects of all seven known KDM families are reviewed as well as our present knowledge of their involvement in cancers. Control of their aberrant behavior by design of chemical inhibitors, that have the potential to be powerful cancer fighting drugs, is an expanding human endeavor and is chronicled at the end of the chapter.

Keywords Epigenetics • Histone lysine methylation • Histone lysine demethylation • KDM family • Fe(II)- and α-ketoglutarate-dependent dioxygeneses • Flavin adenine dinucleotide (FAD)-dependent LSD • Mono/di/tri-methylation • Protein arginine methylation • Jumonji domain Jmj • Combinatorial readout of multiple covalent histone modifications

J.R. Horton (✉) • X. Cheng
Department of Molecular and Cellular Oncology, The University of Texas - MD Anderson Cancer Center, Houston, TX 77030, USA
e-mail: jrhorton@mdanderson.org

M. Gale • Q. Yan
Department of Pathology, Yale School of Medicine, New Haven, CT 06520, USA

A. Kaneda, Y.-i. Tsukada (eds.), *DNA and Histone Methylation as Cancer Targets*, Cancer Drug Discovery and Development, DOI 10.1007/978-3-319-59786-7_7

1 Introduction

Methylation occurs on arginine and lysine residues in histones and is involved in a wide range of biological processes such as gene expression, chromatin organization, dosage compensation, and epigenetic memory. Unlike acetylation, where positive charges on histones are removed, relaxing chromatin and activating genes, methylation or its removal does not affect charges on histones. Histone methylation can be transcriptionally repressive or activating, depending on the position of the methylated residue and the extent of methylation. Histone lysine residues can be monomethylated, dimethylated, or trimethylated [1], while arginine residues can be monomethylated or dimethylated symmetrically or asymmetrically [2]. The methylation of lysines 4, 36, or 79 of histone H3 is typically associated with active transcription, while the methylation of lysines 9 or 27 on histone H3 and lysine 20 on histone H4 contributes to repressed transcription. Methylation with the overall combination of other histone "marks," such as acetylation, phosphorylation, and ubiquitination, as well as the presence of other regulatory factors and DNA methylation ultimately determine chromatin conformation and expression level of the associated gene.

In order to change chromatin structure and gene expression level, histone modifications have to be altered, which can include a reversal of methylation *i.e.* demethylation. Unlike phosphorylation and acetylation, histone methylation was long regarded as irreversible partially because of the stable nature of the carbon-nitrogen bond and lack of evidence for its role in dynamic regulation of gene expression [3]. In addition, in a number of early studies, the half-life of histones and methyl-lysine residues within them appeared to be the same, implying histone methylation was not reversible [4, 5]. However, other studies seemed to show that active turnover of methyl groups did occur at a low but detectable level [6, 7]. Furthermore, in many documented cases, it appeared that different histone methylation patterns were necessary for regulation of gene expression [8].

As early as the 1960s, protein extracts containing lysine demethylase activity were identified and partially purified [9–11]. Decades later, in 2004, as evidence was mounting that histone methylation was dynamic and reversible, the first histone demethylase, a flavin-containing amine oxidase, was finally identified. Lysine-Specific Demethylase 1 (LSD1, also known as KDM1A) provided the first experimental evidence for enzymatic histone demethylation [12]. It was shown to mediate oxidative demethylation on monomethylated or dimethylated H3K4, but not trimethylated H3K4 because the enzymatic mechanism requires a protonated nitrogen [13]. Subsequently, a second and larger class of demethylases containing what was called a Jumonji C (JmjC) domain was theorized [14] and then independently identified through biochemical purification in 2005 [15]. Within a year, more JmjC demethylases were discovered in rapid succession [16–19] and even a crystal structure of a JmjC catalytic domain was published [20]. Unlike KDM1A, the JmjC proteins do not require a protonated nitrogen allowing some JmjC family members to act on trimethylated H3K4 as well [13].

Arginine methylation is also a very stable mark, but unlike lysine methylation, it is still unclear if this modification can be enzymatically reversed. Arginine residues can be monomethylated or asymmetrically or symmetrically dimethylated on R3, R8, R17, and R26 on H3, and R3 on both histones H2A and H4 [21]. A putative

arginine demethylase JMJD6, a JmjC domain-containing protein, was reported to demethylate both asymmetric and symmetric H3R2me2 and H4R3me2 substrates [22]. However, others have not been able to replicate this observation and have found JMJD6 to be a lysine-hydroxylase, catalyzing C-5 hydroxylation of lysine residues in mRNA splicing-regulatory proteins and in histones with no demethylase activity on either H3R2me2 or H4R3me2 peptides [23–25]. Additionally, mutational and structural analysis of JMJD6 suggests that it is not an arginine demethylase and has a novel substrate binding groove and two positively charged surfaces with a stack of aromatic residues located near the active center not found in any JmjC oxygenase family member and may even interact with ssRNA [26, 27]. While it appears JMJD6 may play some role in regulating gene expression, there is still no clear consensus what that role is [25]. Interestingly, it has very recently reported that some JmjC demethylases are also able to demethylate histone and non-histone arginine residues *in vitro* albeit not as efficiently as histone lysine residues; a crystal structure of a known JmjC lysine demethylase (KDM4A) with an H4R3me2s containing-peptide (PDB code 5FWE) was also determined [28].

Arginine residues are not only substrates for methylation, but can also be converted to citrulline by deimination through the action of peptidylarginine deiminases [29]. Deimination has been suggested as a path for arginine demethylation but it appears that these deiminases act only on unmethylated arginines, and not on methylated arginine [30, 31]. As no enzyme has been found that converts citrulline back to arginine, methylation of arginine can only be antagonized by this modification [32].

Thus, since there are no verifiable *in vivo* arginine demethylases at this time, this chapter will only discuss histone lysine (K) demethylases (KDMs). Over the last decade, over 20 KDMs have been discovered representing two distinct classes: the KDM1 family containing two lysine-specific demethylase (LSD) enzymes, and the KDM2–7 families consisting of the JmjC domain-containing enzymes (Table 1). Each KDM demethylates only certain methylated histone residues and sometimes only certain methylated states (mono-, di-, tri) of those residues. The demethylases that primarily act on methylated H3K4 (KDM1 and KDM5) belong to the two different enzyme families; those that primarily act on other histone methylated lysines belong only to the second JmjC family.

The substrate-binding specificities of KDMs are quite diverse. The most prevalent histone lysine substrates are H3K4, H3K9, H3K27, H3K36, H4K20, and H1.4K26. In part, substrate specificity of each demethylase depends on the histone peptide sequence surrounding target lysine residues. However, another important component of KDM specificity is mediated by combinations of additional conserved "helper" domains within KDMs which can include combinations of such "helpers" as the plant homeodomain (PHD) [33], Tudor [34, 35], zinc fingers (such as zf-CXXC and zf-C2HC4) [36–38], F-box [39], AT-rich interactive domain (ARID) [40], tetratricopeptide repeat (TPR) [41] and leucine-rich region (LRR) domains [42, 43]. In addition, selectivity can be conferred by the composition and character of "linker" sequences between the catalytic and neighboring helper domain [44]. Furthermore, KDMs are part of large multimeric and dynamic complexes that contribute yet another level of specificity for gene localization and histone targeting. Finally, alternative splicing of mRNA of JmjC demethylases can lead to different isoforms. These isoforms could have different specificities and/or form different protein complexes.

Table 1 Lysine demethylase families and their histone substrates

Lysine demethylase family	Human family homologs	Common alternative homolog name(s)	Histone substrates
KDM1	KDM1A KDM1B	LSD1 AOF1, LSD2	H3K4me2/1 H3K4me2/1
KDM2	KDM2A KDM2B	JHDM1A, FBXL11 JHDM1B, FBXL10	H3K36me2/1, H3K4me3 H3K36me2/1
KDM3	KDM3A KDM3B KDM3C	JHDM2A, JMJD1A JHDM2B, JMJD1B JMJD1C	H3K9me2/me1 H3K9me2/me1 H3K9me2/me1
KDM4	KDM4A KDM4B KDM4C KDM4D KDM4E	JMJD2, JMJD2A JMJD2B JMJD2C JMJD2D JMJD2E, KDM4DL	H3K9me3/me2, H3K36me3/me2 H3K36me3/me2 H3K36me3/me2 H3K9me3/me2, H3K36me3/me2/me1, H3K56me3
KDM5	KDM5A KDM5B KDM5C KDM5D	JARID1A, RBP2 JARID1B, PLU1 JARID1C, SMCX JARID1D, SMCY	H3K4me3/me2 H3K4me3/me2 H3K4me3/me2 H3K4me3/me2
KDM6	KDM6A KDM6B KDM6C	UTX JMJD3 UTY	H3K27me3/me2 H3K27me3/me2 H3K27me3/me2
KDM7	KDM7A KDM7B KDM7C	JHDM1D, KIAA1718 PHF8 PHF2	H3K9me2/me1, H3K27me2/me1 H4K20me1

Each of these topics must be discussed to understand our limited knowledge of the molecular basis of histone demethylation. Aberrant histone methylation caused by mutation or misregulation of histone demethylases and histone methyltransferases has been observed in several human diseases, particularly cancer. Modulation of histone methylation status for aberrant gene expression in cancers offers medicinal potential for the treatment of cancers via the development of molecular inhibitors of histone demethylases.

2 KDM1 Family Architecture and Mechanism

Unlike other KDMs, the KDM1 family utilizes the cofactor flavin adenine dinucleotide (FAD) to demethylate the methylated lysine substrate via a redox reaction (Fig. 1). The catalytic domain of the KDM1 family, the amine oxidase-like (AOD) domain, is related to the large superfamily of flavin-dependent monoamine oxidases, with MAO-A and MAO-B being the closest homologues [12]. Like other members of this

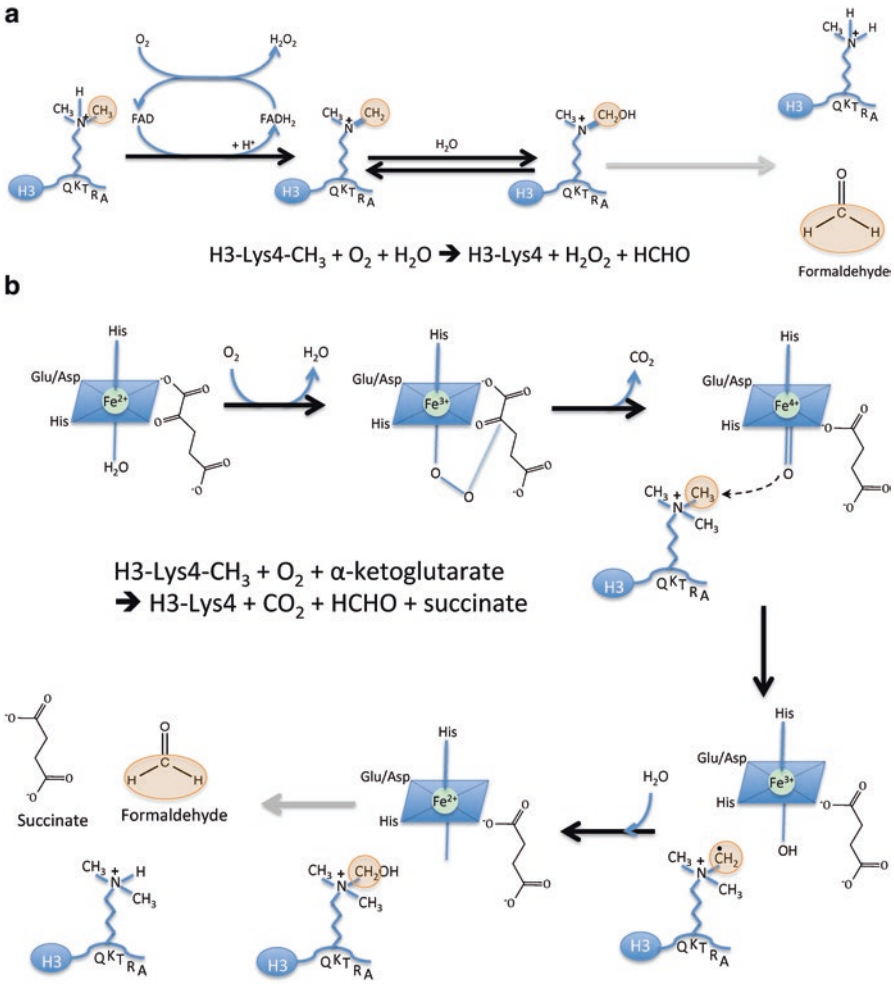

Fig. 1 Reaction mechanisms of (**a**) KDM1/LSD1 demethylase family and (**b**) JmjC demethylases

superfamily, the AOD of the two KDM1 family members can be further subdivided into two separate subdomains, with one subdomain involved in substrate binding and the other forming an expanded Rossmann fold used to bind the cofactor FAD. Each of these subdomains is formed from sequence components spread throughout the primary structure. The substrate-binding subdomain is composed of a six-stranded mixed β-sheet flanked by six α-helices. The two subdomains create a big cavity that defines the demethylase catalytic center at their interface [20, 45–47].

The FAD cofactor, binding to the KDM1A protein, undergoes two-electron reduction by substrate oxidation (Fig. 1a). The oxidized form of FAD is restored by molecular oxygen to generate hydrogen peroxide. The coupled oxidation of methyl-lysine forms a hydrolytically labile imine and $FADH_2$. Molecular oxygen is used as the electron acceptor, and methyl group oxidation is then followed via

hydride transfer from the N-methyl group onto FAD, forming an imine. This imine intermediate is unstable and further hydrolyzed non-enzymatically to release the demethylated lysine and formaldehyde. Thus, during catalysis, each cycle of methyl removal produces a molecule of formaldehyde and of H_2O_2, while consuming an O_2. KDM1/LSDs are incapable of demethylating trimethyl-lysine residues, because the quaternary ammonium group cannot form the requisite imine intermediate.

3 JmjC KDM Architecture and Reaction Mechanism

The JmjC KDM family belongs to a larger superfamily of oxygenases which utilize 2-oxoglutarate (2OG) (also referred to as α-ketoglutarate or α-KG) as a co-substrate and Fe(II) as a cofactor, and couples substrate oxidation to the decarboxylation of 2-oxoglutarate to produce succinate and CO_2 (Fig. 1b). These enzymes are conserved in eukaryotes from yeast to humans [15], and have a double-stranded β-helical (DSBH) or "jelly-roll" fold consisting of eight antiparallel β-strands that form a β-sandwich structure comprised of two four-stranded antiparallel β-sheets. This structure is often referred to as the Jmj or JmjC domain.

The distorted/squashed barrel-like structure is open at one end where the octahedrally coordinated catalytic iron resides in a funnel-shaped active site with three interactions provided by a conserved His-X-Asp/Glu-X_N-His triad from the protein. The co-substrate 2OG is in a compact binding site where its 2-oxo carboxylate group also bidentately binds the iron; the iron ion also has a water molecule at the sixth position where a catalytic oxygen species is expected to reside during the demethylation reaction. The other end of 2OG interacts with the side-chain of a basic residue (Arg/Lys) and with a hydroxyl group from a Ser/Thr or Tyr residue [20, 48].

The JmjC KDM reaction begins by generating a superoxide radical by the complex Fe^{2+}/2OG, which reacts with the C2 atom of 2OG, leading to its decarboxylation to succinate and formation of a Fe^{4+}-oxo species. Afterwards, the highly reactive Fe^{4+}-oxo species abstracts a hydrogen from a lysine ζ-methyl group as the iron is reduced to Fe^{3+}, forming an unstable carbinolamine that will rapidly break down, leading to the release of formaldehyde and loss of a methyl group from the methylated lysine residue. Unlike the KDM1 family, JmjC KDMs do not require lone pair electrons on the target nitrogen atom and thereby can demethylate trimethylated as well as di- and monomethylated lysines.

JmjC demethylases bind methyl-lysine in a highly conserved pocket in the active site through the formation of a network of C–H•••O hydrogen bonds between the methyl groups and the oxygen atoms from the backbone and side chain of active-site residues. Many crystallographic studies have revealed that substrate binding often involves residues from the first and second β-strand of the DSBH, together with strands and loops that extend the JmjC domain. In contrast, "reader" domains such as PHD bind methyl-lysine through cation–π interactions between the methylammonium ion and a cage formed by multiple aromatic residues [49–51].

An additional N-terminal interaction element has been identified in many JmjC KDMs that resides at varying distances away from the JmjC domain and is referred

to as the JmjN domain [20]. In KDM2A and the KDM4 and KDM5 families, it interacts extensively with the catalytic JmjC domain and provides structural integrity without participating in active site formation [17, 52–54]. However, modeling and other recent analysis suggests that the JmjN-like fold exists in all KDM families [54, 55]. Thus, the JmjN domain is not a "domain" per se, but an integral part of the catalytic core. Therefore, it should be considered that the JmjC domain in several KDM families has had additional insertions over evolution, and in one case, in the KDM5 family, other domains have been included in the insertion.

In the following sections, each KDM family is discussed individually. First, a general description of the family and its members is given which includes our present knowledge of their relationship to cancers. A table containing all known NMR and crystal structures containing a family's one or more domains, with cofactors and sometimes peptide substrates, is supplied at the end of each section. It is important to remember that a demethylase's catalytic and other domains do not act in isolation but interact with each other and many other proteins. In fact, there are three main components that confer specificity to a demethylase: the active site of its catalytic domain, the other domains that the demethylase contains, and the other proteins with which the demethylase participates in multicomponent complexes. Therefore, secondly, each of these attributes for each family will be discussed. At the end of the chapter, there will be a short review that highlights the discovery of KDM inhibitors for which the information acquired could aid in drug development.

4 The KDM1 Family

KDM1A was shown to be a histone demethylase by the Shi group in 2004 [12]. At the same time, a second human flavin-dependent histone demethylase, KDM1B, was identified through a domain homology search of genomic databases [12]. In 2009, the Mattevi laboratory isolated and confirmed the flavin-dependent demethylation activity of KDM1B, noting specificity for H3K4me1/2, despite the relatively low sequence identity to KDM1A of less than 25% [56].

The KDM1 family primarily demethylates H3K4me2 and H3K4me1. H3K4 methylation is a gene activation marker [57]. These epigenetic marks are located in open chromatin, primarily in transcription factor binding regions, including promoters and enhancers that positively regulate expression of genes and can be located many thousands of base pairs down- or upstream of a gene [58–60]. These genomic loci are commonly devoid of H3K4me3 [61]. KDM1A appears to regulate histone methylation at promoters, while KDM1B is found in transcriptional elongation complexes and removes H3K4 methyl markings in gene bodies, thereby facilitating gene expression by reducing spurious transcriptional initiation outside of promoters [62]. KDM1B is highly expressed in oocytes and is required for *de novo* DNA methylation of some imprinted genes, a function dependent on its H3K4 demethylase activity [63].

While KDM1A and KDM1B each share a SWIRM domain and a C-terminal catalytic AOD domain, these demethylases have distinct functions and domains that mediate interactions with other biomolecules (Fig. 2) [64]. The N-terminal regions

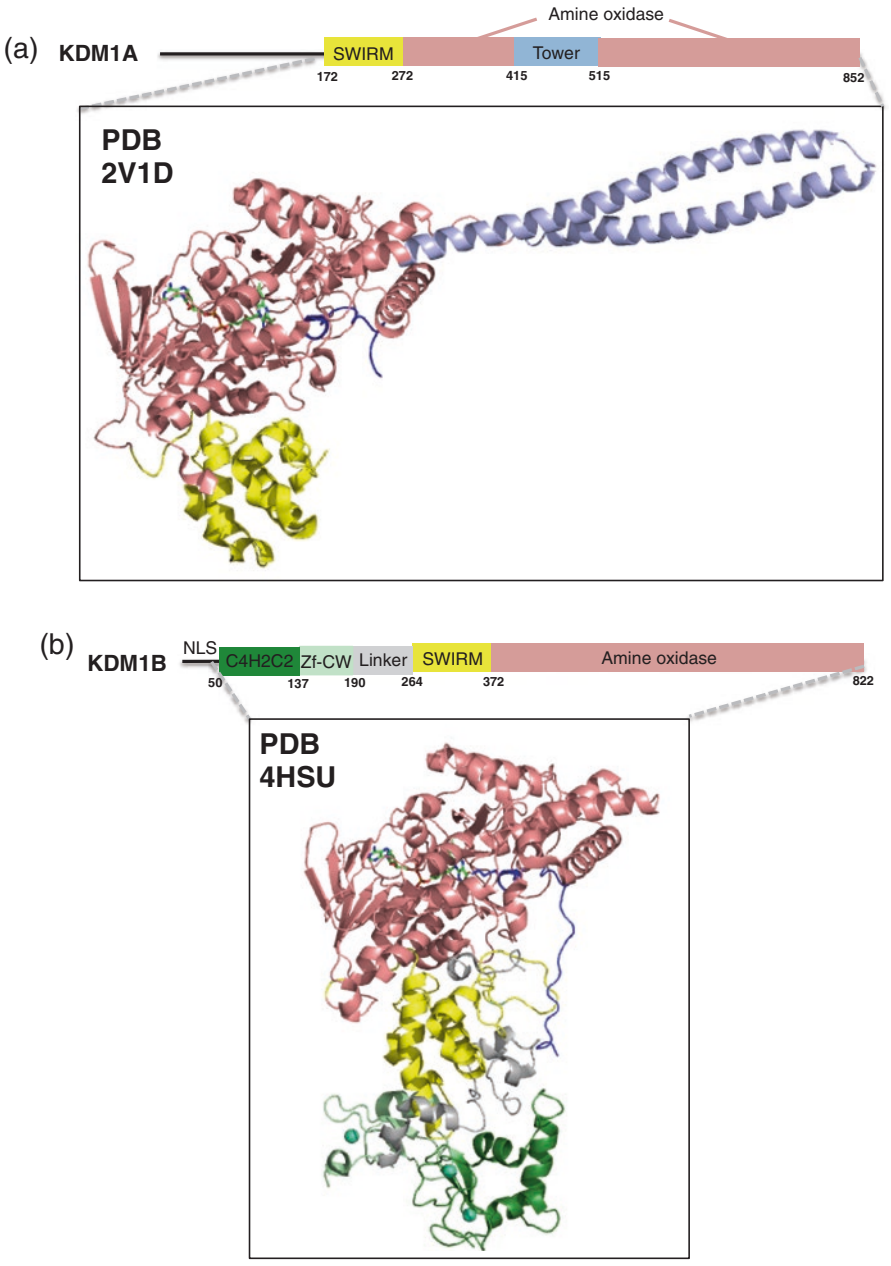

Fig. 2 Representative crystal and domain structures of (**a**) KDM1A and (**b**) KDM1B

of the KDM1 proteins have no predicted conserved structural elements, but do contain nuclear localization signals for nuclear import [63, 65, 66].

There are isoforms of KDM1A resulting from alternative splicing events [67] in which some KDM1A isoforms acquire a new substrate specificity. One of these

isoforms, LSD1n, targets H4K20 methylation, both *in vitro* and *in vivo*, and is involved in neuronal activity–regulated transcription that is necessary for long-term memory formation [68]. Another isoform, LSD1 + 8a, functions as a co-activator by demethylating the repressive H3K9me2 mark. LSD1 + 8a interacts with supervillin; the LSD1 + 8a/supervillin-containing complex demethylates H3K9me2 and thereby regulates neuronal differentiation [69].

KDM1A is overexpressed and/or correlated to poor outcomes such as shorter survival, relapse, high tumor grade, and metastasis in several cancers including prostate cancer [70, 71], bladder cancer [72], neuroblastoma [73], breast cancer [74, 75], non-small cell lung cancer [76], hepatocellular cancer [77], oral cancer [78], colon cancer [79], and sarcomas [80, 81]. Knockdown or inhibition of KDM1A decreased cell growth [71–73, 77–79, 82–86] and migration/invasion [76, 78, 87, 88], as well as increased differentiation [73, 82, 83] in multiple cancer types, both solid and non-solid. The oncogenic activities of KDM1A have been studied extensively in hematological malignancies, and KDM1A was found to be a major contributor to stemness [82, 83]. KDM1A inhibitors are currently in clinical trials for the treatment of particular leukemia subtypes [89]. In contrast to other studies, one report indicates that KDM1A restrains invasion and metastasis in triple-negative breast cancer [90].

Any roles KDM1B may be playing in cancer are just beginning to be elucidated [91, 92]. KDM1B directly ubiquitylates and promotes proteasome-dependent degradation of O-GlcNAc transferase (OGT), and inhibits A549 lung cancer cell growth in a manner dependent on this E3 ligase activity, but not its demethylase activity [92].

4.1 KDM1 Active Site

It has been shown that KDM1A requires a sufficiently long peptide consisting of the first 20 N-terminal amino acids of the H3 histone tail for productive binding [93]. In contrast to many other H3K4 binding proteins where the peptide has an extended conformation, several crystal structures of KDM1A with H3 peptide show that the peptide is severely compressed and has a serpentine shape in a deep active site cavity of KDM1A [94]. The peptide binds in a funnel-shaped pocket adopting a folded conformation in which three structural elements were identified: a helical turn (residues 1–5) located in front of the flavin molecule, a sharp bend (residues 6–9), and a more extended stretch (residues 10–16) that remains partially solvent-exposed on the rim of the binding pocket. The H3 polar residues Arg2, Thr6, Arg8, Lys9 and Thr11, in addition to the N-terminal amino group, lie in well- defined pockets, forming specific and extensive electrostatic and hydrogen- bonding interactions with the surrounding KDM1A residues. The Arg2 residue of the histone H3 tail is essential for stabilization of this tail conformation in the binding site of KDM1A, due to the formation of intrapeptide hydrogen bonds with the side chain of Ser10, and main chain of Gly12 and Gly13. Any disruption of these precise interactions explains the negative effect that nearly all epigenetic modifications (away from H3K4) have on KDM1A–H3 binding [93–95].

In a KDM1B-H3K4me1(1–26) crystal structure, the H3K4me1 peptide extends away from the catalytic cavity and interacts with KDM1B at a second binding site composed of two loops within the linker region of KDM1B [46]. Biochemical analyses indicate that this second binding site is important for substrate recognition and essential for the demethylase activity of KDM1B. KDM1A lacks this second binding site.

4.2 KDM1 Helper Domains

The SWIRM domain was first found in and named after the protein subunits Swi3, Rsc8 and Moira of SWI/SNF-family chromatin remodeling complexes. SWIRM has a compact fold composed of 6 α helices, in which a 20 amino acid long helix (α4) is surrounded by 5 other short helices. The SWIRM domain structure can be divided into the N-terminal part (α1–α3) and the C-terminal part (α4–α6), which are connected to each other by a salt bridge. SWIRM domains are highly conserved amongst chromatin associating proteins and have been shown to bind DNA [96, 97]. However, the residues that compose the typical DNA-binding interface are not conserved and are partially blocked by their interaction in KDM1 proteins with the AOD [45, 98, 99]. This ~85 amino acid domain is believed to help maintain the structural integrity of KDM1 AOD and acts as an anchor site for a histone tail.

In KDM1A, the AOD domain is interrupted with the inclusion of the Tower domain that is absent from KDM1B. KDM1A was originally identified as a component of transcriptional repressor complexes [100, 101] and many of these complexes are formed through this domain. Tower is an ~100 amino acid α-helical, antiparallel coiled-coil domain. This domain is infrequently found in eukaryotic proteins, but is in many prokaryotic proteins involved with intermolecular protein recruitment, membrane docking, and membrane translocation functions [102].

KDM1B lacks a Tower domain, but does contain a novel C4H2C2-type zinc finger (ZnF) and a CW-type zinc finger (Zf-CW) [46, 47]. The ZnF domain is required for KDM1B enzymatic activity through its interaction with the SWIRM domain [103, 104]. Mutations which disrupt the ZnF domains or relays of interactions among the ZnF-SWIRM-AOD may lead to subtle conformational alterations in the AOD that in turn impair the incorporation of FAD, and consequently its enzymatic activity [104]. The surface of the C4H2C2- type zinc finger shows a marked concentration of basic residues, and thus may impact demethylase substrate specificity or positioning within nucleosomal DNA. Additionally, these residues may facilitate interactions with coregulatory molecules or serve to recruit transcriptional machinery, such as phosphorylated RNA polymerase II [62, 104].

4.3 KDM1 in Multicomponent Complexes

The Tower domain of KDM1A forms a complex with the C-terminal domain of CoREST [105], the corepressor for the transcriptional repressor RE1-Silencing Transcription factor (REST) [106–108]. KDM1A is typically associated with CoREST and required for it

to demethylate nucleosome substrates. This subcomplex is found in combination with histone deacetylase (HDAC) 1 or 2, forming a stable larger core complex recruited by many chromatin remodeling multiprotein complexes [100, 101, 109–111]. The CoREST corepressor is necessary for maintaining a repressive chromatin environment in important physiological contexts like neural cell differentiation [105, 112–114].

While structural studies of KDM1A co-crystalized with an H3 substrate peptide revealed that the enzyme active site cannot productively accommodate more than three residues on the N-terminal side of the methylated K4, there is evidence *in vivo* that KDM1A demethylates other substrates. For instance, when associated with the androgen receptor (AR), KDM1A appears to remove repressive methyl groups from H3K9, thereby enhancing AR-dependent gene transcription and resulting in prostate tumor cell proliferation [71]. KDM1A may do this by binding factors that dictate its substrate specificity. Protein kinase C beta 1 (PKCB1)-mediated phosphorylation of H3 threonine-6 also has been proposed as a mechanism to block the H3K4 site and shift the specificity of KDM1A to H3K9 [115]. Recently, EHMT2 (euchromatic histone-lysine N-methyltransferase 2 or G9a) was found to methylate KDM1A at Lys114. KDM1A K114me2, but not unmethylated KDM1A peptide, specifically interacts with the CHD1 (chromodomain-helicase- DNA-binding protein 1) double chromodomain, thus indicating that CHD1 is a reader of KDM1A K114me2. Methylation of KDM1A at Lys114 by EHMT2 and recruitment of CHD1 to AR-binding regions are key events controlling chromatin binding of AR. Thus, the dimethylation of KDM1A at Lys114 appears to ultimately control AR-dependent gene expression [116].

KDM1A appears to be recruited by many CoREST-like and other proteins to form complexes that perform coregulatory or scaffolding functions [64]. In one instance, KDM1A is an integral component of the Mi-2/nucleosome remodeling and deacetylase (NuRD) complex, adding histone demethylation activity to this complex [90]. The NuRD complex contains two other catalytic subunits, the deacetylase HDAC1 and the CHD4 ATPase, both of which are essential for the regulation of gene expression and chromatin remodeling [117]. KDM1A/NuRD complexes regulate several cellular signaling pathways including TGFβ1 signaling pathway that are critically involved in cell proliferation, survival, and epithelial-to-mesenchymal transition [90].

Temporal expression patterns of specific components of KDM1A complexes modulate gene regulatory programs in mammalian development [63, 67, 118, 119]. Any interruption of these patterns, their transcriptional control and/or mutation of components can lead to cancer [64, 120] and other disease [121]. KDM1A is overexpressed in a variety of tumors, and its inactivation or downregulation can inhibit cancer progression [122, 123]. KDM1A targeting inhibitors are an avenue for anticancer drug discovery and will be discussed in a later section of this chapter.

Compared to KDM1A, there is much less known about the multicomponent complexes of KDM1B. In highly transcribed, H3K36me3-enriched coding regions downstream of gene promoters, KDM1B aids in the maintenance of H3K4 and H3K9 methylation by associating with a larger complex that includes Pol II and other elongation factors, as well as the SET-family histone methyltransferases NSD3 and G9a, which methylate histone H3K36 and H3K9 sites, respectively [62]. In addition, the H3K36me3 reader NPAC/ GLYR1 is likely part of this complex as well, which augments the KDM1B demethylation of H3K4me1/2 by binding at its AOD/SWIRM interface [47].

A recent kinetic study showed there is a tight-binding interaction between full-length unmodified histone H3 and KDM1A, which suggests the existence of a secondary binding site on the demethylase surface available for complex formation. The contact between H3 and KDM1A likely occurs through an extensive interaction interface that contributes significantly to its recognition of substrates and products [124]. Apparently, there is still much to discover about KDM1 demethylase function and its control (Table 2).

5 The KDM2 Family

The KDM2 family (Fig. 3) contains the first JmjC KDMs to be discovered and to be established as conserved in eukaryotes from yeast to humans [15]. KDM2 specifically demethylates H3K36me2, and to a lesser extent H3K36me1, which are histone modifications that are associated with transcriptional repression. There have been some indications that KDM2B is also a H3K4me3 demethylase [121], but this observation has only been made *in vivo* and not *in vitro* [135]. In some instances, one could imagine that KDM2B is in a complex with a KDM5 family member, as suggested by one study [136].

KDM2A is over-expressed and correlated to poor prognosis in breast [137, 138], non-small cell lung [139], and gastric cancer [140]. Several studies show that knockdown of KDM2A decreases cell growth [138–140], angiogenesis [138], invasion/migration [139, 140] and metastasis [140]. KDM2A promotes tumorigenicity through upregulation of target genes such as *JAG1* in breast cancer [138] and *DUSP3* in lung cancer [139]. In contrast, one study found that KDM2A knockdown had an opposite effect in breast cancer, increasing invasion, migration, and angiogenesis [141].

KDM2B is implicated in the pathology of breast cancer [142], pancreatic cancer [136], myelodysplastic syndromes [143], and acute myeloid leukemia [144]. Knockdown of KDM2B reduced cancer cell growth [136, 142, 144], as well as impaired stem cell self-renewal [142, 145] and transformation [135, 145, 146]. It is linked to senescence [135, 142, 147] and metabolism [146, 148] control. KDM2B has been shown to regulate cell cycle and senescence associated genes such as *p15* and *p16* [135, 144, 147].

5.1 KDM2 Active Site

Crystal structures of KDM2A with H3K36me2/1 peptides [53] (Table 3) reveal a narrow binding channel that can perfectly fit the specific peptide sequence H3G33 and H3G34 close to H3K36 mark. Any larger side chain in these positions would result in steric hindrance. A pocket binds Pro38 and stabilizes a sharp turn in the H3 backbone. The side chain of Tyr41 binds in a pocket on the demethylase surface through van der Waals interactions and hydrogen binding. Residues Gly33, Gly34,

Table 2 Structures containing domains of KDM1 demethylases

PDB ID	Structure title	Dep. date	Resolution (Å)	Reference
KDM1A/LSD1				
2COM	The solution structure of the SWIRM domain of human LSD1	5/18/05		[99]
2H94	Crystal structure and mechanism of human Lysine-Specific Demethylase-1	6/8/06	2.9	[45]
2IW5	Structural basis for CoREST-dependent demethylation of nucleosomes by the human LSD1 histone demethylase	6/26/06	2.57	[45]
2HKO	Crystal structure of LSD1	7/5/06	2.8	[98]
2DW4	Crystal structure of human LSD1 at 2.3 A resolution	8/2/06	2.3	[125]
2EJR	LSD1-tranylcypromine complex	3/20/07	2.7	[125]
2UXN	Structural basis of histone demethylation by LSD1 revealed by suicide inactivation	3/28/07	2.72	[126]
2UXN	Structural basis of histone demethylation by LSD1 revealed by suicide inactivation	3/28/07	2.72	
2UXX	Human LSD1 histone demethylase-CoREST in complex with an FAD- tranylcypromine adduct	3/30/07	2.74	[126]
2V1D	Structural basis of lsd1-corest selectivity in histone H3 recognition	5/23/07	3.1	[95]
2X0L	Crystal structure of a neuro-specific splicing variant of human histone lysine demethylase LSD1	12/15/09	3	[67]
3ABT	Crystal structure of LSD1 in complex with trans-2-pentafluorophenylcyclopropylamine	12/21/09	3.2	[127]
3ABU	Crystal structure of LSD1 in complex with a 2-PCPA derivative, S1201	12/21/09	3.1	[127]
2XAF	Crystal structure of LSD1-CoREST in complex with para-bromo-(+)-cis-2-phenylcyclopropyl-1-amine	3/31/10	3.25	[128]
2XAG	Crystal structure of LSD1-CoREST in complex with para-bromo-(−)-trans-2-phenylcyclopropyl-1-amine	3/31/10	3.1	[128]
2XAH	Crystal structure of LSD1-CoREST in complex with (+)-trans-2-phenylcyclopropyl-1-amine	3/31/10	3.1	[128]
2XAJ	Crystal structure of LSD1-CoREST in complex with (−)-trans-2-phenylcyclopropyl-1-amine	3/31/10	3.3	[128]
2XAQ	Crystal structure of LSD1-CoREST in complex with a tranylcypromine derivative (mc2584, 13b)	3/31/10	3.2	[128]
2XAS	Crystal structure of LSD1-CoREST in complex with a tranylcypromine derivative (mc2580, 14e)	3/31/10	3.2	[128]
2L3D	The solution structure of the short form SWIRM domain of LSD1	9/13/10		
2Y48	Crystal structure of LSD1-CoREST in complex with a n-terminal snail peptide	1/5/11	3	[129]
4BAY	Phosphomimetic mutant of LSD1-8a splicing variant in complex with CoREST	9/17/12	3.1	[119]

(continued)

Table 2 (continued)

PDB ID	Structure title	Dep. date	Resolution (Å)	Reference
3ZMS	LSD1-CoREST in complex with INSM1 peptide	2/12/13	2.96	[130]
3ZMT	LSD1-CoREST in complex with PRSFLV peptide	2/12/13	3.1	[130]
3ZMU	LSD1-CoREST in complex with PKSFLV peptide	2/12/13	3.2	[130]
3ZMV	LSD1-CoREST in complex with PLSFLV peptide	2/12/13	3	[130]
3ZMZ	LSD1-CoREST in complex with PRSFAV peptide	2/13/13	3	[130]
3ZN0	LSD1-CoREST in complex with PRSFAA peptide	2/13/13	2.8	[130]
3ZN1	LSD1-CoREST in complex with PRLYLV peptide	2/13/13	3.1	[130]
4KUM	Structure of LSD1-CoREST-Tetrahydrofolate complex	5/22/13	3.05	[131]
4CZZ	Histone demethylase LSD1(KDM1A)-CoREST3 Complex	4/23/14	3	[132]
4UV8	LSD1(KDM1A)-CoREST in complex with 1-Benzyl-Tranylcypromine	8/5/14	2.8	[133]
4UV9	LSD1(KDM1A)-CoREST in complex with 1-Ethyl-Tranylcypromine	8/5/14	3	[133]
4UVA	LSD1(KDM1A)-CoREST in complex with 1-Methyl-Tranylcypromine (1R,2S)	8/5/14	2.9	[133]
4UVB	LSD1(KDM1A)-CoREST in complex with 1-Methyl-Tranylcypromine (1S,2R)	8/5/14	2.8	[133]
4UVC	LSD1(KDM1A)-CoREST in complex with 1-Phenyl-Tranylcypromine	8/5/14	3.1	[133]
4UXN	LSD1(KDM1A)-CoREST in complex with Z-Pro derivative of MC2580	8/27/14	2.85	[133]
4XBF	Structure of LSD1:CoREST in complex with ssRNA	12/16/14	2.8	
5AFW	Assembly of methylated LSD1 and CHD1 drives AR-dependent transcription and translocation	1/26/15	1.6	[116]
5IT3	Swirm domain of human Lsd1 (A Tlx-interacting peptide)	3/16/16	1.4	
5L3B	Human LSD1/CoREST: LSD1 D556G mutation	4/6/16	3.3	[134]
5L3C	Human LSD1/CoREST: LSD1 E379K mutation	4/6/16	3.31	[134]
5L3D	Human LSD1/CoREST: LSD1 Y761H mutation	4/6/16	2.6	[134]

KDM1B/LSD2

4FWE	Native structure of LSD2 /AOF1/KDM1b in space group of C2221 at 2.13A	7/1/12	2.13	[104]
4FWF	Complex structure of LSD2/AOF1/KDM1b with H3K4 mimic	7/1/12	2.7	[104]
4FWJ	Native structure of LSD2/AOF1/KDM1b in spacegroup of I222 at 2.9A	7/1/12	2.9	[104]
4GU0	Crystal structure of LSD2 with H3	8/29/12	3.1	[46]
4GU1	Crystal structure of LSD2	8/29/12	2.94	[47]
4GUR	Crystal structure of LSD2-NPAC with H3 in space group P21	8/29/12	2.51	[47]
4GUS	Crystal structure of LSD2-NPAC with H3 in space group P3221	8/29/12	2.23	[47]
4GUT	Crystal structure of LSD2-NPAC	8/29/12	2	[47]
4GUU	Crystal structure of LSD2-NPAC with tranylcypromine	8/29/12	2.3	[47]
4HSU	Crystal structure of LSD2-NPAC with H3(1–26)in space group P21	10/30/12	1.99	[46]

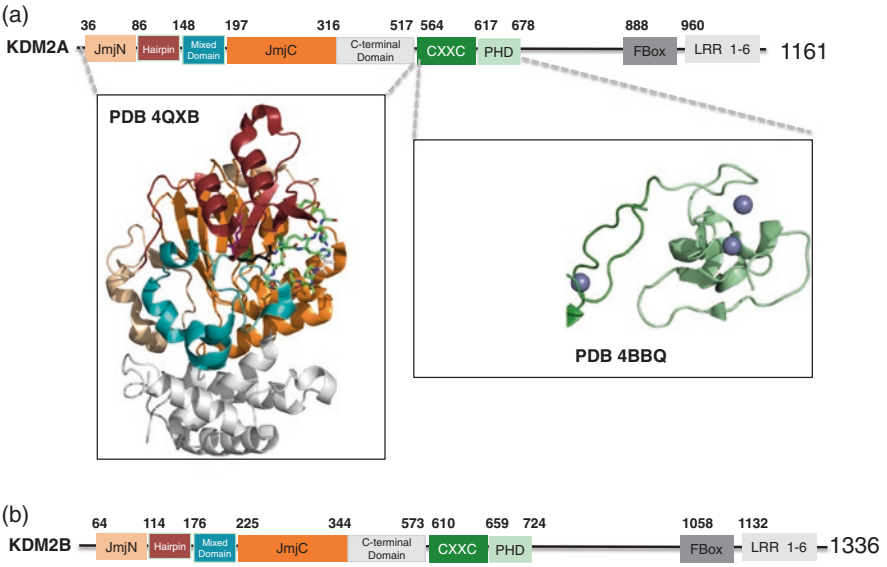

Fig. 3 Representative crystal and domain structures of KDM2 family

Table 3 Structures containing domains of KDM2 demethylases

PDB ID	Structure title	Dep. date	Resolution(Å)	Reference
KDM2A				
4BBQ	Crystal structure of the CXXC and PHD domain of human lysine-specific demethylase 2A (KDM2A)(FBXL11)	9/27/12	2.24	
4TN7	Crystal structure of mouse KDM2A-H3K36ME-NO complex with succinic acid	6/3/14	2.2	[53]
4QWN	Histone demethylase KDM2A-H3K36ME1-alpha-KG complex structure	7/16/14	2.1	[53]
4QX7	Crystal structure of histone demethylase KDM2A-H3K36me2 with alpha-KG	7/18/14	2.34	[53]
4QX8	Crystal structure of histone demethylase KDM2A-H3K36me3 complex with alpha-KG	7/19/14	1.65	[53]
4QXB	crystal structure of histone demethylase KDM2A-H3K36ME3 with NOG	7/19/14	1.6	[53]
4QXC	Crystal structure of histone demethylase KDM2A-H3K36ME2 with NOG	7/19/14	1.75	[53]
4QXH	Crystal structure of histone demethylase KDM2A-H3K36ME1 with NOG	7/20/14	2.2	[53]
KDM2B				
4O64	Human CXXC and PHD domain of KDM2B	4/16/14	2.13	–

Pro38, and Tyr41 are only found near H3K36 and such residues do not flank any other lysine methylation sites on histone H3 or H4.

Surprisingly, KDM2A bound with H3K36me3 peptide, the inactive substrate for KDM2A, could be crystallized. Comparison of structures with H3K36me3 peptide with those with substrate H3K36me2/1 peptide and/or different cofactors suggests that a third methyl group on H3K36me2 may sterically hinder an axial-to-in-plane conversion of the 2OG positioning required for catalysis [149].

5.2 KDM2 Helper Domains and Multicomponent Complexes

Both KDM2 homologs contain a zinc finger CXXC domain that specifically recognizes non-methylated CpG dinucleotides [150], seemingly targeting these histone demethylases to the so-called genomic regions known as CpG islands (CGIs; these contain a high density of CpG dinucleotides where the cytosine nucleotide is primarily not methylated) that are associated with ~70% of mammalian gene promoters and gene regulatory units [151–154]. When KDM2B recognizes non-methylated DNA in CGIs, it recruits the polycomb repressive complex 1 (PRC1) that then contributes to histone H2A Lys119 ubiquitylation (H2AK119ub1) and gene repression [155, 156]. KDM2B associates with a noncanonical PRC1 to regulate adipogenesis [157]. Furthermore, KDM2B, via its F-box domain, functions as a subunit of the CUL1-RING ubiquitin ligase ($CRL1/SCF^{KDM2B}$) complex where SCF is an acronym for combination of Skp, Cullin, F-box proteins. KDM2B targets c-Fos for polyubiquitylation and regulates c-Fos protein levels [158]. Another paper suggests KDM2B has unexpected E3 ubiquitin ligase activity. The F-box in KDM2B shows E3 ligase activity *in vitro*, but has not been characterized further *in vivo* [159].

The F-box domains encoded by KDM2A and KDM2B have 78% protein sequence identity. This suggests that KDM2A may also recognize CpG through its CXXC domain and is likely to form a functional SCF E3 ligase [137]. Interestingly, KDM2A and KDM5B had the highest frequency of genetic amplification and overexpression in breast cancer among 24 KDM genes tested [137]. KDM2A had the highest correlation between copy number and mRNA expression, and high mRNA levels of KDM2A were significantly associated with shorter survival of breast cancer patients. KDM2A has two isoforms: the long isoform that is the whole protein and a short form that lacks the N-terminal JmjC domain but contains all other motifs, including the CXXC and F-box domains. It is this short form of KDM2A that has oncogenic potential and functions as an oncogenic isoform in a subset of breast cancers [137].

6 The KDM3 Family

The KDM3 family (Fig. 4) contains three members in humans, but only two, KDM3A and KDM3B, are fully verified demethylases, which act upon H3K9me2/1. The domains of the KDM3 family encompass a C2HC4 zinc finger followed by a

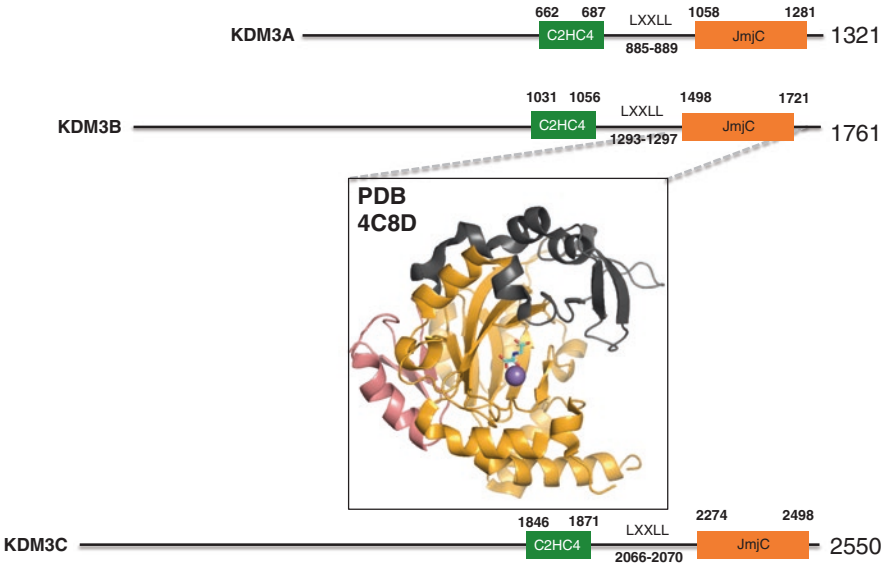

Fig. 4 Representative crystal and domain structures of KDM3 family

~225-residue long JmjC domain which shows 86% similarity between KDM3A and KDM3B. In between these domains lies a LXXLL motif known to be involved in nuclear hormone-receptor interactions [160, 161].

KDM3A is a crucial regulator of spermatogenesis, embryonic stem cell self-renewal, and metabolic gene expression. Both KDM3A and KDM3B may have roles in sex determination [162–168]. KDM3A expression is upregulated in lung cancer [169, 170], gastric cancer [171], neuroblastoma [172], Ewing sarcoma [173], bladder cancer [170], renal cell carcinoma [174], and hepatocellular carcinoma [175]. Additionally, it is implicated in the tumorigenesis of multiple myeloma [176], prostate cancer [177], and colon carcinoma [178, 179]. Knockdown or inhibition of KDM3A inhibited growth [169–171, 173, 174, 176–181] as well as migration or invasion [169, 172, 174, 179] in several tumor cell types. KDM3A was shown to control expression of several well-known proto-oncogenes including *c-Myc* [177], *HOXA1* and *CCND1* [170]. It has been shown to be regulated by hypoxia in cancers [175, 178] and to play a role in angiogenesis [180], further supported by a report that expression of KDM3A is higher in hypoxic environments and near blood vessels in renal cell carcinoma [174]. Contradictorily, one study reports that KDM3A acts as a tumor suppressor in human germ cell-derived tumors like embryonal carcinomas, seminomas, and yolk sac tumors [182].

The biological functions of KDM3B are not as well characterized. The human gene for KDM3B is located at 5q31, a chromosomal area that is often deleted in malignant myeloid disorders, including acute myeloid leukemia and myelodysplasia [183]. The enforced expression of this demethylase in a cell line carrying a 5q deletion inhibits clonogenic growth, indicating that loss of KDM3B may be involved in the pathogenesis of these cancers and that KDM3B may have tumor suppressor activities. Further strengthening its role as a tumor suppressor, high KDM3B expression was

correlated to better disease-free survival after mastectomy in breast cancer patients [184]. However, contrary to the above studies, KDM3B is overexpressed in acute lymphoblastic leukemia and displays specific activity *in vitro* and *in vivo* in leukemogenesis. In this setting, it acts as a transcriptional coactivator to repress differentiation [185]. KDM3B is amplified in non-small cell lung cancer [186].

A third member of the family, KDM3C, has no verifiable demethylase activity on H3K9 peptides *in vitro*, but seems to in cells [187–189]. KDM3C inhibits the neuronal differentiation of human embryonic stem cells and has been found mutated in intracranial germline tumors [188, 190, 191]. KDM3C is reported to play a role in the maintenance of leukemias by functioning as a coactivator for key transcription factors, where its knockdown resulted in apoptosis and impaired growth of cancer cells [189, 190].

6.1 KDM3 Activity and Helper Domains

The C2HC4 zinc finger domain is required for enzymatic activity of KDM3A [192] and the demethylase appears to dimerize through interactions between this domain and the JmjC domain [193]. In addition, if one active site in the KDM3A dimer is mutated, the enzymatic activity of two-step demethylation is significantly decreased. For this KDM family, it appears that the initial conversion of H3K9me2 into H3K9me1 occurs at one active site of the dimer. After the first demethylation step is finished, allosteric regulation of substrate channeling occurs, the monomethylated substrate binds, and conversion of H3K9me1 into H3K9me0 takes place at the second site [193]. Another observation is that one residue, Thr667, contributes to the H3K9me1/2 substrate specificity of wild-type KDM3A: a T667A mutation alters specificity towards H3K9me2 [187]. Thr667 may aid in aligning the methyl group of monomethylated H3K9 correctly in the active site center, presumably bringing it in close proximity to the iron so that the reaction can be catalyzed.

While no papers discussing KDM3 crystal structures have been published, one KDM3 crystal structure has been deposited in the PDB databank (PDB: 4C8D) of the catalytic region of KDM3B (residues 1380–1720) illustrating an unusual JmjC architecture (Table 4). An N-terminal motif proceeding the JmjC domain comprises several α-helices and two three-stranded anti-parallel β-sheets that form β-extension motifs that buttress each side of the central JmjC β-barrel. One of the three-stranded β-sheets is located near the entrance of the active site, implicating it in recognizing the H3 peptide substrate.

Table 4 Structures containing domains of KDM3 demethylases

PDB ID	Structure title	Dep. date	Resolution (Å)	Reference
KDM3B				
4C8D	Crystal structure of JmjC domain of human histone 3 lysine-specific demethylase 3B (KDM3B)	9/30/13	2.18	

6.2 *KDM3 in Multicomponent Complexes*

Several studies have indicated that KDM3A has a role in regulating hypoxia-inducible genes through interaction with transcription factors that are targeted to KDM3A under hypoxic conditions [178, 194–197]. Hypoxic conditions have been linked to enhanced tumor growth [194]. Hypoxia is commonly found in solid tumors where the access of anticancer drugs is restricted, and the hypoxia allows for a selective environment for aggressive cancer cells [196, 198]. KDM3A has been shown to maintain some demethylase activity even under severe hypoxic conditions [199]. KDM3A exhibits hormone-dependent recruitment to androgen-receptor target genes through interaction with the androgen receptor (AR) to upregulate AR target gene expression [192].

7 The KDM4 Family

This demethylase family (Fig. 5) is probably the most examined of all the JmjC demethylase families, especially KDM4A; presently, there are over 55 crystal structures of this enzyme deposited in the PDB which includes complex structures with >20 inhibitors (Table 5, discussed below). There are many excellent published reviews [52, 200–202]. The KDM4 family has specificity for two regions of H3 with different sequences. Members act on H3K9me3/me2 and, in some cases, H3K36me3/

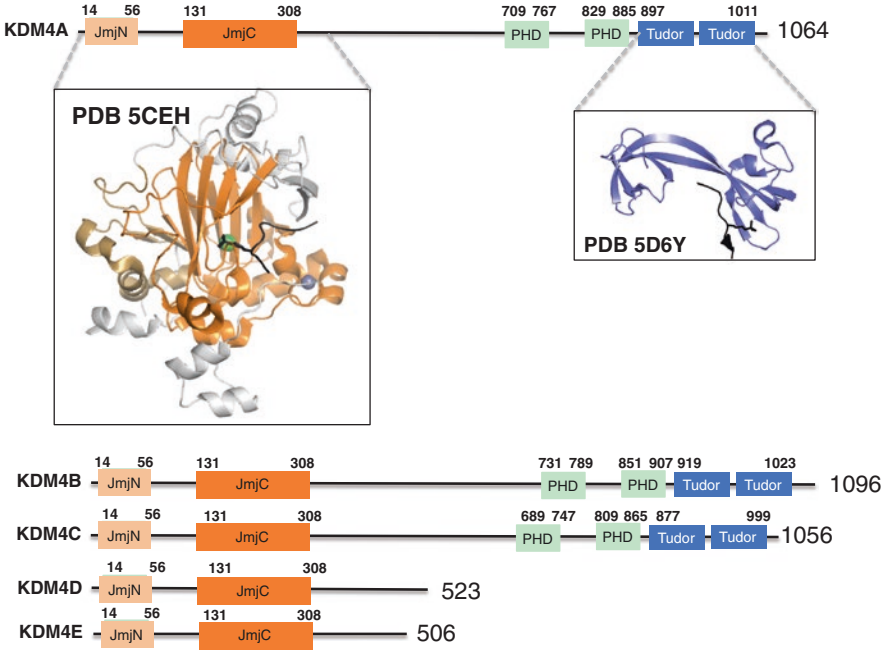

Fig. 5 Representative crystal and domain structures of KDM4 family

Table 5 Structures containing domains of KDM4 demethylases

PDB ID	Structure title	Dep. date	Resolution (Å)	Reference
KDM4A				
2GF7	Double Tudor domain structure	3/21/06	2.2	[206]
2GFA	Double Tudor domain complex structure	3/21/06	2.1	[206]
2QQR	JMJD2A hybrid Tudor domains	7/26/07	1.8	[256]
2QQS	JMJD2A tandem Tudor domains in complex with a trimethylated histone H4-K20 peptide	7/26/07	2.82	[256]
5D6W	Crystal structure of double Tudor domain of human lysine demethylase KDM4A	8/13/15	1.99	
5D6X	Crystal structure of double Tudor domain of human lysine demethylase KDM4A	8/13/15	2.15	
5D6Y	Crystal structure of double Tudor domain of human lysine demethylase KDM4A complexed with histone H3K23me3	8/13/15	2.29	
2OX0	Crystal structure of JMJD2A complexed with histone H3 peptide dimethylated at Lys9	2/19/07	1.95	[253]
2P5B	The complex structure of JMJD2A and trimethylated H3K36 peptide	3/14/07	1.99	[261]
2PXJ	The complex structure of JMJD2A and monomethylated H3K36 peptide	5/14/07	2.00	[261]
2Q8C	Crystal structure of JMJD2A in ternary complex with an histone H3K9me3 peptide and 2-oxoglutarate	6/10/07	2.05	[254]
2Q8D	Crystal structure of JMJD2A in ternary complex with histone H3-K36me2 and succinate	6/10/07	2.29	[254]
2Q8E	Specificity and mechanism of JMJD2A, a trimethyllysine-specific histone demethylase	6/10/07	2.05	[254]
2VD7	Crystal structure of JMJD2A complexed with inhibitor pyridine-2,4- dicarboxylic acid	10/1/07	2.25	[262]
2WWJ	Structure of JMJD2A complexed with inhibitor 10A	10/23/09	2.6	[263]
3NJY	Crystal structure of JMJD2A complexed with 5-carboxy-8-hydroxyquinoline	6/18/10	2.6	[264]
3PDQ	Crystal structure of JMJD2A complexed with bipyridyl inhibitor	10/23/10	1.99	[265]
2YBK	JMJD2A complexed with R-2-hydroxyglutarate	3/8/11	2.4	[266]
2YBP	JMJD2A complexed with R-2-hydroxyglutarate and histone H3K36me3 peptide (30–41)	3/9/11	2.02	[266]
2YBS	JMJD2A complexed with S-2-hydroxyglutarate and histone H3K36me3 peptide (30–41)	3/10/11	2.32	[266]
3RVH	Crystal structure of JMJD2A complexed with inhibitor 8-hydroxy-3-(piperazin-1-yl) quinoline-5-carboxylic acid	5/6/11	2.25	

(continued)

Table 5 (continued)

PDB ID	Structure title	Dep. date	Resolution (Å)	Reference
3U4S	Histone lysine demethylase JMJD2A in complex with T11C peptide substrate crosslinked to N-oxalyl-D-cysteine	10/10/11	2.15	[267]
4AI9	JMJD2A complexed with daminozide	2/8/12	2.25	[268]
4GD4	Crystal structure of JMJD2A complexed with inhibitor, 2-(1H-pyrazol-3-yl)pyridine-4-carboxylic acid	7/31/12	2.33	
4BIS	JMJD2A complexed with 8-hydroxyquinoline-4-carboxylic acid	4/12/13	2.49	[269]
4URA	Crystal structure of human JMJD2A in complex with compound 14a	6/27/14	2.23	
4V2V	JMJD2A complexed with Ni(II), NOG and histone H3K27me3 peptide (25–29) ARK(me3)SA	10/15/14	2	[270]
4V2W	JMJD2A complexed with Ni(II), NOG and histone H3K27me3 peptide (16–35)	10/15/14	1.81	[270]
5A7N	Crystal structure of human JMJD2A in complex with compound 43	7/9/15	2.39	[271]
5A7O	Crystal structure of human JMJD2A in complex with compound 42	7/9/15	2.15	[271]
5A7P	Crystal structure of human JMJD2A in complex with compound 36	7/9/15	2.28	[271]
5A7Q	Crystal structure of human JMJD2A in complex with compound 30	7/9/15	2	[271]
5A7S	Crystal structure of human JMJD2A in complex with compound 44	7/9/15	2.2	[271]
5A7W	Crystal structure of human JMJD2A in complex with compound 35	7/10/15	2.27	[271]
5A80	Crystal structure of human JMJD2A in complex with compound 40	7/11/15	2.28	[271]
5ANQ	Inhibitors of JumonjiC domain-containing histone demethylases	9/7/15	2	[272]
5F2S	Crystal structure of human KDM4A in complex with compound 15	12/2/15	2.08	[273]
5F2W	Crystal structure of human KDM4A in complex with compound 16	12/2/15	2.6	[273]
5F32	Crystal structure of human KDM4A in complex with compound 40	12/2/15	2.05	[273]
5F37	Crystal structure of human KDM4A in complex with compound 58	12/2/15	2.22	[273]
5F39	Crystal structure of human KDM4A in complex with compound 37	12/2/15	2.65	[273]
5F3C	Crystal structure of human KDM4A in complex with compound 52d	12/2/15	2.06	[273]
5F3E	Crystal structure of human KDM4A in complex with compound 54a	12/2/15	2.16	[273]
5F3G	Crystal structure of human KDM4A in complex with compound 53a	12/2/15	2.5	[273]
5F3I	Crystal structure of human KDM4A in complex with compound 54j	12/2/15	2.24	[273]
5FPV	Crystal structure of human JMJD2A in complex with compound KDOAM20A	12/3/15	2.44	[274]

5F5I	Crystal structure of human JMJD2A complexed with KDOOA011340	12/4/15	2.63	[273]
5FWE	JMJD2A complexed with Ni(II), NOG and histone H4(1–15)R3me2s peptide	2/15/16	2.05	
5FY8	Crystal structure of human JMJD2A in complex with D-threo-isocitrate	3/4/16	2.34	
5FYC	Crystal structure of human JMJD2A in complex with succinate	3/7/16	2.26	
5FYH	Crystal structure of human JMJD2A in complex with fumarate	3/7/16	2.35	
5FYI	Crystal structure of human JMJD2A in complex with pyruvate	3/7/16	2.1	
KDM4B				
4LXL	Crystal structure of JMJD2B complexed with pyridine-2,4-dicarboxylic acid and H3K9me3	7/30/13	1.87	
4UC4	Crystal structure of hybrid Tudor domain of human lysine demethylase KDM4B	8/13/14	2.56	
KDM4C				
2XDP	Crystal structure of the Tudor domain of human JMJD2C	5/6/10	1.56	
2XML	Crystal structure of human JMJD2C catalytic domain	7/28/10	2.55	[252]
4XDO	Crystal structure of human KDM4C catalytic domain with OGA	12/19/14	1.97	[275]
4XDP	Crystal structure of human KDM4C catalytic domain bound to tris	12/19/14	2.07	[275]
5FJH	Crystal structure of human JMJD2C catalytic domain in complex with epitherapuetic compound 2-(((2-((2-(dimethylamino)ethyl) (ethyl)amino) -2-oxoethyl)amino)methyl)isonicotinic acid	10/9/15	2.1	
5FJK	Crystal structure of human JMJD2C catalytic domain in complex 6-ethyl- 5-methyl-7-oxo-4,7-dihydropyrazolo(1,5-a)pyrimidine-3-carbonitrile			
KDM4D				
3DXT	Crystal structure of the catalytic core domain of JMJD2D	7/25/08	1.8	
3DXU	The crystal structure of core JMJD2D complexed with FE and N-oxalylglycine	7/25/08	2.2	
4HON	Crystal structure of human JMJD2D/KDM4D in complex with an H3K9me3 peptide and 2-oxoglutarate	10/22/12	1.8	[276]
4HOO	Crystal structure of human JMJD2D/KDM4D apoenzyme	10/22/12	2.49	[276]
4D6Q	Crystal structure of human JMJD2D in complex with 2,4-PDCA	11/14/14	1.29	
4D6R	Crystal structure of human JMJD2D in complex with N-oxalylglycine and bound o-toluenesulfonamide	11/14/14	1.4	
4D6S	Crystal structure of human JMJD2D in complex with N-oxalylglycine and bound 5,6-dimethylbenzimidazole	11/14/14	1.4	
5F5A	Crystal structure of human JMJD2D complexed with KDOAM16	12/4/15	1.41	[273]
5F5C	Crystal structure of human JMJD2D complexed with KDOPP7	12/4/15	1.88	[273]

(continued)

Table 5 (continued)

PDB ID	Structure title	Dep. date	Resolution (Å)	Reference
5FP3	Crystal structure of human JMJD2D complexed with 3-(4-phenylbutanamido)pyridine-4-carboxylic acid	11/27/15	2.05	[277]
5FP4	Crystal structure of human KDM4D in complex with 3-(4- phenylbutanamido)pyridine-4-carboxylic acid	11/27/15	2	[277]
5FP8	Crystal structure of human KDM4D in complex with 3-4-methylthiophen-2- ylmethylaminopyridine-4-carboxylic acid	11/27/15	1.98	[277]
5FP9	Crystal structure of human KDM4D in complex with 3-aminopyridine-4- carboxylic acid(w/S-oxy cysteine)	11/27/15	2	[277]
5FPA	Crystal structure of human KDM4D in complex with 3H,4H-pyrido-3,4-d- pyrimidin-4-one	11/27/15	1.96	[277]
5FPB	Crystal structure of human KDM4D in complex with 2-1H-pyrazol-4-yloxy- 3H,4H-pyrido-3,4-d-pyrimidin-4-one	11/27/15	1.91	[277]

me2. H3K9me3 demethylation promotes an open chromatin state, contributing to the transcriptional activation of promoter regions [200]. KDM4A and KDM4B occupancy is fairly evenly distributed across different genomic regions, while KDM4C localizes predominantly to H3K4me3-containing promoter regions [203–205].

In humans, this family contains five known members. The KDM4A-C proteins share more than 50% sequence identity; each contains JmjN, JmjC, two plant homeodomains (PHD) and two hybrid Tudor domains that form a bilobal structure, with each lobe resembling a normal Tudor domain. KDM4D and KDM4E, in contrast, are considerably shorter proteins that lack the C-terminal region, including the PHD and Tudor domains [17, 52]. Biochemical studies indicate that KDM4A-C catalyze the removal of H3K9 and H3K36 di- and trimethyl marks. However, *in vivo,* KDM4A seems to demethylate only trimethylated residues [19] and has a greater affinity for H3K9me3 over H3K36me3 [16, 20, 206]. KDM4D can only demethylate H3K9me3/me2 [17, 52]. KDM4E meanwhile, catalyzes the removal of two methyl groups from H3K9me3 and also H3K56me3 [207, 208].

The KDM4 family members are associated with cancer in several ways, summarized for most family members below (reviewed in [52, 200, 201, 209]). Several members are involved in hypoxia [210, 211] and DNA mismatch repair [212]. KDM4A, B, and C are required for the survival of acute myeloid leukemia cells [213].

KDM4A expression is upregulated and/or correlates to poor outcomes in many cancers including breast [214, 215], prostate [17, 216, 217], lung [218–220], bladder [220], gastric [221], and endometrial carcinoma [222, 223]. KDM4A overexpression led to the development of prostatic intraepithelial neoplasia, and combined overexpression of KDM4A and ETV1 resulted in prostate carcinoma formation in *Pten*$^{+/-}$ mice [217]. Furthermore, overexpression of KDM4A has been shown to cause localized copy gains and DNA re-replication in tumor cells [224]. Knockdown or knockout of KDM4A inhibits growth [217, 221–223, 225–228], migration/invasion [222, 223, 227], and metastasis [87] in several cancer models, and provokes apoptosis [218, 221, 226] and senescence [219]. KDM4A regulates target genes such as *p27* [223], *YAP1* (*yes-associated protein 1*) [217], *ARHI* (*aplasia Ras homolog member I*) [215], *CHD5* (*chromodomain helicase DNA-binding domain 5*), and activating protein 1 (AP1) family genes [87]. It is associated with cancer-related proteins such as the androgen receptor (AR) [223], p53 [226], and SIRT2 (sirtuin 2) [228].

KDM4B is overexpressed and correlates to adverse outcomes in many cancers including endometrial cancer [223], luminal breast cancer [214], colorectal cancer [229], bladder [230], lung [230], prostate [17, 231], gastric [232–234], hepatocellular carcinoma [235], and osteosarcoma [236]. Knockdown of KDM4B inhibits growth [211, 225, 229, 230, 232, 237–239], migration/invasion [223, 229, 233], and metastasis [233], and induced DNA damage [239] and apoptosis [232, 239, 240]. It is known to associate with nuclear receptors to drive cancers such as AR [223, 231] and ERα (estrogen receptor α) [211, 237, 238], regulating target genes such as *c-Myc* [223], *CDK6* (*cyclin-dependent kinase 6*) [230], and ERα target genes such as *CCND1* [211, 237].

KDM4C is amplified in basal-like breast cancer [214, 241], esophageal squamous cell carcinomas [242], sarcomatoid lung carcinoma [243], lymphomas [244], and medulloblastoma [245, 246]. Likewise, it is overexpressed and/or associated with

negative patient outcomes in basal-like breast cancer [214], esophageal squamous cell carcinoma [242], prostate cancer [17], osteosarcoma [236], and esophageal squamous cell carcinoma [247]. KDM4C knockdown or inhibition prevents growth of several cancer types [17, 210, 244, 248], as well as breast cancer metastasis to the lung [210]. Overexpression of KDM4C was able to transform normal-like breast epithelial cells [241]. KDM4C was reported to interact with HIF1α (hypoxia inducible factor 1 α) [210] and FGF2 (fibroblast growth factor 2) [236], as well as to target p53 pathway gene *MDM2* (mouse double minute 2 homolog) [249]. In contrast, one study reports that KDM4C expression is associated with improved breast cancer survival and response to therapy [250]. KDM4D is overexpressed in basal-like breast cancer [214]. KDM4D knockdown blocked the proliferation of colon cancer cells, but surprisingly, KDM4D was shown to bind p53 and activate *p21* expression [251].

7.1 KDM4 Active Site

Binding specificity in KDM4 members originates from amino acids surrounding lysines 9 and 36 on histone H3, whereas space and electrostatic environment in the methyl group–binding pocket of these enzymes allow for di- and trimethyl and not the monomethylated lysine residues to position a methyl group productively toward the Fe^{2+} atom in the catalytic center. Crystal structures and modeling punctuates the importance of certain residues in KDM4 demethylases for defining H3K36me3 recognition [225]. In KDM4A and KDM4B, residues Ile71, Asn86, and Asp135 engage in van der Waals interactions or hydrogen bonds with H3 residues H39 and R40 on the C-terminal side of H3K36me3 while the side chains of Leu75, His90, and Asp139 in KDM4D cannot avoid steric clashes with H39 and R40. The crystal structure of the KDM4D-peptide complex also shows that the R42 side chain of H3 lies in close proximity to Lys91 and Lys92 on the surface of KDM4D, resulting in potential electrostatic repulsion between the enzyme and H3K36me3 peptide. In KDM4A, the corresponding residues, Ile87 and Gln88, possess uncharged side chains, alleviating this electrostatic repulsion. Ile71, Asn86, Ile87, and Gln88 in KDM4A are strictly conserved in KDM4B and KDM4C and mutations of these residues to the corresponding amino acids in KDM4D and KDM4E (i.e., I71L, N86H, I87K, and Q88K) disrupt H3K36me3 demethylation *in vitro* and *in vivo* [252].

In KDM4A-C, the C–H•••O hydrogen-bonding network in the active site places one of the three methyl groups of the trimethylated lysine close to the Fe^{2+} and in an ideal position for catalysis. When dimethylated or monomethylated lysines bind at the active site, the methyl groups are sequestered away from the metal ion by C–H•••O hydrogen bonds. Therefore, the catalysis-competent methyl position is energetically disfavored. For a dimethylated lysine, a rotational movement could allow one of the methyl groups to gain access to Fe^{2+} for catalysis, probably with less efficiency than a trimethylated lysine [253, 254]. A monomethylated lysine would be completely sequestered and cannot reach the proper positioning for catalysis. Ser288

(whose hydroxyl group forms C–H•••O hydrogen bonds with methyl groups) is frequently substituted by Ala in other JmjC demethylases, such as KDM4D and KDM6A (A1238). The substitution of Ser288 in KDM4A with Ala enhances its activity, especially on dimethylated substrates, indicative of this residue's role in the determination of the methylation state specificity [20, 254].

7.2 KDM4 Helper Domains

The functions of the two PHD domains in KDM4A-C remain unknown. However, it appears that differential tandem Tudor domain (TTD) binding properties across the KDM4 demethylase family may distinguish the targets of the KDM4 family in the genome. The TTD domain has two shared β-strands that interdigitate to form a bilobal structure, with each lobe resembling a normal Tudor domain. The KDM4A TTD recognizes both H3K4me3 and H4K20me3 [206, 255, 256], while the KDM4B TTD binds methylated H4K20 [257], and the KDM4C TTD is specialized to recognize only methylated H3K4 [203, 258]. In the crystal structure of the KDM4A TTD, the second Tudor domain uses a cluster of aromatic residues, Phe932, Trp967 and Tyr973, to establish an open cage pocket for binding the side chain of H3K4me3 or H4K20me3 while the side chains of the other Tudor domain form intermolecular contacts [206]. However, the H3 and H4 peptides contact the Tudor domains in opposite orientations and at different surfaces of the second hybrid Tudor domain, while the side chains of the other Tudor domain form intermolecular contacts [35, 259].

7.3 KDM4 in Multicomponent Complexes

Recall that H3K4 trimethylation is a hallmark of active promoters that are usually devoid of H3K9 trimethylation, a mark of inactive chromatin. Through its Tudor domain, KDM4A could be recruited to active gene promoters where it would demethylate H3K9 ensuring amplification of gene transcription. As one example of a KDM4 family member in an epigenetic modifying complex, KDM4B is physically associated with and an integral component of the H3K4 methyltransferase mixed-lineage leukemia 2 (MLL2) complex [238]. This complex could potentially be a Tudor domain-independent instance (possibly through PHD) in which KDM4B can simultaneously demethylate H3K9 while H3K4 becomes trimethylated. This KDM4B/MLL2 complex co-purifies with estrogen receptor α (ERα) and is required for ERα-regulated transcription [238]. ERα exhibits greater stability when KDM4B is overexpressed, and ERα can upregulate KDM4B. This creates a positive feedback loop between these two molecules to amplify the estrogen signal [260]. A similar mechanism has been proposed for AR signaling [231]. In this manner, KDM4B has an oncogenic role in both breast and prostate cancers. Another report finds KDM4B and KDM4C work distinctly and combinatorially in different multicomponent complexes in embryonic stem cells that affect their differentiation [204].

8 The KDM5 Family

The human KDM5 family (Fig. 6 and Table 6), specific for the demethylation of H3K4me3/2, encompasses four enzymes: KDM5A/JARID1A/RBP2 (retinoblastoma-binding protein 2), KDM5B/JARID1B/PLU-1, KDM5C/JARID1C/SMCX (selected mouse cDNA on the X), and KDM5D/JARID1D/SMCY (selected mouse cDNA on the Y) [278]. KDM5 members show a high degree of homology in sequence and domain organization [54, 279]. In addition to the catalytic JmjC domain, each contains a JmjN domain, an ARID DNA-binding motif, two or three PHD finger domains and a C5CH2-type zinc finger domain. The KDM5 family is unique among JmjC-containing histone demethylases in that there are identifiable domains, the ARID and PHD, between the JmjN and JmjC. Despite the fact that all members of KDM5 catalyze the demethylation of the same histone mark, they appear to have exclusive functional properties probably because of their different expression profiles and presence in distinct protein complexes [278, 279].

This family of KDMs is the only one to demethylate the H3K4me3 mark. In genome-wide studies, this mark broadly correlates with RNA polymerase II occupancy at sites of active gene expression, and is thought to provide an additional layer of transcriptional regulation. H3K4me3 is known to be associated with transcriptionally active genes or in combination with repressive histone marks [280], such as H3K27me3, at the promoters and transcriptional start sites at the 5′-end of important developmental genes [280, 281], keeping them in the "poised for activation" state.

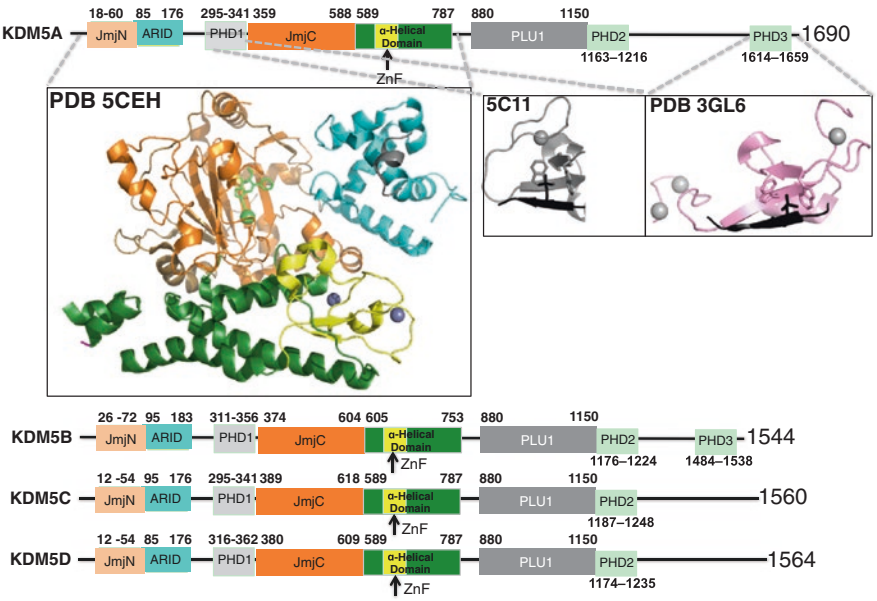

Fig. 6 Representative crystal and domain structures of KDM5 family

Table 6 Structures containing domains of KDM5 demethylases

PDB ID	Structure title	Dep. date	Resolution (Å)	Reference
KDM5A				
2JXJ	NMR structure of the ARID domain from the histone H3K4 demethylase RBP2	11/20/07		
2KGG	Crystal structure of JARID1A-PHD3 complexed with H3(1–9)K4me3 peptide	3/11/09	1.9	[325]
2KGI	Solution structure of JARID1A C-terminal PHD finger in complex with H3(1–9)K4me3	3/12/09		[325]
3GL6	Crystal structure of JARID1A-PHD3 complexed with H3(1–9)K4me3 peptide	3/11/09	1.9	[325]
5C11	Crystal Structure of JARID1A PHD finger bound to histone H3C4me3 peptide	6/12/15	2.8	
5CEH	Structure of histone lysine demethylase KDM5A in complex with selective inhibitor	7/6/15	3.14	[283]
5E6H	A linked Jumonji domain of the KDM5A lysine demethylase	10/9/15	2.24	[54]
5IVJ	Linked KDM5A Jmj domain bound to the inhibitor N11 [3-({1-[2-(4,4-difluoropiperidin-1-yl)ethyl]-5-fluoro-1H-indazol-3-yl}amino)pyridine-4-carboxylic acid]			[282]
5IVV	Linked KDM5A Jmj domain bound to the inhibitor N12 [3-((1-methyl-1H-pyrrolo[2,3-b]pyridin-3-yl)amino) isonicotinic acid]			[282]
5IVY	Linked KDM5A Jmj domain bound to the inhibitor N16 [3-(2-(4-chlorophenyl)acetamido)isonicotinic acid]			[282]
5IW0	Linked KDM5A Jmj domain bound to the inhibitor N19 [2-(5-((4-chloro-2-methylbenzyl)oxy)-1H-pyrazol-1-yl)isonicotinic acid]			[282]
5IVB	A high resolution structure of a linked KDM5A Jmj domain with alpha-ketoglutarate			[282]
5IVC	Linked KDM5A Jmj domain bound to the inhibitor N3 (4′-[(2-phenylethyl)carbamoyl][2,2′-bipyridine]-4-carboxylic acid)			[282]
5IVE	Linked KDM5A Jmj domain bound to the inhibitor N8 (5-methyl-7-oxo-6-(propan-2-yl)-4,7-dihydropyrazolo[1,5-a]pyrimidine-3-carbonitrile)			[282]
5IVF	Linked KDM5A Jmj domain bound to the inhibitor N10 8-(1-methyl-1H-imidazol-4-yl)-2-(4,4,4-trifluorobutoxy)pyrido[3,4-d]pyrimidin-4-ol			[282]
KDM5B				
2EQY	Solution structure of the ARID domain of Jarid1b protein	03/30/07		
2MA5	Solution NMR structure of PHD type zinc finger domain of lysine-specific demethylase 5B (PLU-1/JARID1B) from *Homo sapiens*, Northeast Structural Genomics Consortium (NESG) Target HR7375C	6/28/13		
2MNY	NMR structure of KDM5B PHD1 finger	4/16/14		[322]

Table 6 (continued)

PDB ID	Structure title	Dep. date	Resolution (Å)	Reference
2MNZ	NMR structure of KDM5B PHD1 finger in complex with H3K4me0(1-10aa)	4/16/14		[322]
5A1F	Crystal structure of the catalytic domain of PLU1 in complex with N-oxalylglycine	4/29/15	2.1	[274]
5A3N	Crystal structure of human PLU-1 (JARID1B) in complex with KDOAM25a	6/2/15	2	
5A3P	Crystal structure of the catalytic domain of human PLU1 (JARID1B)	6/2/15	2.01	[274]
5A3T	Crystal structure of human PLU-1 (JARID1B) in complex with KDM5-C49 (2-(((2-((2-(dimethylamino) ethyl)(ethyl)amino)-2-oxoethyl)amino)methyl) isonicotinic acid)	6/2/15	1.9	[274]
5A3W	Crystal structure of human PLU-1 (JARID1B) in complex with pyridine-2, 6-dicarboxylic acid (PDCA)	6/3/15	2	[274]
5FPL	Crystal structure of human JARID1B in complex with CCT363901	12/2/15	2.35	
5FPU	Crystal structure of human JARID1B in complex with GSKJ1	12/3/15	2.24	[274]
5FUN	Crystal structure of human JARID1B in complex with GSK467	1/28/16	2.3	[274]
5FUP	Crystal structure of human JARID1B in complex with 2-oxoglutarate	1/28/16	2.15	[274]
5FV3	Crystal structure of human JARID1B construct c2 in complex with N- oxalylglycine	2/2/16	2.37	[274]
5FYT	Crystal structure of the catalytic domain of human JARID1B in complex with 3D fragment (5-fluoro-2-oxo-2,3-dihydro-1H-indol-3-yl)acetic acid (N09996a)	3/9/16	1.87	
5FYU	Crystal structure of the catalytic domain of human JARID1B in complex with 3D fragment 3-amino-4-methyl-1,3-dihydro-2H-indol-2-one (N10042a)	3/9/16	2.06	
5FYY	Crystal structure of the catalytic domain of human JARID1B in complex with N05798a	3/10/16	2.18	
5FYZ	Crystal structure of the catalytic domain of human JARID1B in complex with 3D fragment 2-(2-oxo-2,3-dihydro-1H-indol-3-yl)acetonitrile (N10063a)	3/10/16	1.75	
5FZ0	Crystal structure of the catalytic domain of human JARID1B in complex with N11213a	3/10/16	2.42	
5FZ1	Crystal structure of the catalytic domain of human JARID1B in complex with Maybridge fragment 2,4-dichloro-N-pyridin-3-ylbenzamide (E48115b) (ligand modeled based on PANDDA event map)	3/10/16	2.39	
5FZ3	Crystal structure of the catalytic domain of human JARID1B in complex with Maybridge fragment 3,6-Dihydroxybenzonorbornane (N08776b) (ligand modelled based on PANDDA event map)	3/10/16	2.5	
5FZ4	Crystal structure of the catalytic domain of human JARID1B in complex with 3D fragment (3R)-1-[(3-phenyl-1,2,4-oxadiazol-5-yl)methyl]pyrrolidin-3-ol (N10057a) (ligand modelled based on PANDDA event map, SGC - Diamond I04-1 fragment screening)	3/10/16	2.07	

5FZ6	Crystal structure of the catalytic domain of human JARID1B in complex with Maybridge fragment N05859b (ligand modelled based on PANDDA event map, SGC - Diamond I04-1 fragment screening)	3/11/16	2.33	
5FZ7	Crystal structure of the catalytic domain of human JARID1B in complex with Maybridge fragment ethyl 2-amino-4-thiophen-2-ylthiophene-3- carboxylate (N06131b) (ligand modelled based on PANDDA event map, SGC - Diamond I04-1 fragment screening)	3/11/16	2.3	
5FZ9	Crystal structure of the catalytic domain of human JARID1B in complex with Maybridge fragment thieno(3,2-b)thiophene-5-carboxylic acid (N06263b) (ligand modelled based on PANDDA event map, SGC - Diamond I04-1 fragment screening)	3/12/16	2.06	
5FZA	Crystal structure of the catalytic domain of human JARID1B in complex with 3D fragment 2-piperidin-4-yloxy-5-(trifluoromethyl)pyridine (N10072a) (ligand modelled based on PANDDA event map)	3/12/16	2.1	
5FZB	Crystal structure of the catalytic domain of human JARID1B in complex with Maybridge fragment 4-Pyridylthiourea (N06275b) (ligand modelled based on PANDDA event map, SGC - Diamond I04-1 fragment screening)	3/12/16	2.18	
5FZC	Crystal structure of the catalytic domain of human JARID1B in complex with Maybridge fragment 4,5-dihydronaphtho(1,2-b)thiophene-2- carboxylicacid (N11181a) (ligand modelled based on PANDDA event map, SGC - Diamond I04-1 fragment screening)	3/14/16	2.05	
5FZH	Crystal structure of the catalytic domain of human JARID1B in complex with Maybridge fragment 4,5-dihydronaphtho(1,2-b)thiophene-2- carboxylicacid (N11181a) (ligand modelled based on PANDDA event map, SGC - Diamond I04-1 fragment screening)	3/14/16	2.09	
5FZK	Crystal structure of the catalytic domain of human JARID1B in complex with 3D fragment N,3-dimethyl-N-(pyridin-3-ylmethyl)-1,2-oxazole-5- carboxamide (N10051a) (ligand modelled based on PANDDA event map, SGC - Diamond I04-1 fragment screening)	3/14/16	2.05	
5FZL	Crystal structure of the catalytic domain of human JARID1B in complex with 3D fragment 3-methyl-N-pyridin-4-yl-1,2-oxazole-5-carboxamide (N09954a) (ligand modelled based on PANDDA event map, SGC - Diamond I04-1 fragment screening)	3/14/16	2.55	
KDM5C				
2JRZ	Solution structure of the Bright/ARID domain from the human JARID1C protein	07/10/2007		[329]
5FWJ	Crystal structure of human JARID1C in complex with KDM5-C49	2/17/16	2.1	[274]
KDM5D				
2E6R	Solution structure of the PHD domain in SmcY protein	07/03/2007		
2YQE	Solution structure of the ARID domain of JARID1D protein	04/01/2008		

Recently, crystal structures of truncated KDM5A, KDM5B, and KDM5C proteins have been determined [54, 274, 282, 283]. In truncated KDM5 proteins, the ARID and PHD1 domains between JmjN and JmjC are dispensable to activity, while the C5HC2 zinc finger motif is required for its *in vivo* [284] and *in vitro* activity [54, 274]. The active KDM5A and KDM5B structures showed that the domain arrangement of this KDM family most closely resembles that of KDM6, despite the fact that the catalytic domain shares the greatest sequence identity with the KDM4 family (33%). The fold of the catalytic JmjC domain is highly conserved with that of KDM6A (PDB ID 3AVS; r.m.s. deviation = 0.46 Å over 107 Cα) and other JmjC demethylases, despite the fact that this region retains only 16% sequence identity with KDM6A. There is a C-terminal helical domain composed of four helices, and a zinc finger C5HC2 motif was found, similar to the GATA-like motif in the KDM6 family (see below).

KDM5 family enzymes have been studied in several types of cancer and cancer processes (for reviews, please see [278, 279]). KDM5A and KDM5B are reported to be amplified or overexpressed in many cancers, and have been shown to play key roles in cancer cell proliferation, drug resistance and metastasis. KDM5A is amplified or over-expressed in several cancers including breast [285], lung [286, 287], hepatocellular [288], and gastric [289, 290] cancers. It is linked to proliferation and senescence control by antagonizing the functions of retinoblastoma protein (pRB) [291–293] and suppressing the expression of cyclin-dependent kinase inhibitor genes such as *p21*, *p27*, and *p16* [286, 288, 289]. In three different genetically-engineered mouse tumor models, knockout of KDM5A significantly prolonged survival [293, 294]. KDM5A has also been shown to play a role in epithelial-mesenchymal transition [287, 295], invasion [286, 294], and metastasis [294, 296]. Additionally, expression of KDM5A is implicated in anti-cancer drug resistance in lung cancer [297], breast cancer [285], and glioblastoma [298].

KDM5B is reported to be overexpressed in breast [284, 299], lung [300], bladder [301], diffuse large B-cell lymphoma [302], prostate [303], colorectal [304], glioma [305], ovarian [306], and hepatocellular [307, 308] cancers. KDM5B has been shown to repress expression of tumor suppressor genes such as *BRCA1* and *HOXA5*, as well as cell cycle checkpoint genes such as *p15*, *p27*, and *p21* [284, 305, 307, 309]. Furthermore, KDM5B expression is linked to stem cell-like properties and resistance to a targeted therapy in melanoma [310, 311]. Many recent studies link expression of KDM5B to poor prognosis, chemoresistance, and metastasis in a variety of cancers [306, 308, 312–315].

Several studies indicate that KDM5 enzymes may have tumor suppressive functions in particular contexts. Breast cancer patients with high expression of KDM5A had a better response to docetaxel [184]. Migration and invasion are suppressed in triple negative breast cancer cells when KDM5B is artificially overexpressed [316]. Finally, KDM5C and KDM5D are inactivated or deleted in renal cell carcinoma [317] and prostate cancer [318], respectively. KDM5C knockdown significantly increased growth of renal cell carcinoma cells in a xenograft model [319].

8.1 KDM5 Active Site

Modeling places a trimethylated lysine residue in the active site of KDM5A, surrounded on four sides by Trp470, Tyr472, Asn585, and the metal-ligand water molecule. The aromatic indole ring of Trp470 would be in parallel with the hydrophobic portion of the target lysine. The side chains of Tyr472 and Asn585 would each coordinate one methyl group, whereas the third methyl group would be in close proximity to a metal ligand-coordinated water molecule. During the catalytic cycle, this site would be occupied by the dioxygen O_2 molecule that initiates the demethylation reaction by abstracting a hydrogen atom from the substrate.

8.2 KDM5 Helper Domains

The ARID domain binds double-stranded DNA and may be involved in anchoring KDM5 proteins onto linear or nucleosome-wrapped nucleic acid [303, 320, 321]. In the KDM5A structure containing an ARID domain [283], the domain adopts the canonical fold but differs slightly in its loop conformations compared to the NMR structure of the isolated KDM5A ARID domain [320] and may block part of the substrate binding site, suggesting that ARID-PHD1 may interfere with substrate binding until interaction with nucleosome.

The PHD1 domains of both KDM5A and KDM5B have been shown to bind to unmodified H3K4me0 [316, 322–324], whereas both of their PHD3 domains have been shown to bind to H3K4me3 [316, 325]. Though KDM5B's PHD3 domain favors binding to H3K4me3, it will also bind to lower methylation states of H3K4 [316, 325]. The PHD2 domain of KDM5B apparently does not recognize histone [316]. Of note, binding of the PHD1 domain of KDM5D to H3K4me0 is ~30X weaker than that of KDM5B, even though their sequences are very similar. This is likely because the Leu326 residue in the KDM5B sequence is replaced by a phenylalanine in KDM5D, where this bulky side chain may cause steric hindrance and obstruct this interaction with a peptide [316]. The binding of these PHD domains to both the substrate and the product of KDM5 demethylases may seem unusual. Yet, binding of PHD1 to H3K4me0 may provide an anchoring mechanism for KDM5A/B to sense H3K4me3 through PHD3 and slide along the H3K4me3-enriched promoters, demethylating other nearby methylated H3K4 and further spreading the transcriptionally inactive state of chromatin. Interestingly, such a model was proposed in one of the first papers to identify that a KDM5 family member is capable of erasing methyl groups of trimethylated H3K4 [326].

As mentioned above, the C5HC2 zinc finger motif is required for activity. In KDM6A, the interaction of a similar zinc finger domain with the KDM6 JmjC domain is required for activity, and in a KDM6A crystal structure with peptide, the zinc finger domain undergoes rearrangement and aids in recognition of a portion of histone H3 around the substrate H3K27 [327]. A future structure of a KDM5 demethylase with peptide may reveal something similar.

8.3 KDM5 in Multicomponent Complexes

KDM5A interacts with the Sin3B/HDAC complex, and KDM5A and Sin3B/HDAC cooperate in transcriptional repression of a subset of E2F4 target genes through deacetylation, demethylation, and nucleosome repositioning [328]. Similarly, KDM5B copurifies and colocalizes with components of the NuRD complex, indicating that KDM5B and NuRD may cooperate in transcriptional repression [316]. The NuRD complex contains two catalytic subunits, the deacetylase HDAC1 and the CHD4 ATPase, both of which are essential for the regulation of gene expression and chromatin remodeling.

9 The KDM6 Family

This KDM family contains three human demethylases (Fig. 7). KDM6A consists of 1401 amino acids and contains a JmjC catalytic domain and 6 tetratricopeptide repeat (TPR) protein-protein interaction domains [41, 330]. KDM6B consists of 1679 amino acids, but it does not appear to contain any characterized domains other than the JmjC domain [331]; however, sequence analysis suggests that it

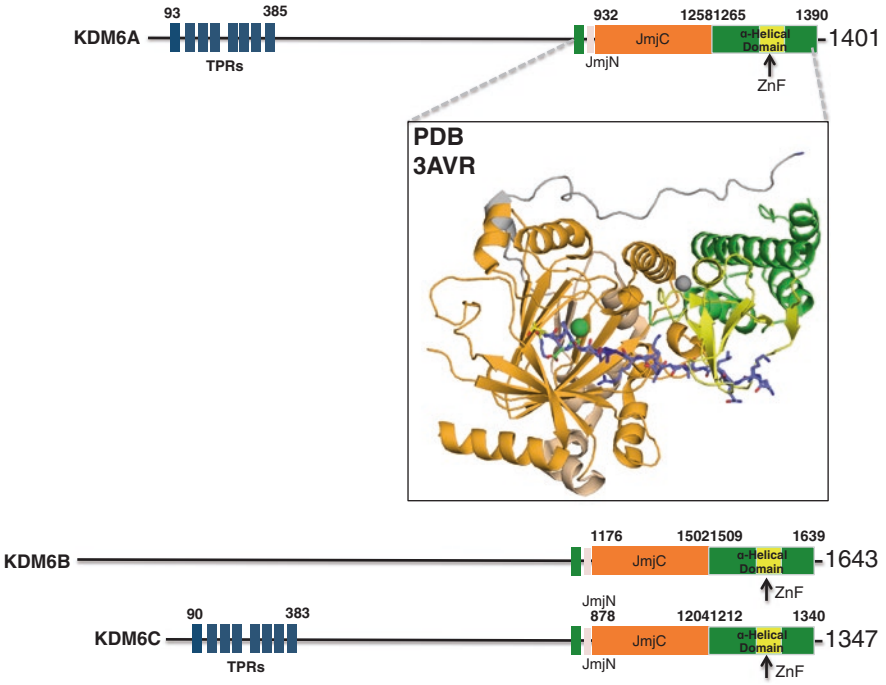

Fig. 7 Representative crystal and domain structures of KDM6 family

may also contain similar TPR domains as KDM6A. These two enzymes have 84% sequence similarity in the JmjC domain [330]. KDM6C consists of 1347 amino acids [332] and shares 83% amino acid identity with KDM6A throughout its sequence [333]. It was once thought to be enzymatically inactive [330, 334], but minimal demethylase activity was later demonstrated and appears to be due to a subtle sequence divergence in the JmjC catalytic domain [332]. KDM6C is located on the Y chromosome and partially compensates for some KDM6A functions, some which may be demethylase-independent, as it was demonstrated using knockout mouse models [335]. KDM6C may activate transcription in a gene-specific manner, as there has been no observation of a decrease in global levels of H3K27me3 upon overexpression of KDM6C in HEK 293 T cells. It is thought that this demethylase may be required in male sex determination during development [332].

KDM6 family members have both pro- and anti-oncogenic roles in cancer, depending on the cell type (reviewed in [336–338]). KDM6A is often classified as a tumor suppressor. Inactivating mutations have been reported in medulloblastoma [339], bladder cancer [340, 341], T-cell acute lymphoblastic leukemia (T-ALL) [342, 343], acute lymphoblastic leukemia [344], renal cell carcinoma [317], chronic myeloamonocytic leukemia [345], and in many other solid and non-solid tumors [346]. Its expression was necessary and sufficient to arrest the cell cycle in human fibroblasts by targeting genes encoding Rb-binding proteins, and depleting KDM6A increased proliferation [347]. Re-expression of KDM6A in KDM6A-null esophageal carcinoma cell lines slowed proliferation [346], and knockdown of KDM6A enhanced *in vitro* and *in vivo* growth of bladder cancer cells [341].

KDM6A knockout in T-ALL cells increased T-ALL kinetics and decreased lifespan of recipient mice. Overexpression of KDM6A in T-ALL cell lines decreased growth and induced apoptosis [343]. Similarly, knockdown of KDM6A boosted development of T-ALL in mice and sensitized cells to treatment with the EZH2 inhibitor 3-DZNep [342]. In the TAL1-positive subgroup of T-ALL, however, KDM6A is oncogenic, and its knockdown attenuated cell growth and induced apoptosis, while overexpression increased cell growth [348].

There are divergent reports of KDM6A's role in breast cancer as well. While one study reports that low KDM6A expression predicts poor survival in breast cancer [347], another reports that high KDM6A expression is associated with poor prognosis in breast cancer [349]. The latter is supported by a study that finds KDM6A is overexpressed in breast cancer and correlated to tumor grade [350]. Additionally, knockdown of KDM6A decreased breast cancer cell proliferation, invasion, and lung colonization [349].

KDM6B can act as a tumor suppressor through interactions with p53 [351, 352] and activation of *p16* [351, 353, 354], promoting senescence after oncogene induction [353, 354] and differentiation of cancer stem cells [351]. In support, KDM6B expression is reduced in several cancer types [353, 355]. KDM6B knockdown decreased p15 expression, with a concurrent increase in proliferation and decrease in apoptosis in colorectal cancer cells, where low expression predicts poor patient prognosis [355].

On the other hand, KDM6B expression is increased in melanoma [356]. Depletion of KMD6B in melanoma boosted self-renewal, trans-endothelial migration, metastasis, angiogenesis, and macrophage recruitment [356]. Similarly, knockdown of KDM6B reduced tumor growth and induced apoptosis in diffuse large B-cell lymphoma cells [357]. In T-ALL, KDM6B was critical for tumor initiation and maintenance through control of NOTCH1 target genes like *HEY1, HES1*, and *NRARP* [343]. Treatment with the pan-KDM6/5 inhibitor GSK-J4 [358] has anti-tumor effects on K27 M H3.3 mutants in brainstem gliomas [359], ovarian cancer cells [360], T-ALL cells [343], and TAL1-positive T-ALL patient derived xenografts [348]. KDM6C may play a role in prostate cancer tumorigenesis [361, 362], but its roles have yet to be fully elucidated.

9.1 KDM6 Helper Domains

A domain lies C-terminal to the JmjC domain of KDM6 demethylases that contains a four α-helix bundle which is bisected between the third and fourth helices by a Zn^{2+}-coordinated GATA-like domain of novel topology [363] containing four conserved cysteine residues that coordinate a zinc ion to stabilize the structure. The JmjC and GATA-like zinc-binding domains in KDM6 proteins pack against each other with a large buried surface area (~4000 $Å^2$). This zinc-binding domain is required for optimal stability and the catalytic competence of the truncated KDM6 proteins observed in crystal structures.

Of note, this zinc-binding domain is involved in recognizing an N-terminal portion (H3A17 to H3T22) of the histone H3 target site [327] (Table 7). The zinc-binding domain undergoes a significant conformational change upon binding to the N-terminal portion of histone H3, and this change exposes a hydrophobic patch composed of His1320, His1329, Leu1342, and Val1356 by displacing Tyr1354, which was masking this hydrophobic patch. Among the residues in the N-terminal portion of histone H3, H3A17 and H3L20 exhibit extensive interactions with this hydrophobic patch. Because H3L20 is found only in the context of the H3K27 target, the zinc-binding domain is likely to serve as a substrate determinant for KDM6A. Thus, KDM6A recognizes a relatively large portion of histone H3 with two domains and this contributes to the highly specific activity of KDM6A toward H3K27.

It is noted here that possible “cross-talk” can exist between different epigenetic marks on a histone molecule. Histone H3A17 and H3A26 can be methylated by CARM1/PRMT4, and the zinc-binding domain and the JmjC domain of KDM6A interact with Arg17 and Arg26, respectively. Because KDM6A tightly holds the charged side chains of the histone H3A17 and H3A26 residues, methylation of Arg17 and Arg26 would decrease or block H3 peptide binding and subsequent KDM6A demethylase activity.

Table 7 Structures containing domains of KDM6

PDB ID	Structure title	Dep. date	Resolution (Å)	Reference
KDM6A				
3AVR	Catalytic fragment of UTX/KDM6A bound with histone H3K27me3 peptide, N-oxyalylglycine, and Ni(II)	3/7/11	1.8	[327]
3AVS	Catalytic fragment of UTX/KDM6A bound with N-oxyalylglycine, and Ni(II)	3/7/11	1.85	[327]
KDM6B				
2XUE	Crystal structure of JMJD3	10/19/10	2	[358]
2XXZ	Crystal structure of the human JMJD3 Jumonji domain	11/12/10	1.8	
4ASK	Crystal structure of JMJD3 with GSK-J1	5/1/12	1.86	[358]
4EYU	The free structure of the mouse C-terminal domain of KDM6B	5/1/12	2.3	[358]
4EZ4	Free KDM6B structure	5/2/12	2.99	[358]
4EZH	The crystal structure of KDM6B bound with H3K27me3 peptide	5/2/12	2.52	[358]
5FP3	Cell penetrant inhibitors of the JMJD2 (KDM4) and JARID1 (KDM5) families of histone lysine demethylases	11/27/15	2.05	[277]
KDM6C				
3ZLI	Crystal structure of JmjC domain of human histone demethylase UTY	1/31/13	1.8	[332]
3ZPO	Crystal structure of JmjC domain of human histone demethylase UTY with bound GSK J1	2/28/13	2	[332]

9.2 KDM6 in Multicomponent Complexes

Protein-protein interaction residues in KDM6 demethylases have not been identified, although the TPR repeats are suspected. Similar to the H3K9me3 epigenetic mark, H3K27me3 is tightly associated with inactive gene promoters and acts in opposition to H3K4me3. Like KDM4A-C, KDM6A and B are part of the MLL2 complex [364, 365] and appear to be involved in differentiation, development, and disease [338, 342, 366, 367].

10 The KDM7 Family

The KDM7 family consists of three members (Fig. 8). Each member harbors two domains in its respective N-terminal half: a PHD domain that binds H3K4me3 and a JmjC domain that demethylates H3K27me2/1 via KDM7A, H3K9me2/1 and H4K20me1 via KDM7B, and H3K9me1 via KDM7C [44, 368]. However, KDM7C

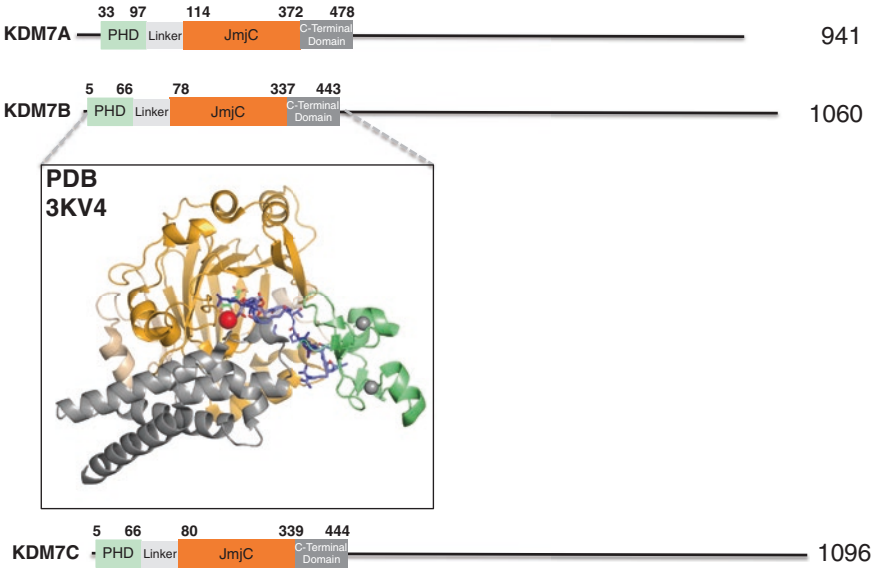

Fig. 8 Representative crystal and domain structures of KDM7 family

activity has not been observed *in vitro* [369]. However, *in vivo*, KDM7C becomes active through a protein kinase A (PKA)-dependent histone lysine demethylase complex, PHF2–ARID5B [370, 371]. KDM7 family members have been implicated as both oncogenic and tumor suppressive. KDM7A expression was upregulated by nutrient starvation, and under those conditions its expression suppressed xenograft tumor growth by restraining angiogenesis [372].

KDM7B is overexpressed in prostate cancer [216, 373], breast cancer [374], laryngeal and hypopharyngeal cancer [375], non-small cell lung cancer [376], and esophageal cancer [377]. It was shown to target and promote expression of oncomiRs miR-21 [376] and miR-125b [373]. Knockdown of KDM7B in cancer cells attenuates growth [216, 373, 376, 377] as well as migration/invasion [216, 377], and induces apoptosis [216, 373, 376]. In contrast, KDM7B expression and activity is critical for response to all-*trans* retinoic acid treatment by acute promyelocytic leukemia cells [378].

KDM7C expression is increased in esophageal squamous cell carcinoma and associated with poor overall survival [379]. However, most studies point to a tumor suppressor function for KDM7C in cancer. It is deleted and/or downregulated in breast cancer [380], head and neck squamous cell carcinoma [381], as well as colon and stomach cancers [382]. KDM7C was shown to associate with p53, and knockdown of KDM7C in p53 competent cells led to decreased sensitivity to genotoxic drugs, as well as reduced drug-induced expression of p21 [382]. Finally, KDM7C was shown to be necessary for treatment-induced mesenchymal to epithelial transition (MET) in breast cancer cells, which led to loss of their tumor initiating ability [383].

10.1 KDM7 Active Site

In the structure of KDM7B with histone peptide, the target H3K9me2 lies in the active site right next to the Fe^{2+} and the 2OG inactive analog N-oxalylglycine (NOG) [44] (Table 8). One of its terminal N-CH_3 groups projects toward the aromatic ring of Tyr234, and the other methyl group points toward Asp249 and Asn333, forming two hydrogen bonds of C–H•••O type. The dimethylated terminal nitrogen atom carrying the lone pair of electrons forms a hydrogen bond with one of the oxygen atoms of NOG. The active site cannot accommodate a trimethylated lysine because the third methyl group would cause repulsive tension with NOG. Phe279 makes van der Waals contacts with Ile248 and Ile318, forming a hydrophobic core supporting the backbone of Fe^{2+}-coordinating residues His247, Asp249, and His319. Substitution of Phe279 to serine is associated with inherited X-linked mental retardation [384–387].

In *C. elegans* KDM7A, NOG is stabilized by residues Asn421, Thr492, and Tyr505 [388]. The methylated side chain of H3K9me2 (or H3K27me2) is checked by Phe482 and Phe498 through hydrophobic interactions. One of the methyl groups of dimethylated lysine interacts with the side chains of Asp497 and Asn581 through two C–H•••O hydrogen bonds.

KDM7C appears to be an inactive demethylase. The metal binding site in KDM7C closely resembles the Fe^{2+} sites in other JmjC domains [369]. However, KDM7C contains a tyrosine (Tyr321) in the place of the fifth ligand, and the longer side chain of Tyr321 makes the Fe^{2+} move away from the corresponding binding site in KDM7B, an active demethylase. The small movement of the ferrous iron, induced by the presence of Tyr321, could position the reactive oxygen in a non-reactive mode.

10.2 KDM7 Helper Domains

KDM7A/B structures provided one of the first examples of how helper domains can both upregulate and/or downregulate JmjC demethylase activity through contributions associated with steric effects. The presence of H3K4me3 on the same peptide as H3K9me2 makes the doubly methylated peptide a significantly better substrate of KDM7B, resulting in a 12-fold increase in enzymatic activity as revealed by activity assays [44, 389–391]. By contrast, the presence of H3K4me3 diminishes the H3K9me2 demethylase activity of KDM7A with no adverse effect on its H3K27me2 activity, because the distance between the H3K4me3 and H3K27me2 marks is long enough for occupation of the PHD and JmjC domain pockets simultaneously [44, 388]. Differences in substrate specificity between the two enzymes are explained by a bent conformation of KDM7B, allowing each of its domains to engage their respective targets, and an extended conformation of KDM7A, which prevents its JmjC domain from accessing H3K9me2 when its PHD domain engages H3K4me3. Thus, the structural linkage between the PHD domain binding to H3K4me3 and the placement of the catalytic JmjC domains relative to this ‘on’ H3K4me3 epigenetic mark determine which repressive marks are removed by both

Table 8 Structures containing domains of KDM7

PDB ID	Structure title	Dep. date	Resolution (Å)	Reference
KDM7A				
3KV5	Structure of KIAA1718, human Jumonji demethylase, in complex with N-oxalylglycine	11/29/09	2.39	[44]
3KV6	Structure of KIAA1718, human Jumonji demethylase, in complex with alpha-ketoglutarate	11/29/09	2.89	[44]
3KV9	Structure of KIAA1718 Jumonji domain	11/29/09	2.29	[44]
3KVA	Structure of KIAA1718 Jumonji domain in complex with alpha-ketoglutarate	11/29/09	2.79	[44]
3KVB	Structure of KIAA1718 Jumonji domain in complex with N-oxalylglycine	11/29/09	2.69	[44]
3N9L	ceKDM7A from C.elegans, complex with H3K4me3 peptide and NOG	05/31/10	2.80	[388]
3N9M	ceKDM7A from C.elegans, alone	05/31/10	2.49	[388]
3N9N	ceKDM7A from C.elegans, complex with H3K4me3K9me2 peptide and NOG	05/31/10	2.30	[388]
3N9O	ceKDM7A from C.elegans, complex with H3K4me3 peptide, H3K9me2 peptide and NOG	05/31/10	2.31	[388]
3N9P	ceKDM7A from C.elegans, complex with H3K4me3K27me2 peptide and NOG	05/31/10	2.39	[388]
3N9Q	ceKDM7A from C.elegans, complex with H3K4me3 peptide, H3K27me2 peptide and NOG	05/31/10	2.30	[388]
3PUQ	CEKDM7A from C.Elegans, complex with alpha-KG	12/06/10	2.25	[395]
3PUR	CEKDM7A from C.Elegans, complex with D-2-HG	12/06/10	2.10	[395]
3U78	E67-2 selectively inhibits KIAA1718, a human histone H3 lysine 9 Jumonji demethylase	10/13/11	2.69	[396]

1WEP	Solution structure of PHD domain in PHF8	05/25/04		
3K3N	Crystal structure of the catalytic core domain of human PHF8	10/03/09	2.40	[397]
3K3O	Crystal structure of the catalytic core domain of human PHF8 complexed with alpha-ketoglutarate	10/03/09	2.10	[397]
2WWU	Crystal structure of the catalytic domain of PHD finger protein 8	10/29/09	2.15	[398]
3KV4	Structure of PHF8 in complex with histone H3	11/29/09	2.19	[44]
4DO0	Crystal structure of human PHF8 in complex with daminozide	02/09/12	2.55	
KDM7C				
3KQI	Crystal structure of PHF2 PHD domain complexed with H3K4me3 peptide	11/17/09	1.78	[399]
3PTR	PHF2 Jumonji domain	12/03/10	1.95	[369]
3PU3	PHF2 Jumonji domain-NOG complex	12/03/10	1.95	[369]
3PU8	PHF2 Jumonji-NOG-Fe(II) complex	12/03/10	1.94	[369]
3PUA	PHF2 Jumonji-NOG-Ni(II)	12/03/10	1.89	[369]
3PUS	PHF2 Jumonji-NOG-Ni(II)	12/06/10	2.08	[369]

demethylases. Thus, the KDM7A and KDM7B JmjC domains on their own are promiscuous enzymes; it is the associated PHD domains and linker—a determinant for the relative positioning of the two domains—that are mainly responsible for substrate specificity. It should also be noted that KDM helper domains can affect the orientation of peptide binding: a peptide in complex with a KDM6 demethylase has an opposite orientation across the JmjC domain compared to a peptide in complex with a KDM7 demethylase [44, 327, 388].

A structural study on *C. elegans* KDM7A suggested that the extended conformation between the PHD and Jumonji domains might enable a trans-histone peptide-binding mechanism, in which H3K4me3 associated with the PHD domain and the H3K9me2 bound to the Jumonji domain could be coming from two separate histone H3 molecules of the same nucleosome or two neighboring nucleosomes [388]. However, this trans-binding mechanism can be excluded for human KDM7A because the presence of an H3K4me3 *in trans* or *in cis* with H3K9me2 substrate peptide strongly inhibits KDM7A activity toward H3K9me2 [44]. Nevertheless, the trans-binding mechanism is an attractive model for KDM7B if the flexible loop between the PHD and JmjC enables the enzyme to adopt an extended conformation to allow binding of two peptides simultaneously. The trans-binding mechanism could explain the finding that KDM7B also functions *in vivo* as an H4K20me1 demethylase while its PHD domain interacts with H3K4me3/me2 in the context of nucleosome [392, 393]. However, if this were the case, an explanation would be needed as to why KDM7B is only active on monomethylated H4K20, whereas it is active on mono- and dimethylated H3K9 and H3K27. One possibility is that only H4K20me1 co-exists with H3K4me3/me2 *in vivo*.

10.3 KDM7 in Multicomponent Complexes

The C-terminal halves show little homology among the family members and do not contain any known domains. Nonetheless, C-terminal parts of members are essential for their gene regulatory functions. For example, it was found that KDM7B binds to RNA polymerase I/II, KMT2, HCF1, E2F1, ZNF711 and RAR, under the control of the C-terminal portion of KDM7B [389, 390, 392, 394]. In addition, KDM7C is associated with p53 through its C-terminal region [382]. It appears probable that the variability of the C-terminal halves of KDM7 members provides functional diversity by choosing different histone demethylase partners for transcription.

11 Molecular Basis of KDM Inhibition and Development of Inhibitors into Drugs

At present, current epigenetic therapies primarily involve inhibitors of DNA demethylation and histone deacetylation [400]. Considering the significant implication of KDMs in the development of various diseases, a thorough understanding of their

molecular mechanism and effective therapeutic inhibition is of considerable interest, but at its infancy. Further characterization of many demethylases is proceeding through both functional studies and the development of small molecule inhibitors targeted against them. These studies will be invaluable for our understanding and treatment of cancer. There are two possible ways by which a demethylase-inhibiting drug may be able to halt or even prevent cancers. It can repress oncogenes and/or activate tumor-suppressor genes that are deregulated by methylation processes [401, 402] or overcome resistance to chemotherapy [283, 403, 404]. Transient and reversible drug resistance develops in certain cancer cell populations during treatment with cancer drugs. KDM5A is as at least one chromatin-modifying enzyme required for establishing a drug-tolerant subpopulation [297]. Reduced methylation of H3K4 has also been linked to poor prognosis in cancer patients [405].

The many crystal structures of demethylases have revealed substantially conserved Fe^{2+} and 2OG binding sites; yet, differences in Fe^{2+} and 2OG binding sites are idiosyncratic to each KDM family and may be able to be exploited for the development of selective inhibitors. For instance, N198 in KDM4A and N1156 in KDM6A establish a hydrogen bond at the back of the pocket with the carboxylic moiety of 2OG, while in KDM2A and KDM7 family members, the asparagine is replaced by a tyrosine that causes a different Fe^{2+} coordination of the carboxylic moiety of the cofactor and a loss of the hydrogen bond. In a KDM4A-inhibitor structure [263], a π-π stacking interaction with F185 at the front part of the pocket can be observed; this phenylalanine is only conserved within the KDM4 and KDM5 families [406]. KDM2A/6A/7 show a threonine at this location that would prohibit a π-ring system at this position. Another example is the invariant cysteine in the active site of the KDM5 family (Cys-481 in KDM5A), which spatially replaces residues in other KDMs (i.e. Pro-1388 of KDM6B). Exploring the interaction between this noncatalytic cysteine and studied inhibitors could provide an avenue for improved potency, selectivity, and prolonged on-target residence times of inhibitors specific for the KDM5 family. For example, an approach of using reversible covalent inhibitors that target noncatalytic cysteine residues to achieve prolonged and tunable residence time has recently been demonstrated with protein kinases [407]. Both reversible [408] and irreversible inhibitors [122, 123, 409, 410] have been made against KDM1A, and some of these inhibitors have entered into clinical trials as drugs for cancers such as acute myeloid leukemia [411] and small cell lung carcinoma [412, 413].

The pace of inquiry in the KDM inhibitor field is accelerating: the number of papers published and applications for patents in the last several years are a testament to the presupposition that study in this area will lead to great discovery of KDM chemical probes and drug candidates [122, 273, 277, 411, 414–416]. A comprehensive review is beyond the scope of this chapter. A few highlights in this area will be discussed.

11.1 Inhibitors of KDM1 Demethylases

There are many compounds that are KDM1 inhibitors (Fig. 9a). The AOD catalytic domain of KDM1 is homologous to those of the monoamine oxidases (MAOs) A and B and this has facilitated studies for this KDM family. Consequently, several

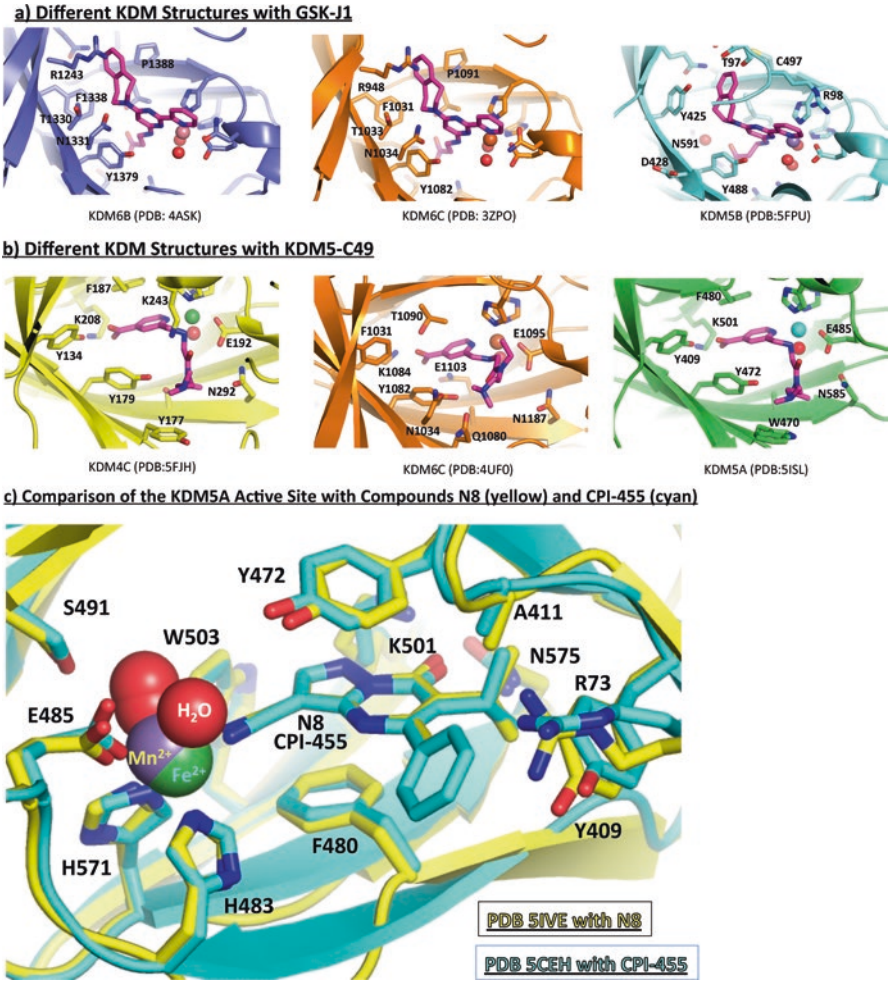

Fig. 9 Crystal structures containing (**a**) GSK-J1, (**b**) KDM5-C49 and (**c**) compounds N8 and CPI-455

well-studied MAO inhibitors, including phenelzine and tranylcypromine (TCP), an FDA-approved treatment for psychological disorders [417], have been demonstrated to also inhibit KDM1A [418, 419]. A mechanism-based irreversible inhibitor, TCP forms a covalent adduct with the FAD cofactor within the active site of the enzyme [94, 126, 419]. The application of TCP as an inhibitor of KDM1A has provided promising proof-of-principle data in mouse models and leukemia cell lines [82, 83]. However, such non-selective amine oxidase inhibitors could obviously have adverse effects and are not ideal solutions for KDM1 inhibitors. Therefore, derivatives of tranylcypromine have been made, and the first structures with enhanced potency and target selectivity for KDM1A were obtained through

modification of the phenyl group of TCP using crystal structures of KDM1A with TCP or a KDM1-selective peptide-based inhibitor [127, 420].

Since KDM1 can specifically recognize the twenty-one amino acids from the N-terminal tail of histone H3, inhibitors containing these twenty-one amino acid long peptides from the histone H3 N-terminal tail with modifications on target lysine have been synthesized; a propargyl-Lys-derivatized peptide functions as a potent and selective time-dependent inactivator of KDM1A [421]. However, even a H3 peptide with methionine replacement for the target lysine appears to be a good inhibitor (K_i = 40 nM) and a structure was determined [95]. Peptides derived from SNAIL1 and INSM1 sequences could also act as KDM1A inhibitors [130]. SNAIL1 is a transcription factor that binds to the KDM1A active site through its SNAG (Snail/GFI) domain with the N-terminal 21 residues adopting a similar conformation to the H3 substrate and acts as a competitive inhibitor. INSM1 (insulinoma-associated protein) is another member of the same family of transcription factors as SNAIL1 and binds to KDM1A with similar affinity. However, crystal structures showed that only the first nine and eight residues of the two transcription factor peptides, respectively, bind in an ordered conformation. Several such small peptides exhibited competitive inhibition and crystal structures of both of these with KDM1A were determined (see Table 2). In addition, novel and potent cyclic peptide inhibitors of KDM1A have been developed [422]; an advantage of cyclic peptides is their significant stability to hydrolysis in plasma.

11.2 Inhibitors of JmjC Demethylases

Many different types of compounds inhibit the JmjC demethylases (Fig. 9b). The majority of JmjC KDM inhibitors identified to date incorporate carboxylic acids/carboxylic acid analogs, leading to use of pro-drug ester forms for sufficient cellular activity. The inhibitors occupy the 2OG binding site and may contain moieties that occupy other potential binding sites such as the region where the methyl-lysine binds. There has been a rapid increase in reports of JmjC KDM inhibitors both in the scientific literature and in patents in the last few years; several excellent reviews and reports of new molecular inhibitor scaffolds have appeared recently [271, 277, 414, 423–426]. However, many of these KDM inhibitors lack the desired selectivity, potency and pharmacokinetic properties (particularly cell permeability) necessary to be considered as probe molecules for the investigation of individual KDM function in cancer or for development as cancer drugs. There are basically three types of JmjC demethylase inhibitors: 2OG mimetics, compounds that target peptide binding sites, and compounds that interfere with the action of helper domains. We discuss select compounds from each category below, as well as some of the challenges associated with their use.

11.3 TCA Cycle Intermediates and 2OG Mimetics

The development of JmjC demethylase inhibitors is likely to pose challenges with respect to reaching sufficient potency, given the intracellular competition by excess cofactor and cofactor-like compounds. Cancer-associated mutations in tricarboxylic acid (TCA) cycle enzymes lead to abnormal accumulation of TCA cycle metabolites that have been linked to oncogenic transformation. These metabolites are themselves inhibitors of KDMs when they exist in a cell at high concentrations. Mutations to these enzymes are common in tumors and can result in very substantial increases in the concentrations of succinate, fumarate, or 2-hydroxyglutarate (2HG) [427–430]. 2HG is a five-carbon dicarboxylic acid with a chiral center at the second carbon atom; therefore, there are two possible enantiomers of 2HG: ((*S/R*)-2HG). Mutations cause isocitrate dehydrogenase (IDH) 1 and 2 to convert 2OG into 2HG, as well as produce 2OG from isocitrate [431]. IDH mutants exclusively produce the (R) enantiomer of 2HG, and the levels of (R)-2HG in IDH mutant tumors can be extremely elevated, ranging from 1 mM to as high as 35 mM [432–434]. Succinate, a co-product of the JmjC demethylase reaction, fumarate, and 2HG all inhibit JmjC demethylases, though rather weakly (in the μM to mM range for KDM2A, KDM4A, KDM4C and KDM5B, as shown with isolated proteins and in cells [266, 395, 435]), via competition with 2OG [254, 436]. A number of KDM4A and KDM6C crystal structures with these compounds have been solved (see Tables 5 and 7).

The 2OG analog NOG has generally been used as an inhibitor for *in vitro* studies [17]. In NOG, the C-3 methylene group of 2OG is replaced with an NH group to give an N-oxalyl amide derivative that likely stalls the catalytic reaction by hindering oxygen binding to the active site iron. NOG has been utilized in many crystallizations of JmjC demethylases, especially those in which peptide is present. Often structures also include a non-catalytic metal ion such as Ni^{2+}, Co^{2+}, or Mg^{2+} as a substitute for Fe^{2+}. Metal chelating compounds such as diols can also inhibit JmjC KDMs at high concentration. For example, the common buffer TRIS inhibits KDM4C with a K_i = 11 mM and a crystal structure with TRIS has been solved with the compound clearly in the active site when the crystal was grown in the absence of 2OG [275].

Analysis of the X-ray crystal structure of KDM4A in complex with NOG and a trimethylated peptide [253] led to the design and synthesis of NOG derivatives substituted with an alkyl-linked dimethylaniline group in order to mimic the interactions of the trimethylated peptide with the protein [437]. These derivatives maintained the inhibitory action of NOG against KDM4A, and illustrate a strategy of linking the 2OG and peptide substrate binding sites to further increase JmjC KDM inhibition.

11.4 Daminozide and Hydroxamic Acid-Based JmjC KDM Inhibitors

Daminozide is selective for the KDM2/7 families over other members of the human JmjC KDMs [KDM2A (IC_{50} = 1.5 μM) and KDM7B (IC_{50} = 0.55 μM)] [268]. Crystallographic studies revealed that daminozide chelates the active site iron via its

dimethylamino nitrogen lone pair and C-4 carbonyl group, with its C-1 carbonyl occupying the same site as the 2OG C-5 carboxylate. This selectivity may be engendered by the more hydrophobic region created by the Tyr257, Val255 and Ile191 residues adjacent to the iron ion in the KDM2/7 families compared to the more hydrophobic residues in the corresponding regions in KDM4A and other JmjC demethylases.

11.5 Pyridine Derivatives

A screen using known inhibitors of other 2OG dependent oxygenases identified 2,4-pyridinedicarboxylic acid (2,4-PDCA), which showed potent inhibitory activity on KDM4E (IC_{50} = 1.4 μM) [262]. The structure of KDM4A (and later other KDMs-see Tables 5 and 6) with bound 2,4-PDCA showed that 2,4-PDCA functions in a 2OG competitive manner. 2,4-PDCA binds the Ni^{2+} cation in a bidentate manner via its N-atom and 2-carboxylate, whereas the 4-carboxylate mimics 2OG binding by forming two hydrogen bonds with a Lys and a Tyr in the active site. Many compounds have a similar binding mechanism; however, the minimal binding requirements in the 2OG site appear to one atom binding to metal and one binding to the Lys residue in JmjC demethylase binding sites [282].

There are two other inhibitors that are pyridine derivatives and have been studied in greater detail, both biochemically and structurally, than other inhibitors amongst several KDM families: GSK-J1/J4 (4) and KDM5-C49/C70. GSK-J4 and KDM5-C70 are cell permeable prodrug ethyl esters that are hydrolyzed by an esterase within the cell to generate GSK-J1 and KDM5-C49, respectively. GSK-J1 is a potent inhibitor of the H3K27 histone demethylases KDM6A and KDM6B with *in vitro* IC_{50} values of 56 and 18 μM, respectively [358]. However, GSK-J1 is a good inhibitor for other KDM families as well, particularly KDM5 [438, 439]. GSK-J1 contains a propanoic acid moiety that mimics 2OG binding, and a pyridyl-pyrimidine biaryl chelates the active site Fe^{2+}, inducing a shift in its position. GSK-J4 is still one of the few inhibitors revealed to have cell activity. GSK-J4 has anticancer effects against acute lymphoblastic leukemia and pediatric brainstem glioma [343, 359], as well as the ability to target ovarian cancer stem cells [360]. GSK-J1 has been crystalized with members of the KDM5 and KDM6 families (Tables 6 and 7).

KDM5-C49/C70 is reported to be a potent and selective inhibitor for the KDM5 family, but is a good inhibitor for the KDM4 and KDM6 families as well [274, 282]. KDM5-C49 is a 2,4-PDCA analog and shows nanomolar inhibitory potencies in enzymatic assays across several JmjC families. KDM5-C70 also lead to cell cycle arrest in a multiple myeloma cells and breast cancer cell lines with an observed increase in global H3K4me3 levels [274, 282].

A pan-inhibitor, JIB-04, was identified in an unbiased cellular screen, and shown to effectively and specifically inhibit several KDM families' activity *in vivo* as well as *in vitro* [440]. Furthermore, JIB-04 could specifically inhibit KDM function in cancer cells, as well as in tumors *in vivo*. JIB-04 is not a competitive inhibitor of 2OG, and the exact molecular mechanism is unclear. There is relative selectivity of

JIB-04 toward KDM5B *versus* KDM5C *in vitro*, which correlated with an increased cellular potency overall *in vivo* and a propensity for cell type specificity not observed with GSK-J4 in one study [54]. High-throughput screening also identified 2,4-PDCA-related 8-hydroxyquinoline compounds as inhibitors of KDM demethylases that were further developed [264, 269, 414]. Natural products such as flavonoids and catechols have been demonstrated to inhibit a number of 2OG oxygenases, including the JmjC KDMs [416, 441].

11.6 A Compound Showing Some Selectivity

Two similar compounds have been crystallized with variant truncated constructs of KDM5A [282, 283]. One compound, CPI-455, is cell permeable while the other, N8, is not. However, both are amongst the most effective KDM5 inhibitors *in vitro* and are more selective for the KDM5 family than other KDM families. The only difference between the two compounds is a substitution of a methyl group in N8 with a phenyl group in CPI-455 (Fig. 9b). Interestingly, the addition of a methyl group to the phenyl group of CPI-455 to produce CPI-4203 makes this inhibitor less cell permeable and an inactive or very weak control for cell assays [283]. Our lack of understanding of how these small changes make compounds less or more cell permeable reflect our present lack of knowledge of the characteristics required to endow compounds with properties for permeability.

The position occupied by these inhibitors (Fig. 10c) completely overlaps the binding site of 2OG, demonstrating a competitive mode of action, as suggested by biochemical assays [282, 283]. The nitrile group of these KDM5 inhibitors makes a single interaction with the active-site metal ion, while a ring nitrogen atom forms a hydrogen bond with the side chain of Lys501. The carbonyl oxygen off the ring is within hydrogen bonding distance to the side chains of Asn575, as well as Lys501. In the KDM5 structure with 2OG, the side chain Asn575 bridges between Lys501 and Tyr409, which form hydrogen bonds with the carboxylic group of 2OG. In contrast to the structure with 2OG, the side chain of Tyr409 is pushed away by the bulky pyrazolopyrimidine ring and is rotated nearly 90° from that of the 2OG-bound form, resulting in a van der Waals contact with the isopropyl substituent on these compounds [54]. In the CPI-455 structure, Tyr409 as well as Arg73 is pushed even further away from the active site because of the phenyl ring substitution of the methyl group in N8. In both structures, the central pyrimidine ring sandwiches between the aromatic rings of Tyr472 and Phe480. The phenyl group in CPI-455 forms an edge-to-face aromatic contact with Tyr409 and points toward solvent.

All amino acids within 4 Å of the inhibitor are conserved in the KDM5 family; hence, N8 and CPI-455 inhibit all KDM5 family members. The selectivity of these compounds for KDM5 versus KDM2, KDM3 and KDM6 proteins derives from conformational and sequence differences within their active sites. For

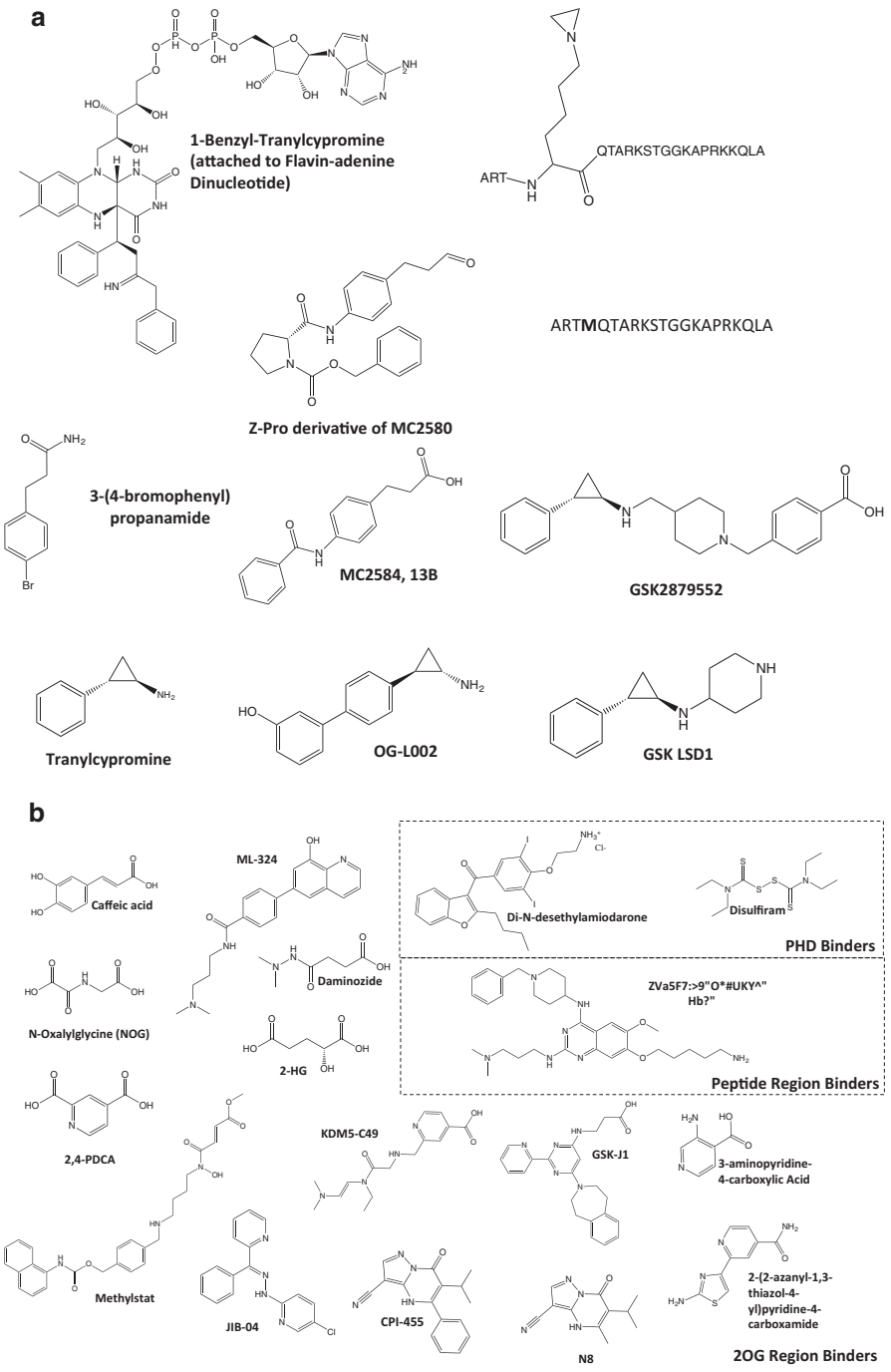

Fig. 10 Representative inhibitors of (**a**) KDM1 family and (**b**) JmjC demethylase families

instance, KDM6B is more constricted in the region flanking the phenyl and isopropyl substituents off the pyrazolopyrimidine ring of these compounds. The scaffold of CPI-455 is being further developed by improving the interactions with the Tyr409 side chain with modifications of both the isopropyl and phenyl groups to improve inhibition of KDM5 demethylases and the cell potency of the compound [442].

11.7 Inhibitors to Substrate Binding Regions

An inhibitor of G9a methyltransferase (BIX-01294) and its analog E67 also inhibited the human H3K9me2 demethylase KDM7A [396]. These compounds act as H3 substrate analogues and therefore, both enzymes can recognize methyl-lysine residues either as product or as substrate. Compound E67 was shown to inhibit KDM7A and KDM7B with IC_{50} values in the low-micromolar range in an *in vitro* mass spectrometric demethylation assay, but was inactive against KDM5C. E67 exhibited cytotoxicity at concentrations around 50 μM against mouse and human primary fibroblasts. A crystal structure confirmed binding of this compound to the active site of the enzyme [396]. A compound that mimics both Lys and 2OG was synthesized which appeared to selectively inhibit KDMs [443]. In addition, its prodrug methylstat selectively inhibited JmjC demethylases in cells and could inhibit cell growth of an esophageal carcinoma cell line.

11.8 Inhibitors to PHD Binding Helper Domains

Helper domains of JmjC KDMs can be tractable targets and provide promising leads for development of inhibitors targeting noncatalytic domains of JmjC KDMs. For instance, small molecule inhibitors targeting the PHD3 domain of KDM5A were identified through application of an assay that uses 96-well polystyrene plates activated with synthetic ligand for covalent and oriented capture of a protein fusion to KDM5A PHD3 which allowed screening for molecules that displaced histone H3K4me3 binding to PHD3 [444]. Screening of the NIH Clinical Collection 1 library identified compounds such as disulfiram, phenothiazine, aminodarone, and tegaserod maleate as inhibitors (Fig. 10a). Disulfiram inhibits KDM5A PHD3 and other PHD fingers not by acting as a ligand, but through ejection of structural zinc, thus revealing a general susceptibility specific to PHD fingers as a histone reader domain. The compounds were further tested through affinity pull-downs, fluorescence polarization, and histone reader specificity studies. Inhibitors based on aminodarone derivatives were identified to be potent against KDM5A-PHD3, with IC50 values in the 25–40 μM range [444].

12 Conclusions

Crystal structures of catalytic domains exist for every human KDM family. Additionally, there is a quickly growing number of structures of these domains with inhibitors containing different chemical moieties in the active site. However, there is a substantial need for developing new types of inhibitors, likely aided by improving our understanding of all of these structures. Because we know that some catalytic domains are inactive when expressed alone, these structures need to be further supplemented by solution studies and greater biochemical analysis of KDM selectivity.

There are still much to learn about these demethylases. For instance, very little is known about large parts of some KDM demethylases, such as the second half of the KDM5 and KDM7 families. Discovery is just beginning on how KDM domains interact with each other and how these domains interact with other proteins in multicomponent complexes. Recent advances in single-particle cryo-electron microscopy (cryo-EM) may aide in this regard [445]. These advances are enabling generation of numerous near-atomic resolution structures for well-ordered protein complexes with sizes ≥200 kDa. Cryo-EM should allow structure determination of the large KDMs with all their domains, complexes with their interacting proteins and nucleosomes as well as information about the dynamic conformational states of these domains and complexes.

Future detailed structural information from both X-ray crystallography and cryo-EM will offer further understanding about the molecular basis of histone demethylation, *i.e.* how demethylases exert their substrate specificities and function in histone regulation. In turn, this will allow better development of inhibitors, which may potentially be utilized as drugs in mankind's battle against various cancers where demethylases play a substantial role.

Acknowledgements The work in the Cheng laboratory is supported by NIH grant GM114306-02; the work in the Yan laboratory is supported by American Cancer Society Research Scholar Grant (RSG-13-384-01-DMC) and DoD Breast Cancer Research Program Award (W81XWH-14-1-0308). National Science Foundation Graduate Research Fellowship (DGE-1122492) supports M.G. in the Yan laboratory. X.C. is a Georgia Research Alliance Eminent Scholar.

References

1. Bannister AJ, Kouzarides T (2004) Histone methylation: recognizing the methyl mark. Methods Enzymol 376:269–288
2. Bedford MT, Richard S (2005) Arginine methylation an emerging regulator of protein function. Mol Cell 18(3):263–272
3. Jenuwein T, Allis CD (2001) Translating the histone code. Science 293(5532):1074–1080
4. Lee CT, Duerre JA (1974) Changes in histone methylase activity of rat brain and liver with ageing. Nature 251(5472):240–242
5. Byvoet P et al (1972) The distribution and turnover of labeled methyl groups in histone fractions of cultured mammalian cells. Arch Biochem Biophys 148(2):558–567

6. Borun TW, Pearson D, Paik WK (1972) Studies of histone methylation during the HeLa S-3 cell cycle. J Biol Chem 247(13):4288–4298
7. Annunziato AT, Eason MB, Perry CA (1995) Relationship between methylation and acetylation of arginine-rich histones in cycling and arrested HeLa cells. Biochemistry 34(9):2916–2924
8. Bannister AJ, Schneider R, Kouzarides T (2002) Histone methylation: dynamic or static? Cell 109(7):801–806
9. Kim S, Benoiton L, Paik WK (1964) Epsilon-alkyllysinase. Purification and properties of the enzyme. J Biol Chem 239:3790–3796
10. Paik WK, Kim S (1973) Enzymatic demethylation of calf thymus histones. Biochem Biophys Res Commun 51(3):781–788
11. Paik WK, Kim S (1974) Epsilon-alkyllysinase. New assay method, purification, and biological significance. Arch Biochem Biophys 165(1):369–378
12. Shi Y et al (2004) Histone demethylation mediated by the nuclear amine oxidase homolog LSD1. Cell 119(7):941–953
13. Shi Y, Whetstine JR (2007) Dynamic regulation of histone lysine methylation by demethylases. Mol Cell 25(1):1–14
14. Trewick SC, McLaughlin PJ, Allshire RC (2005) Methylation: lost in hydroxylation? EMBO Rep 6(4):315–320
15. Tsukada Y et al (2006) Histone demethylation by a family of JmjC domain-containing proteins. Nature 439(7078):811–816
16. Whetstine JR et al (2006) Reversal of histone lysine trimethylation by the JMJD2 family of histone demethylases. Cell 125(3):467–481
17. Cloos PA et al (2006) The putative oncogene GASC1 demethylates tri- and dimethylated lysine 9 on histone H3. Nature 442(7100):307–311
18. Fodor BD et al (2006) Jmjd2b antagonizes H3K9 trimethylation at pericentric heterochromatin in mammalian cells. Genes Dev 20(12):1557–1562
19. Klose RJ et al (2006) The transcriptional repressor JHDM3A demethylates trimethyl histone H3 lysine 9 and lysine 36. Nature 442(7100):312–316
20. Chen Z et al (2006) Structural insights into histone demethylation by JMJD2 family members. Cell 125(4):691–702
21. Di Lorenzo A, Bedford MT (2011) Histone arginine methylation. FEBS Lett 585(13):2024–2031
22. Chang B et al (2007) JMJD6 is a histone arginine demethylase. Science 318(5849):444–447
23. Webby CJ et al (2009) Jmjd6 catalyses lysyl-hydroxylation of U2AF65, a protein associated with RNA splicing. Science 325(5936):90–93
24. Unoki M et al (2013) Lysyl 5-hydroxylation, a novel histone modification, by Jumonji domain containing 6 (JMJD6). J Biol Chem 288(9):6053–6062
25. Bottger A et al (2015) The oxygenase Jmjd6 – a case study in conflicting assignments. Biochem J 468(2):191–202
26. Mantri M et al (2010) Crystal structure of the 2-oxoglutarate- and Fe(II)-dependent lysyl hydroxylase JMJD6. J Mol Biol 401(2):211–222
27. Hong X et al (2010) Interaction of JMJD6 with single-stranded RNA. Proc Natl Acad Sci U S A 107(33):14568–14572
28. Walport LJ et al (2016) Arginine demethylation is catalysed by a subset of JmjC histone lysine demethylases. Nat Commun 7:11974
29. Thompson PR, Fast W (2006) Histone citrullination by protein arginine deiminase: is arginine methylation a green light or a roadblock? ACS Chem Biol 1(7):433–441
30. Hidaka Y, Hagiwara T, Yamada M (2005) Methylation of the guanidino group of arginine residues prevents citrullination by peptidylarginine deiminase IV. FEBS Lett 579(19):4088–4092
31. Raijmakers R et al (2007) Methylation of arginine residues interferes with citrullination by peptidylarginine deiminases in vitro. J Mol Biol 367(4):1118–1129
32. Cuthbert GL et al (2004) Histone deimination antagonizes arginine methylation. Cell 118(5):545–553
33. Musselman CA, Kutateladze TG (2011) Handpicking epigenetic marks with PHD fingers. Nucleic Acids Res 39(21):9061–9071

34. Pek JW, Anand A, Kai T (2012) Tudor domain proteins in development. Development 139(13):2255–2266
35. Lu R, Wang GG (2013) Tudor: a versatile family of histone methylation 'readers'. Trends Biochem Sci 38(11):546–555
36. Laity JH, Lee BM, Wright PE (2001) Zinc finger proteins: new insights into structural and functional diversity. Curr Opin Struct Biol 11(1):39–46
37. Klug A (2010) The discovery of zinc fingers and their applications in gene regulation and genome manipulation. Annu Rev Biochem 79:213–231
38. Gamsjaeger R et al (2007) Sticky fingers: zinc-fingers as protein-recognition motifs. Trends Biochem Sci 32(2):63–70
39. Wang Z et al (2014) Roles of F-box proteins in cancer. Nat Rev Cancer 14(4):233–247
40. Wilsker D et al (2002) ARID proteins: a diverse family of DNA binding proteins implicated in the control of cell growth, differentiation, and development. Cell Growth Differ 13(3):95–106
41. Blatch GL, Lassle M (1999) The tetratricopeptide repeat: a structural motif mediating protein-protein interactions. BioEssays 21(11):932–939
42. Ng A, Xavier RJ (2011) Leucine-rich repeat (LRR) proteins: integrators of pattern recognition and signaling in immunity. Autophagy 7(9):1082–1084
43. Ng AC et al (2011) Human leucine-rich repeat proteins: a genome-wide bioinformatic categorization and functional analysis in innate immunity. Proc Natl Acad Sci U S A 108(Suppl 1):4631–4638
44. Horton JR et al (2010) Enzymatic and structural insights for substrate specificity of a family of Jumonji histone lysine demethylases. Nat Struct Mol Biol 17(1):38–43
45. Stavropoulos P, Blobel G, Hoelz A (2006) Crystal structure and mechanism of human lysine-specific demethylase-1. Nat Struct Mol Biol 13(7):626–632
46. Chen F et al (2013) Structural insight into substrate recognition by histone demethylase LSD2/KDM1b. Cell Res 23(2):306–309
47. Fang R et al (2013) LSD2/KDM1B and its cofactor NPAC/GLYR1 endow a structural and molecular model for regulation of H3K4 demethylation. Mol Cell 49(3):558–570
48. Hou H, Yu H (2010) Structural insights into histone lysine demethylation. Curr Opin Struct Biol 20(6):739–748
49. Musselman CA et al (2012) Perceiving the epigenetic landscape through histone readers. Nat Struct Mol Biol 19(12):1218–1227
50. Taverna SD et al (2007) How chromatin-binding modules interpret histone modifications: lessons from professional pocket pickers. Nat Struct Mol Biol 14(11):1025–1040
51. Kamps JJ et al (2015) Chemical basis for the recognition of trimethyllysine by epigenetic reader proteins. Nat Commun 6:8911
52. Berry WL, Janknecht R (2013) KDM4/JMJD2 histone demethylases: epigenetic regulators in cancer cells. Cancer Res 73(10):2936–2942
53. Cheng Z et al (2014) A molecular threading mechanism underlies Jumonji lysine demethylase KDM2A regulation of methylated H3K36. Genes Dev 28(16):1758–1771
54. Horton JR et al (2016) Characterization of a linked Jumonji domain of the KDM5/JARID1 family of histone H3 lysine 4 demethylases. J Biol Chem 291(6):2631–2646
55. Pilka ES, James T, Lisztwan JH (2015) Structural definitions of Jumonji family demethylase selectivity. Drug Discov Today 20(6):743–749
56. Karytinos A et al (2009) A novel mammalian flavin-dependent histone demethylase. J Biol Chem 284(26):17775–17782
57. Sims RJ 3rd, Nishioka K, Reinberg D (2003) Histone lysine methylation: a signature for chromatin function. Trends Genet 19(11):629–639
58. Barski A et al (2007) High-resolution profiling of histone methylations in the human genome. Cell 129(4):823–837
59. Maston GA et al (2012) Characterization of enhancer function from genome-wide analyses. Annu Rev Genomics Hum Genet 13:29–57
60. Wang Y, Li X, Hu H (2014) H3K4me2 reliably defines transcription factor binding regions in different cells. Genomics 103(2–3):222–228
61. Heintzman ND et al (2009) Histone modifications at human enhancers reflect global cell-type-specific gene expression. Nature 459(7243):108–112

62. Fang R et al (2010) Human LSD2/KDM1b/AOF1 regulates gene transcription by modulating intragenic H3K4me2 methylation. Mol Cell 39(2):222–233
63. Ciccone DN et al (2009) KDM1B is a histone H3K4 demethylase required to establish maternal genomic imprints. Nature 461(7262):415–418
64. Burg JM et al (2015) KDM1 class flavin-dependent protein lysine demethylases. Biopolymers 104(4):213–246
65. Jin Y et al (2014) Nuclear import of human histone lysine-specific demethylase LSD1. J Biochem 156(6):305–313
66. Kubicek S, Jenuwein T (2004) A crack in histone lysine methylation. Cell 119(7):903–906
67. Zibetti C et al (2010) Alternative splicing of the histone demethylase LSD1/KDM1 contributes to the modulation of neurite morphogenesis in the mammalian nervous system. J Neurosci 30(7):2521–2532
68. Wang J et al (2015) LSD1n is an H4K20 demethylase regulating memory formation via transcriptional elongation control. Nat Neurosci 18(9):1256–1264
69. Laurent B et al (2015) A specific LSD1/KDM1A isoform regulates neuronal differentiation through H3K9 demethylation. Mol Cell 57(6):957–970
70. Kahl P et al (2006) Androgen receptor coactivators lysine-specific histone demethylase 1 and four and a half LIM domain protein 2 predict risk of prostate cancer recurrence. Cancer Res 66(23):11341–11347
71. Metzger E et al (2005) LSD1 demethylates repressive histone marks to promote androgen-receptor-dependent transcription. Nature 437(7057):436–439
72. Kauffman EC et al (2011) Role of androgen receptor and associated lysine-demethylase coregulators, LSD1 and JMJD2A, in localized and advanced human bladder cancer. Mol Carcinog 50(12):931–944
73. Schulte JH et al (2009) Lysine-specific demethylase 1 is strongly expressed in poorly differentiated neuroblastoma: implications for therapy. Cancer Res 69(5):2065–2071
74. Serce N et al (2012) Elevated expression of LSD1 (Lysine-specific demethylase 1) during tumour progression from pre-invasive to invasive ductal carcinoma of the breast. BMC Clin Pathol 12:13
75. Lim S et al (2010) Lysine-specific demethylase 1 (LSD1) is highly expressed in ER-negative breast cancers and a biomarker predicting aggressive biology. Carcinogenesis 31(3):512–520
76. Lv T et al (2012) Over-expression of LSD1 promotes proliferation, migration and invasion in non-small cell lung cancer. PLoS One 7(4):e35065
77. Zhao ZK et al (2013) Overexpression of LSD1 in hepatocellular carcinoma: a latent target for the diagnosis and therapy of hepatoma. Tumour Biol 34(1):173–180
78. Wang Y et al (2016) The histone demethylase LSD1 is a novel oncogene and therapeutic target in oral cancer. Cancer Lett 374(1):12–21
79. Ding J et al (2013) LSD1-mediated epigenetic modification contributes to proliferation and metastasis of colon cancer. Br J Cancer 109(4):994–1003
80. Schildhaus HU et al (2011) Lysine-specific demethylase 1 is highly expressed in solitary fibrous tumors, synovial sarcomas, rhabdomyosarcomas, desmoplastic small round cell tumors, and malignant peripheral nerve sheath tumors. Hum Pathol 42(11):1667–1675
81. Bennani-Baiti IM et al (2012) Lysine-specific demethylase 1 (LSD1/KDM1A/AOF2/BHC110) is expressed and is an epigenetic drug target in chondrosarcoma, Ewing's sarcoma, osteosarcoma, and rhabdomyosarcoma. Hum Pathol 43(8):1300–1307
82. Harris WJ et al (2012) The histone demethylase KDM1A sustains the oncogenic potential of MLL-AF9 leukemia stem cells. Cancer Cell 21(4):473–487
83. Schenk T et al (2012) Inhibition of the LSD1 (KDM1A) demethylase reactivates the all-trans-retinoic acid differentiation pathway in acute myeloid leukemia. Nat Med 18(4):605–611
84. Yatim A et al (2012) NOTCH1 nuclear interactome reveals key regulators of its transcriptional activity and oncogenic function. Mol Cell 48(3):445–458
85. Theisen ER et al (2016) Therapeutic opportunities in Ewing sarcoma: EWS-FLI inhibition via LSD1 targeting. Oncotarget 7(14):17616–17630
86. Sankar S et al (2014) Reversible LSD1 inhibition interferes with global EWS/ETS transcriptional activity and impedes Ewing sarcoma tumor growth. Clin Cancer Res 20(17):4584–4597

87. Ding X et al (2013) Epigenetic activation of AP1 promotes squamous cell carcinoma metastasis. Sci Signal 6(273):ra28 1–13, S0–15
88. Lin T et al (2010) Requirement of the histone demethylase LSD1 in Snai1-mediated transcriptional repression during epithelial-mesenchymal transition. Oncogene 29(35):4896–4904
89. Morera L, Lubbert M, Jung M (2016) Targeting histone methyltransferases and demethylases in clinical trials for cancer therapy. Clin Epigenetics 8:57
90. Wang Y et al (2009) LSD1 is a subunit of the NuRD complex and targets the metastasis programs in breast cancer. Cell 138(4):660–672
91. Katz TA et al (2014) Inhibition of histone demethylase, LSD2 (KDM1B), attenuates DNA methylation and increases sensitivity to DNMT inhibitor-induced apoptosis in breast cancer cells. Breast Cancer Res Treat 146(1):99–108
92. Yang Y et al (2015) Histone demethylase LSD2 acts as an E3 ubiquitin ligase and inhibits cancer cell growth through promoting proteasomal degradation of OGT. Mol Cell 58(1):47–59
93. Forneris F et al (2005) Human histone demethylase LSD1 reads the histone code. J Biol Chem 280(50):41360–41365
94. Yang M et al (2007) Structural basis of histone demethylation by LSD1 revealed by suicide inactivation. Nat Struct Mol Biol 14(6):535–539
95. Forneris F et al (2007) Structural basis of LSD1-CoREST selectivity in histone H3 recognition. J Biol Chem 282(28):20070–20074
96. Da G et al (2006) Structure and function of the SWIRM domain, a conserved protein module found in chromatin regulatory complexes. Proc Natl Acad Sci U S A 103(7):2057–2062
97. Qian C et al (2005) Structure and chromosomal DNA binding of the SWIRM domain. Nat Struct Mol Biol 12(12):1078–1085
98. Yang M et al (2006) Structural basis for CoREST-dependent demethylation of nucleosomes by the human LSD1 histone demethylase. Mol Cell 23(3):377–387
99. Tochio N et al (2006) Solution structure of the SWIRM domain of human histone demethylase LSD1. Structure 14(3):457–468
100. Ballas N et al (2001) Regulation of neuronal traits by a novel transcriptional complex. Neuron 31(3):353–365
101. Shi Y et al (2003) Coordinated histone modifications mediated by a CtBP co-repressor complex. Nature 422(6933):735–738
102. Barta ML et al (2012) The structures of coiled-coil domains from type III secretion system translocators reveal homology to pore-forming toxins. J Mol Biol 417(5):395–405
103. Yang Z et al (2010) AOF1 is a histone H3K4 demethylase possessing demethylase activity-independent repression function. Cell Res 20(3):276–287
104. Zhang Q et al (2013) Structure-function analysis reveals a novel mechanism for regulation of histone demethylase LSD2/AOF1/KDM1b. Cell Res 23(2):225–241
105. Andres ME et al (1999) CoREST: a functional corepressor required for regulation of neural-specific gene expression. Proc Natl Acad Sci U S A 96(17):9873–9878
106. Chong JA et al (1995) REST: a mammalian silencer protein that restricts sodium channel gene expression to neurons. Cell 80(6):949–957
107. Schoenherr CJ, Anderson DJ (1995) Silencing is golden: negative regulation in the control of neuronal gene transcription. Curr Opin Neurobiol 5(5):566–571
108. Schoenherr CJ, Anderson DJ (1995) The neuron-restrictive silencer factor (NRSF): a coordinate repressor of multiple neuron-specific genes. Science 267(5202):1360–1363
109. You A et al (2001) CoREST is an integral component of the CoREST- human histone deacetylase complex. Proc Natl Acad Sci U S A 98(4):1454–1458
110. Hakimi MA et al (2002) A core-BRAF35 complex containing histone deacetylase mediates repression of neuronal-specific genes. Proc Natl Acad Sci U S A 99(11):7420–7425
111. Humphrey GW et al (2001) Stable histone deacetylase complexes distinguished by the presence of SANT domain proteins CoREST/kiaa0071 and Mta-L1. J Biol Chem 276(9):6817–6824
112. Abrajano JJ et al (2009) REST and CoREST modulate neuronal subtype specification, maturation and maintenance. PLoS One 4(12):e7936

113. Qureshi IA, Gokhan S, Mehler MF (2010) REST and CoREST are transcriptional and epigenetic regulators of seminal neural fate decisions. Cell Cycle 9(22):4477–4486
114. Lakowski B, Roelens I, Jacob S (2006) CoREST-like complexes regulate chromatin modification and neuronal gene expression. J Mol Neurosci 29(3):227–239
115. Metzger E et al (2010) Phosphorylation of histone H3T6 by PKCbeta(I) controls demethylation at histone H3K4. Nature 464(7289):792–796
116. Metzger E et al (2016) Assembly of methylated KDM1A and CHD1 drives androgen receptor-dependent transcription and translocation. Nat Struct Mol Biol 23(2):132–139
117. Basta J, Rauchman M (2015) The nucleosome remodeling and deacetylase complex in development and disease. Transl Res 165(1):36–47
118. Wang J et al (2007) Opposing LSD1 complexes function in developmental gene activation and repression programmes. Nature 446(7138):882–887
119. Toffolo E et al (2014) Phosphorylation of neuronal lysine-specific demethylase 1LSD1/KDM1A impairs transcriptional repression by regulating interaction with CoREST and histone deacetylases HDAC1/2. J Neurochem 128(5):603–616
120. McGrath J, Trojer P (2015) Targeting histone lysine methylation in cancer. Pharmacol Ther 150:1–22
121. Pedersen MT, Helin K (2010) Histone demethylases in development and disease. Trends Cell Biol 20(11):662–671
122. Zheng YC et al (2015) A systematic review of histone lysine-specific demethylase 1 and its inhibitors. Med Res Rev 35(5):1032–1071
123. Zheng YC et al (2016) Irreversible LSD1 inhibitors: application of tranylcypromine and its derivatives in cancer treatment. Curr Top Med Chem 16(19):2179–2188
124. Burg JM et al (2016) Lysine-specific demethylase 1A (KDM1A/LSD1): product recognition and kinetic analysis of full-length histones. Biochemistry 55(11):1652–1662
125. Mimasu S et al (2008) Crystal structure of histone demethylase LSD1 and tranylcypromine at 2.25 A. Biochem Biophys Res Commun 366(1):15–22
126. Yang M et al (2007) Structural basis for the inhibition of the LSD1 histone demethylase by the antidepressant trans-2-phenylcyclopropylamine. Biochemistry 46(27):8058–8065
127. Mimasu S et al (2010) Structurally designed trans-2-phenylcyclopropylamine derivatives potently inhibit histone demethylase LSD1/KDM1. Biochemistry 49(30):6494–6503
128. Binda C et al (2010) Biochemical, structural, and biological evaluation of tranylcypromine derivatives as inhibitors of histone demethylases LSD1 and LSD2. J Am Chem Soc 132(19):6827–6833
129. Baron R et al (2011) Molecular mimicry and ligand recognition in binding and catalysis by the histone demethylase LSD1-CoREST complex. Structure 19(2):212–220
130. Tortorici M et al (2013) Protein recognition by short peptide reversible inhibitors of the chromatin-modifying LSD1/CoREST lysine demethylase. ACS Chem Biol 8(8):1677–1682
131. Luka Z et al (2014) Crystal structure of the histone lysine specific demethylase LSD1 complexed with tetrahydrofolate. Protein Sci 23(7):993–998
132. Barrios AP et al (2014) Differential properties of transcriptional complexes formed by the CoREST family. Mol Cell Biol 34(14):2760–2770
133. Vianello P et al (2014) Synthesis, biological activity and mechanistic insights of 1-substituted cyclopropylamine derivatives: a novel class of irreversible inhibitors of histone demethylase KDM1A. Eur J Med Chem 86:352–363
134. Pilotto S et al (2016) LSD1/KDM1A mutations associated to a newly described form of intellectual disability impair demethylase activity and binding to transcription factors. Hum Mol Genet 25(12):2578–2587
135. He J et al (2008) The H3K36 demethylase Jhdm1b/Kdm2b regulates cell proliferation and senescence through p15(Ink4b). Nat Struct Mol Biol 15(11):1169–1175
136. Tzatsos A et al (2013) KDM2B promotes pancreatic cancer via Polycomb-dependent and -independent transcriptional programs. J Clin Invest 123(2):727–739
137. Liu H et al (2016) Integrated genomic and functional analyses of histone demethylases identify oncogenic KDM2A isoform in breast cancer. Mol Carcinog 55(5):977–990

138. Chen JY et al (2016) Lysine demethylase 2A promotes stemness and angiogenesis of breast cancer by upregulating Jagged1. Oncotarget 7(19):27689–27710
139. Wagner KW et al (2013) KDM2A promotes lung tumorigenesis by epigenetically enhancing ERK1/2 signaling. J Clin Invest 123(12):5231–5246
140. Huang Y et al (2015) Histone demethylase KDM2A promotes tumor cell growth and migration in gastric cancer. Tumour Biol 36(1):271–278
141. Rizwani W et al (2014) Mammalian lysine histone demethylase KDM2A regulates E2F1-mediated gene transcription in breast cancer cells. PLoS One 9(7):e100888
142. Kottakis F et al (2014) NDY1/KDM2B functions as a master regulator of polycomb complexes and controls self-renewal of breast cancer stem cells. Cancer Res 74(14):3935–3946
143. Karoopongse E et al (2014) The KDM2B- let-7b -EZH2 axis in myelodysplastic syndromes as a target for combined epigenetic therapy. PLoS One 9(9):e107817
144. Nakamura S et al (2013) JmjC-domain containing histone demethylase 1B-mediated p15(Ink4b) suppression promotes the proliferation of leukemic progenitor cells through modulation of cell cycle progression in acute myeloid leukemia. Mol Carcinog 52(1):57–69
145. He J, Nguyen AT, Zhang Y (2011) KDM2b/JHDM1b, an H3K36me2-specific demethylase, is required for initiation and maintenance of acute myeloid leukemia. Blood 117(14):3869–3880
146. Ueda T et al (2015) Fbxl10 overexpression in murine hematopoietic stem cells induces leukemia involving metabolic activation and upregulation of Nsg2. Blood 125(22):3437–3446
147. Tzatsos A et al (2009) Ndy1/KDM2B immortalizes mouse embryonic fibroblasts by repressing the Ink4a/Arf locus. Proc Natl Acad Sci U S A 106(8):2641–2646
148. Yu X et al (2015) A systematic study of the cellular metabolic regulation of Jhdm1b in tumor cells. Mol BioSyst 11(7):1867–1875
149. Hausinger RP (2004) FeII/alpha-ketoglutarate-dependent hydroxylases and related enzymes. Crit Rev Biochem Mol Biol 39(1):21–68
150. Zhou JC et al (2012) Recognition of CpG island chromatin by KDM2A requires direct and specific interaction with linker DNA. Mol Cell Biol 32(2):479–489
151. Blackledge NP, Klose R (2011) CpG island chromatin: a platform for gene regulation. Epigenetics 6(2):147–152
152. Blackledge NP et al (2010) CpG islands recruit a histone H3 lysine 36 demethylase. Mol Cell 38(2):179–190
153. Long HK, Blackledge NP, Klose RJ (2013) ZF-CxxC domain-containing proteins, CpG islands and the chromatin connection. Biochem Soc Trans 41(3):727–740
154. Blackledge NP, Thomson JP, Skene PJ (2013) CpG island chromatin is shaped by recruitment of ZF-CxxC proteins. Cold Spring Harb Perspect Biol 5(11):a018648
155. Farcas AM et al (2012) KDM2B links the polycomb repressive complex 1 (PRC1) to recognition of CpG islands. elife 1:e00205
156. Wu X, Johansen JV, Helin K (2013) Fbxl10/Kdm2b recruits polycomb repressive complex 1 to CpG islands and regulates H2A ubiquitylation. Mol Cell 49(6):1134–1146
157. Inagaki T et al (2015) The FBXL10/KDM2B scaffolding protein associates with novel polycomb repressive complex-1 to regulate adipogenesis. J Biol Chem 290(7):4163–4177
158. Han XR et al (2016) KDM2B/FBXL10 targets c-Fos for ubiquitylation and degradation in response to mitogenic stimulation. Oncogene 35(32):4179–4190
159. Janzer A et al (2012) The H3K4me3 histone demethylase Fbxl10 is a regulator of chemokine expression, cellular morphology, and the metabolome of fibroblasts. J Biol Chem 287(37):30984–30992
160. Heery DM et al (1997) A signature motif in transcriptional co-activators mediates binding to nuclear receptors. Nature 387(6634):733–736
161. Plevin MJ, Mills MM, Ikura M (2005) The LxxLL motif: a multifunctional binding sequence in transcriptional regulation. Trends Biochem Sci 30(2):66–69
162. Kuroki S et al (2013) Epigenetic regulation of mouse sex determination by the histone demethylase Jmjd1a. Science 341(6150):1106–1109
163. Liu Z et al (2015) Knockout of the histone demethylase Kdm3b decreases spermatogenesis and impairs male sexual behaviors. Int J Biol Sci 11(12):1447–1457

164. Okada Y et al (2007) Histone demethylase JHDM2A is critical for Tnp1 and Prm1 transcription and spermatogenesis. Nature 450(7166):119–123
165. Loh YH et al (2007) Jmjd1a and Jmjd2c histone H3 Lys 9 demethylases regulate self-renewal in embryonic stem cells. Genes Dev 21(20):2545–2557
166. Tateishi K et al (2009) Role of Jhdm2a in regulating metabolic gene expression and obesity resistance. Nature 458(7239):757–761
167. Inagaki T et al (2009) Obesity and metabolic syndrome in histone demethylase JHDM2a-deficient mice. Genes Cells 14(8):991–1001
168. Kuroki S et al (2013) JMJD1C, a JmjC domain-containing protein, is required for long-term maintenance of male germ cells in mice. Biol Reprod 89(4):93
169. Zhan M et al (2016) JMJD1A promotes tumorigenesis and forms a feedback loop with EZH2/let-7c in NSCLC cells. Tumour Biol 37(8):11237–11247
170. Cho HS et al (2012) The JmjC domain-containing histone demethylase KDM3A is a positive regulator of the G1/S transition in cancer cells via transcriptional regulation of the HOXA1 gene. Int J Cancer 131(3):E179–E189
171. Yang H et al (2015) Elevated JMJD1A is a novel predictor for prognosis and a potential therapeutic target for gastric cancer. Int J Clin Exp Pathol 8(9):11092–11099
172. Tee AE et al (2014) The histone demethylase JMJD1A induces cell migration and invasion by up-regulating the expression of the long noncoding RNA MALAT1. Oncotarget 5(7):1793–1804
173. Parrish JK et al (2015) The histone demethylase KDM3A is a microRNA-22-regulated tumor promoter in Ewing sarcoma. Oncogene 34(2):257–262
174. Guo X et al (2011) The expression of histone demethylase JMJD1A in renal cell carcinoma. Neoplasma 58(2):153–157
175. Yamada D et al (2012) Role of the hypoxia-related gene, JMJD1A, in hepatocellular carcinoma: clinical impact on recurrence after hepatic resection. Ann Surg Oncol 19(Suppl 3):S355–S364
176. Ohguchi H et al (2016) The KDM3A-KLF2-IRF4 axis maintains myeloma cell survival. Nat Commun 7:10258
177. Fan L et al (2016) Regulation of c-Myc expression by the histone demethylase JMJD1A is essential for prostate cancer cell growth and survival. Oncogene 35(19):2441–2452
178. Krieg AJ et al (2010) Regulation of the histone demethylase JMJD1A by hypoxia-inducible factor 1 alpha enhances hypoxic gene expression and tumor growth. Mol Cell Biol 30(1):344–353
179. Uemura M et al (2010) Jumonji domain containing 1A is a novel prognostic marker for colorectal cancer: in vivo identification from hypoxic tumor cells. Clin Cancer Res 16(18):4636–4646
180. Osawa T et al (2013) Inhibition of histone demethylase JMJD1A improves anti-angiogenic therapy and reduces tumor-associated macrophages. Cancer Res 73(10):3019–3028
181. Park SJ et al (2013) The histone demethylase JMJD1A regulates adrenomedullin-mediated cell proliferation in hepatocellular carcinoma under hypoxia. Biochem Biophys Res Commun 434(4):722–727
182. Ueda J et al (2014) The hypoxia-inducible epigenetic regulators Jmjd1a and G9a provide a mechanistic link between angiogenesis and tumor growth. Mol Cell Biol 34(19):3702–3720
183. Hu Z et al (2001) A novel nuclear protein, 5qNCA (LOC51780) is a candidate for the myeloid leukemia tumor suppressor gene on chromosome 5 band q31. Oncogene 20(47):6946–6954
184. Paolicchi E et al (2013) Histone lysine demethylases in breast cancer. Crit Rev Oncol Hematol 86(2):97–103
185. Kim JY et al (2012) KDM3B is the H3K9 demethylase involved in transcriptional activation of lmo2 in leukemia. Mol Cell Biol 32(14):2917–2933
186. Baik SH et al (2009) DNA profiling by array comparative genomic hybridization (CGH) of peripheral blood mononuclear cells (PBMC) and tumor tissue cell in non-small cell lung cancer (NSCLC). Mol Biol Rep 36(7):1767–1778
187. Brauchle M et al (2013) Protein complex interactor analysis and differential activity of KDM3 subfamily members towards H3K9 methylation. PLoS One 8(4):e60549
188. Wang J et al (2014) Epigenetic regulation of miR-302 by JMJD1C inhibits neural differentiation of human embryonic stem cells. J Biol Chem 289(4):2384–2395

189. Chen M et al (2015) JMJD1C is required for the survival of acute myeloid leukemia by functioning as a coactivator for key transcription factors. Genes Dev 29(20):2123–2139
190. Sroczynska P et al (2014) shRNA screening identifies JMJD1C as being required for leukemia maintenance. Blood 123(12):1870–1882
191. Wang L et al (2014) Novel somatic and germline mutations in intracranial germ cell tumours. Nature 511(7508):241–245
192. Yamane K et al (2006) JHDM2A, a JmjC-containing H3K9 demethylase, facilitates transcription activation by androgen receptor. Cell 125(3):483–495
193. Goda S et al (2013) Control of histone H3 lysine 9 (H3K9) methylation state via cooperative two-step demethylation by Jumonji domain containing 1A (JMJD1A) homodimer. J Biol Chem 288(52):36948–36956
194. Lim S et al (2010) Epigenetic regulation of cancer growth by histone demethylases. Int J Cancer 127(9):1991–1998
195. Pollard PJ et al (2008) Regulation of Jumonji-domain-containing histone demethylases by hypoxia-inducible factor (HIF)-1alpha. Biochem J 416(3):387–394
196. Sar A et al (2009) Identification and characterization of demethylase JMJD1A as a gene upregulated in the human cellular response to hypoxia. Cell Tissue Res 337(2):223–234
197. Wellmann S et al (2008) Hypoxia upregulates the histone demethylase JMJD1A via HIF-1. Biochem Biophys Res Commun 372(4):892–897
198. Lin Q, Yun Z (2010) Impact of the hypoxic tumor microenvironment on the regulation of cancer stem cell characteristics. Cancer Biol Ther 9(12):949–956
199. Beyer S et al (2008) The histone demethylases JMJD1A and JMJD2B are transcriptional targets of hypoxia-inducible factor HIF. J Biol Chem 283(52):36542–36552
200. Guerra-Calderas L et al (2015) The role of the histone demethylase KDM4A in cancer. Cancer Genet 208(5):215–224
201. Labbe RM, Holowatyj A, Yang ZQ (2013) Histone lysine demethylase (KDM) subfamily 4: structures, functions and therapeutic potential. Am J Transl Res 6(1):1–15
202. Del Rizzo PA, Trievel RC (2014) Molecular basis for substrate recognition by lysine methyltransferases and demethylases. Biochim Biophys Acta 1839(12):1404–1415
203. Pack LR, Yamamoto KR, Fujimori DG (2016) Opposing Chromatin Signals Direct and Regulate the Activity of Lysine Demethylase 4C (KDM4C). J Biol Chem 291(12):6060–6070
204. Das PP et al (2014) Distinct and combinatorial functions of Jmjd2b/Kdm4b and Jmjd2c/Kdm4c in mouse embryonic stem cell identity. Mol Cell 53(1):32–48
205. Zhang X et al (2009) Genome-wide analysis of mono-, di- and trimethylation of histone H3 lysine 4 in *Arabidopsis thaliana*. Genome Biol 10(6):R62
206. Huang Y et al (2006) Recognition of histone H3 lysine-4 methylation by the double tudor domain of JMJD2A. Science 312(5774):748–751
207. Yu Y et al (2012) Histone H3 lysine 56 methylation regulates DNA replication through its interaction with PCNA. Mol Cell 46(1):7–17
208. Jack AP et al (2013) H3K56me3 is a novel, conserved heterochromatic mark that largely but not completely overlaps with H3K9me3 in both regulation and localization. PLoS One 8(2):e51765
209. Young LC, Hendzel MJ (2013) The oncogenic potential of Jumonji D2 (JMJD2/KDM4) histone demethylase overexpression. Biochem Cell Biol 91(6):369–377
210. Luo W et al (2012) Histone demethylase JMJD2C is a coactivator for hypoxia-inducible factor 1 that is required for breast cancer progression. Proc Natl Acad Sci U S A 109(49):E3367–E3376
211. Yang J et al (2010) The histone demethylase JMJD2B is regulated by estrogen receptor alpha and hypoxia, and is a key mediator of estrogen induced growth. Cancer Res 70(16):6456–6466
212. Awwad SW, Ayoub N (2015) Overexpression of KDM4 lysine demethylases disrupts the integrity of the DNA mismatch repair pathway. Biol Open 4(4):498–504
213. Agger K et al (2016) Jmjd2/Kdm4 demethylases are required for expression of Il3ra and survival of acute myeloid leukemia cells. Genes Dev 30(11):1278–1288
214. Ye Q et al (2015) Genetic alterations of KDM4 subfamily and therapeutic effect of novel demethylase inhibitor in breast cancer. Am J Cancer Res 5(4):1519–1530

215. Li LL et al (2014) JMJD2A contributes to breast cancer progression through transcriptional repression of the tumor suppressor ARHI. Breast Cancer Res 16(3):R56
216. Bjorkman M et al (2012) Systematic knockdown of epigenetic enzymes identifies a novel histone demethylase PHF8 overexpressed in prostate cancer with an impact on cell proliferation, migration and invasion. Oncogene 31(29):3444–3456
217. Kim TD et al (2016) Histone demethylase JMJD2A drives prostate tumorigenesis through transcription factor ETV1. J Clin Invest 126(2):706–720
218. Xu W et al (2016) Jumonji domain containing 2A predicts prognosis and regulates cell growth in lung cancer depending on miR-150. Oncol Rep 35(1):352–358
219. Mallette FA, Richard S (2012) JMJD2A promotes cellular transformation by blocking cellular senescence through transcriptional repression of the tumor suppressor CHD5. Cell Rep 2(5):1233–1243
220. Kogure M et al (2013) Deregulation of the histone demethylase JMJD2A is involved in human carcinogenesis through regulation of the G(1)/S transition. Cancer Lett 336(1):76–84
221. Hu CE et al (2014) JMJD2A predicts prognosis and regulates cell growth in human gastric cancer. Biochem Biophys Res Commun 449(1):1–7
222. Wang HL et al (2014) Expression and effects of JMJD2A histone demethylase in endometrial carcinoma. Asian Pac J Cancer Prev 15(7):3051–3056
223. Qiu MT et al (2015) KDM4B and KDM4A promote endometrial cancer progression by regulating androgen receptor, c-myc, and p27kip1. Oncotarget 6(31):31702–31720
224. Black JC et al (2013) KDM4A lysine demethylase induces site-specific copy gain and rereplication of regions amplified in tumors. Cell 154(3):541–555
225. Chu CH et al (2014) KDM4B as a target for prostate cancer: structural analysis and selective inhibition by a novel inhibitor. J Med Chem 57(14):5975–5985
226. Kim TD et al (2012) The JMJD2A demethylase regulates apoptosis and proliferation in colon cancer cells. J Cell Biochem 113(4):1368–1376
227. Li BX et al (2011) Effects of RNA interference-mediated gene silencing of JMJD2A on human breast cancer cell line MDA-MB-231 in vitro. J Exp Clin Cancer Res 30:90
228. Xu W et al (2015) SIRT2 suppresses non-small cell lung cancer growth by targeting JMJD2A. Biol Chem 396(8):929–936
229. Liu Y et al (2013) An epigenetic role for PRL-3 as a regulator of H3K9 methylation in colorectal cancer. Gut 62(4):571–581
230. Toyokawa G et al (2011) The histone demethylase JMJD2B plays an essential role in human carcinogenesis through positive regulation of cyclin-dependent kinase 6. Cancer Prev Res (Phila) 4(12):2051–2061
231. Coffey K et al (2013) The lysine demethylase, KDM4B, is a key molecule in androgen receptor signalling and turnover. Nucleic Acids Res 41(8):4433–4446
232. Li W et al (2011) Histone demethylase JMJD2B is required for tumor cell proliferation and survival and is overexpressed in gastric cancer. Biochem Biophys Res Commun 416(3–4):372–378
233. Zhao L et al (2013) JMJD2B promotes epithelial-mesenchymal transition by cooperating with beta-catenin and enhances gastric cancer metastasis. Clin Cancer Res 19(23):6419–6429
234. Han F et al (2016) JMJD2B is required for Helicobacter pylori-induced gastric carcinogenesis via regulating COX-2 expression. Oncotarget 7(25):38626–38637
235. Lu JW et al (2015) JMJD2B as a potential diagnostic immunohistochemical marker for hepatocellular carcinoma: a tissue microarray-based study. Acta Histochem 117(1):14–19
236. Li X, Dong S (2015) Histone demethylase JMJD2B and JMJD2C induce fibroblast growth factor 2: mediated tumorigenesis of osteosarcoma. Med Oncol 32(3):53
237. Kawazu M et al (2011) Histone demethylase JMJD2B functions as a co-factor of estrogen receptor in breast cancer proliferation and mammary gland development. PLoS One 6(3):e17830
238. Shi L et al (2011) Histone demethylase JMJD2B coordinates H3K4/H3K9 methylation and promotes hormonally responsive breast carcinogenesis. Proc Natl Acad Sci U S A 108(18):7541–7546
239. Chen L et al (2014) Jumonji domain-containing protein 2B silencing induces DNA damage response via STAT3 pathway in colorectal cancer. Br J Cancer 110(4):1014–1026

240. Sun BB et al (2014) Silencing of JMJD2B induces cell apoptosis via mitochondria-mediated and death receptor-mediated pathway activation in colorectal cancer. J Dig Dis 15(9):491–500
241. Liu G et al (2009) Genomic amplification and oncogenic properties of the GASC1 histone demethylase gene in breast cancer. Oncogene 28(50):4491–4500
242. Yang ZQ et al (2000) Identification of a novel gene, GASC1, within an amplicon at 9p23-24 frequently detected in esophageal cancer cell lines. Cancer Res 60(17):4735–4739
243. Italiano A et al (2006) Molecular cytogenetic characterization of a metastatic lung sarcomatoid carcinoma: 9p23 neocentromere and 9p23-p24 amplification including JAK2 and JMJD2C. Cancer Genet Cytogenet 167(2):122–130
244. Rui L et al (2010) Cooperative epigenetic modulation by cancer amplicon genes. Cancer Cell 18(6):590–605
245. Ehrbrecht A et al (2006) Comprehensive genomic analysis of desmoplastic medulloblastomas: identification of novel amplified genes and separate evaluation of the different histological components. J Pathol 208(4):554–563
246. Northcott PA et al (2009) Multiple recurrent genetic events converge on control of histone lysine methylation in medulloblastoma. Nat Genet 41(4):465–472
247. Sun LL et al (2013) Histone demethylase GASC1, a potential prognostic and predictive marker in esophageal squamous cell carcinoma. Am J Cancer Res 3(5):509–517
248. Ozaki Y et al (2015) The oncogenic role of GASC1 in chemically induced mouse skin cancer. Mamm Genome 26(11–12):591–597
249. Ishimura A et al (2009) Jmjd2c histone demethylase enhances the expression of Mdm2 oncogene. Biochem Biophys Res Commun 389(2):366–371
250. Berdel B et al (2012) Histone demethylase GASC1 – a potential prognostic and predictive marker in invasive breast cancer. BMC Cancer 12:516
251. Kim TD et al (2012) Regulation of tumor suppressor p53 and HCT116 cell physiology by histone demethylase JMJD2D/KDM4D. PLoS One 7(4):e34618
252. Hillringhaus L et al (2011) Structural and evolutionary basis for the dual substrate selectivity of human KDM4 histone demethylase family. J Biol Chem 286(48):41616–41625
253. Ng SS et al (2007) Crystal structures of histone demethylase JMJD2A reveal basis for substrate specificity. Nature 448(7149):87–91
254. Couture JF et al (2007) Specificity and mechanism of JMJD2A, a trimethyllysine-specific histone demethylase. Nat Struct Mol Biol 14(8):689–695
255. Kim J et al (2006) Tudor, MBT and chromo domains gauge the degree of lysine methylation. EMBO Rep 7(4):397–403
256. Lee J et al (2008) Distinct binding modes specify the recognition of methylated histones H3K4 and H4K20 by JMJD2A-tudor. Nat Struct Mol Biol 15(1):109–111
257. Mallette FA et al (2012) RNF8- and RNF168-dependent degradation of KDM4A/JMJD2A triggers 53BP1 recruitment to DNA damage sites. EMBO J 31(8):1865–1878
258. Pedersen MT et al (2014) The demethylase JMJD2C localizes to H3K4me3-positive transcription start sites and is dispensable for embryonic development. Mol Cell Biol 34(6):1031–1045
259. Ozboyaci M et al (2011) Molecular recognition of H3/H4 histone tails by the tudor domains of JMJD2A: a comparative molecular dynamics simulations study. PLoS One 6(3):e14765
260. Gaughan L et al (2013) KDM4B is a master regulator of the estrogen receptor signalling cascade. Nucleic Acids Res 41(14):6892–6904
261. Chen Z et al (2007) Structural basis of the recognition of a methylated histone tail by JMJD2A. Proc Natl Acad Sci U S A 104(26):10818–10823
262. Rose NR et al (2008) Inhibitor scaffolds for 2-oxoglutarate-dependent histone lysine demethylases. J Med Chem 51(22):7053–7056
263. Rose NR et al (2010) Selective inhibitors of the JMJD2 histone demethylases: combined nondenaturing mass spectrometric screening and crystallographic approaches. J Med Chem 53(4):1810–1818
264. King ON et al (2010) Quantitative high-throughput screening identifies 8-hydroxyquinolines as cell-active histone demethylase inhibitors. PLoS One 5(11):e15535

265. Chang KH et al (2011) Inhibition of histone demethylases by 4-carboxy-2,2′-bipyridyl compounds. ChemMedChem 6(5):759–764
266. Chowdhury R et al (2011) The oncometabolite 2-hydroxyglutarate inhibits histone lysine demethylases. EMBO Rep 12(5):463–469
267. Woon EC et al (2012) Linking of 2-oxoglutarate and substrate binding sites enables potent and highly selective inhibition of JmjC histone demethylases. Angew Chem Int Ed Engl 51(7):1631–1634
268. Rose NR et al (2012) Plant growth regulator daminozide is a selective inhibitor of human KDM2/7 histone demethylases. J Med Chem 55(14):6639–6643
269. Hopkinson RJ et al (2013) 5-carboxy-8-hydroxyquinoline is a broad spectrum 2-oxoglutarate oxygenase inhibitor which causes iron translocation. Chem Sci 4(8):3110–3117
270. Williams ST et al (2014) Studies on the catalytic domains of multiple JmjC oxygenases using peptide substrates. Epigenetics 9(12):1596–1603
271. Korczynska M et al (2016) Docking and linking of fragments to discover Jumonji histone demethylase inhibitors. J Med Chem 59(4):1580–1598
272. Roatsch M et al (2016) Substituted 2-(2-aminopyrimidin-4-yl)pyridine-4-carboxylates as potent inhibitors of JumonjiC domain-containing histone demethylases. Future Med Chem 8(13):1553–1571
273. Bavetsias V et al (2016) 8-Substituted pyrido[3,4-d]pyrimidin-4(3H)-one derivatives as potent, cell permeable, KDM4 (JMJD2) and KDM5 (JARID1) histone lysine demethylase inhibitors. J Med Chem 59(4):1388–1409
274. Johansson C et al (2016) Structural analysis of human KDM5B guides histone demethylase inhibitor development. Nat Chem Biol 12(7):539–545
275. Wigle TJ et al (2015) A high-throughput mass spectrometry assay coupled with redox activity testing reduces artifacts and false positives in lysine demethylase screening. J Biomol Screen 20(6):810–820
276. Krishnan S, Trievel RC (2013) Structural and functional analysis of JMJD2D reveals molecular basis for site-specific demethylation among JMJD2 demethylases. Structure 21(1):98–108
277. Westaway SM et al (2016) Cell penetrant inhibitors of the KDM4 and KDM5 families of histone lysine demethylases. 2. Pyrido[3,4-d]pyrimidin-4(3H)-one derivatives. J Med Chem 59(4):1370–1387
278. Blair LP et al (2011) Epigenetic regulation by lysine demethylase 5 (KDM5) enzymes in cancer. Cancers (Basel) 3(1):1383–1404
279. Rasmussen PB, Staller P (2014) The KDM5 family of histone demethylases as targets in oncology drug discovery. Epigenomics 6(3):277–286
280. Voigt P, Tee WW, Reinberg D (2013) A double take on bivalent promoters. Genes Dev 27(12):1318–1338
281. Bernstein BE et al (2006) A bivalent chromatin structure marks key developmental genes in embryonic stem cells. Cell 125(2):315–326
282. Horton JR et al (2016) Structural basis for KDM5A histone lysine demethylase inhibition by diverse compounds. Cell Chemical Biology 23(7):769–781
283. Vinogradova M et al (2016) An inhibitor of KDM5 demethylases reduces survival of drug-tolerant cancer cells. Nat Chem Biol 12(7):531–538
284. Yamane K et al (2007) PLU-1 is an H3K4 demethylase involved in transcriptional repression and breast cancer cell proliferation. Mol Cell 25(6):801–812
285. Hou J et al (2012) Genomic amplification and a role in drug-resistance for the KDM5A histone demethylase in breast cancer. Am J Transl Res 4(3):247–256
286. Teng YC et al (2013) Histone demethylase RBP2 promotes lung tumorigenesis and cancer metastasis. Cancer Res 73(15):4711–4721
287. Wang S et al (2013) RBP2 induces epithelial-mesenchymal transition in non-small cell lung cancer. PLoS One 8(12):e84735
288. Liang X et al (2013) Histone demethylase retinoblastoma binding protein 2 is overexpressed in hepatocellular carcinoma and negatively regulated by hsa-miR-212. PLoS One 8(7):e69784

289. Zeng J et al (2010) The histone demethylase RBP2 is overexpressed in gastric cancer and its inhibition triggers senescence of cancer cells. Gastroenterology 138(3):981–992
290. Jiping Z et al (2013) MicroRNA-212 inhibits proliferation of gastric cancer by directly repressing retinoblastoma binding protein 2. J Cell Biochem 114(12):2666–2672
291. Fattaey AR et al (1993) Characterization of the retinoblastoma binding proteins RBP1 and RBP2. Oncogene 8(11):3149–3156
292. Benevolenskaya EV et al (2005) Binding of pRB to the PHD protein RBP2 promotes cellular differentiation. Mol Cell 18(6):623–635
293. Lin W et al (2011) Loss of the retinoblastoma binding protein 2 (RBP2) histone demethylase suppresses tumorigenesis in mice lacking Rb1 or Men1. Proc Natl Acad Sci USA 108(33):13379–13386
294. Cao J et al (2014) Histone demethylase RBP2 is critical for breast cancer progression and metastasis. Cell Rep 6(5):868–877
295. Zhou D et al (2016) RBP2 induces stem-like cancer cells by promoting EMT and is a prognostic marker for renal cell carcinoma. Exp Mol Med 48:e238
296. Liang X et al (2015) Histone demethylase RBP2 promotes malignant progression of gastric cancer through TGF-beta1-(p-Smad3)-RBP2-E-cadherin-Smad3 feedback circuit. Oncotarget 6(19):17661–17674
297. Sharma SV et al (2010) A chromatin-mediated reversible drug-tolerant state in cancer cell subpopulations. Cell 141(1):69–80
298. Banelli B et al (2015) The histone demethylase KDM5A is a key factor for the resistance to temozolomide in glioblastoma. Cell Cycle 14(21):3418–3429
299. Cancer Genome Atlas, N (2012) Comprehensive molecular portraits of human breast tumours. Nature 490(7418):61–70
300. Hayami S et al (2010) Overexpression of the JmjC histone demethylase KDM5B in human carcinogenesis: involvement in the proliferation of cancer cells through the E2F/RB pathway. Mol Cancer 9:59
301. Li X et al (2013) Connexin 26 is down-regulated by KDM5B in the progression of bladder cancer. Int J Mol Sci 14(4):7866–7879
302. Liggins AP et al (2010) A panel of cancer-testis genes exhibiting broad-spectrum expression in haematological malignancies. Cancer Immun 10:8
303. Xiang Y et al (2007) JARID1B is a histone H3 lysine 4 demethylase up-regulated in prostate cancer. Proc Natl Acad Sci U S A 104(49):19226–19231
304. Ohta K et al (2013) Depletion of JARID1B induces cellular senescence in human colorectal cancer. Int J Oncol 42(4):1212–1218
305. Dai B et al (2014) Overexpressed KDM5B is associated with the progression of glioma and promotes glioma cell growth via downregulating p21. Biochem Biophys Res Commun 454(1):221–227
306. Wang L et al (2015) Overexpression of JARID1B is associated with poor prognosis and chemotherapy resistance in epithelial ovarian cancer. Tumour Biol 36(4):2465–2472
307. Wang D et al (2016) Depletion of histone demethylase KDM5B inhibits cell proliferation of hepatocellular carcinoma by regulation of cell cycle checkpoint proteins p15 and p27. J Exp Clin Cancer Res 35:37
308. Tang B et al (2015) JARID1B promotes metastasis and epithelial-mesenchymal transition via PTEN/AKT signaling in hepatocellular carcinoma cells. Oncotarget 6(14):12723–12739
309. Scibetta AG et al (2007) Functional analysis of the transcription repressor PLU-1/JARID1B. Mol Cell Biol 27(20):7220–7235
310. Roesch A et al (2010) A temporarily distinct subpopulation of slow-cycling melanoma cells is required for continuous tumor growth. Cell 141(4):583–594
311. Roesch A et al (2013) Overcoming intrinsic multidrug resistance in melanoma by blocking the mitochondrial respiratory chain of slow-cycling JARID1B(high) cells. Cancer Cell 23(6):811–825
312. Wang Z et al (2015) KDM5B is overexpressed in gastric cancer and is required for gastric cancer cell proliferation and metastasis. Am J Cancer Res 5(1):87–100

313. Lin CS et al (2015) Silencing JARID1B suppresses oncogenicity, stemness and increases radiation sensitivity in human oral carcinoma. Cancer Lett 368(1):36–45
314. Kuo YT et al (2015) JARID1B expression plays a critical role in chemoresistance and stem cell-like phenotype of neuroblastoma cells. PLoS One 10(5):e0125343
315. Bamodu OA et al (2016) Aberrant KDM5B expression promotes aggressive breast cancer through MALAT1 overexpression and downregulation of hsa-miR-448. BMC Cancer 16:160
316. Klein BJ et al (2014) The histone-H3K4-specific demethylase KDM5B binds to its substrate and product through distinct PHD fingers. Cell Rep 6(2):325–335
317. Dalgliesh GL et al (2010) Systematic sequencing of renal carcinoma reveals inactivation of histone modifying genes. Nature 463(7279):360–363
318. Komura K et al (2016) Resistance to docetaxel in prostate cancer is associated with androgen receptor activation and loss of KDM5D expression. Proc Natl Acad Sci USA 113(22):6259–6264
319. Niu X et al (2012) The von Hippel-Lindau tumor suppressor protein regulates gene expression and tumor growth through histone demethylase JARID1C. Oncogene 31(6):776–786
320. Tu S et al (2008) The ARID domain of the H3K4 demethylase RBP2 binds to a DNA CCGCCC motif. Nat Struct Mol Biol 15(4):419–421
321. Yao W, Peng Y, Lin D (2010) The flexible loop L1 of the H3K4 demethylase JARID1B ARID domain has a crucial role in DNA-binding activity. Biochem Biophys Res Commun 396(2):323–328
322. Zhang Y et al (2014) The PHD1 finger of KDM5B recognizes unmodified H3K4 during the demethylation of histone H3K4me2/3 by KDM5B. Protein Cell 5(11):837–850
323. Torres IO et al (2015) Histone demethylase KDM5A is regulated by its reader domain through a positive-feedback mechanism. Nat Commun 6:6204
324. Chakravarty S et al (2015) Histone peptide recognition by KDM5B-PHD1: a case study. Biochemistry 54(37):5766–5780
325. Wang GG et al (2009) Haematopoietic malignancies caused by dysregulation of a chromatin-binding PHD finger. Nature 459(7248):847–851
326. Klose RJ et al (2007) The retinoblastoma binding protein RBP2 is an H3K4 demethylase. Cell 128(5):889–900
327. Sengoku T, Yokoyama S (2011) Structural basis for histone H3 Lys 27 demethylation by UTX/KDM6A. Genes Dev 25(21):2266–2277
328. van Oevelen C et al (2008) A role for mammalian Sin3 in permanent gene silencing. Mol Cell 32(3):359–370
329. Koehler C et al (2008) Backbone and sidechain 1H, 13C and 15N resonance assignments of the Bright/ARID domain from the human JARID1C (SMCX) protein. Biomol NMR Assign 2(1):9–11
330. Hong S et al (2007) Identification of JmjC domain-containing UTX and JMJD3 as histone H3 lysine 27 demethylases. Proc Natl Acad Sci U S A 104(47):18439–18444
331. Hubner MR, Spector DL (2010) Role of H3K27 demethylases Jmjd3 and UTX in transcriptional regulation. Cold Spring Harb Symp Quant Biol 75:43–49
332. Walport LJ et al (2014) Human UTY(KDM6C) is a male-specific N-methyl lysyl demethylase. J Biol Chem 289(26):18302–18313
333. Greenfield A et al (1998) The UTX gene escapes X inactivation in mice and humans. Hum Mol Genet 7(4):737–742
334. Lan F et al (2007) A histone H3 lysine 27 demethylase regulates animal posterior development. Nature 449(7163):689–694
335. Shpargel KB et al (2012) UTX and UTY demonstrate histone demethylase-independent function in mouse embryonic development. PLoS Genet 8(9):e1002964
336. Arcipowski KM, Martinez CA, Ntziachristos P (2016) Histone demethylases in physiology and cancer: a tale of two enzymes, JMJD3 and UTX. Curr Opin Genet Dev 36:59–67
337. Perrigue PM, Najbauer J, Barciszewski J (2016) Histone demethylase JMJD3 at the intersection of cellular senescence and cancer. Biochim Biophys Acta 1865(2):237–244
338. Van der Meulen J, Speleman F, Van Vlierberghe P (2014) The H3K27me3 demethylase UTX in normal development and disease. Epigenetics 9(5):658–668

339. Robinson G et al (2012) Novel mutations target distinct subgroups of medulloblastoma. Nature 488(7409):43–48
340. Gui Y et al (2011) Frequent mutations of chromatin remodeling genes in transitional cell carcinoma of the bladder. Nat Genet 43(9):875–878
341. Nickerson ML et al (2014) Concurrent alterations in TERT, KDM6A, and the BRCA pathway in bladder cancer. Clin Cancer Res 20(18):4935–4948
342. Van der Meulen J et al (2015) The H3K27me3 demethylase UTX is a gender-specific tumor suppressor in T-cell acute lymphoblastic leukemia. Blood 125(1):13–21
343. Ntziachristos P et al (2014) Contrasting roles of histone 3 lysine 27 demethylases in acute lymphoblastic leukaemia. Nature 514(7523):513–517
344. Mar BG et al (2012) Sequencing histone-modifying enzymes identifies UTX mutations in acute lymphoblastic leukemia. Leukemia 26(8):1881–1883
345. Jankowska AM et al (2011) Mutational spectrum analysis of chronic myelomonocytic leukemia includes genes associated with epigenetic regulation: UTX, EZH2, and DNMT3A. Blood 118(14):3932–3941
346. van Haaften G et al (2009) Somatic mutations of the histone H3K27 demethylase gene UTX in human cancer. Nat Genet 41(5):521–523
347. Wang JK et al (2010) The histone demethylase UTX enables RB-dependent cell fate control. Genes Dev 24(4):327–332
348. Benyoucef A et al (2016) UTX inhibition as selective epigenetic therapy against TAL1-driven T-cell acute lymphoblastic leukemia. Genes Dev 30(5):508–521
349. Kim JH et al (2014) UTX and MLL4 coordinately regulate transcriptional programs for cell proliferation and invasiveness in breast cancer cells. Cancer Res 74(6):1705–1717
350. Patani N et al (2011) Histone-modifier gene expression profiles are associated with pathological and clinical outcomes in human breast cancer. Anticancer Res 31(12):4115–4125
351. Ene CI et al (2012) Histone demethylase Jumonji D3 (JMJD3) as a tumor suppressor by regulating p53 protein nuclear stabilization. PLoS One 7(12):e51407
352. Williams K et al (2014) The histone lysine demethylase JMJD3/KDM6B is recruited to p53 bound promoters and enhancer elements in a p53 dependent manner. PLoS One 9(5):e96545
353. Agger K et al (2009) The H3K27me3 demethylase JMJD3 contributes to the activation of the INK4A-ARF locus in response to oncogene- and stress-induced senescence. Genes Dev 23(10):1171–1176
354. Barradas M et al (2009) Histone demethylase JMJD3 contributes to epigenetic control of INK4a/ARF by oncogenic RAS. Genes Dev 23(10):1177–1182
355. Tokunaga R et al (2016) The prognostic significance of histone lysine demethylase JMJD3/KDM6B in colorectal cancer. Ann Surg Oncol 23(2):678–685
356. Park WY et al (2016) H3K27 demethylase JMJD3 employs the NF-kappaB and BMP signaling pathways to modulate the tumor microenvironment and promote melanoma progression and metastasis. Cancer Res 76(1):161–170
357. Zhang Y et al (2016) JMJD3 promotes survival of diffuse large B-cell lymphoma subtypes via distinct mechanisms. Oncotarget 7(20):29387–29399
358. Kruidenier L et al (2012) A selective jumonji H3K27 demethylase inhibitor modulates the proinflammatory macrophage response. Nature 488(7411):404–408
359. Hashizume R et al (2014) Pharmacologic inhibition of histone demethylation as a therapy for pediatric brainstem glioma. Nat Med 20(12):1394–1396
360. Sakaki H et al (2015) GSKJ4, a selective Jumonji H3K27 demethylase inhibitor, effectively targets ovarian cancer stem cells. Anticancer Res 35(12):6607–6614
361. Dutta A et al (2016) Identification of an NKX3.1-G9a-UTY transcriptional regulatory network that controls prostate differentiation. Science 352(6293):1576–1580
362. Lau YF, Zhang J (2000) Expression analysis of thirty one Y chromosome genes in human prostate cancer. Mol Carcinog 27(4):308–321
363. Omichinski JG et al (1993) NMR structure of a specific DNA complex of Zn-containing DNA binding domain of GATA-1. Science 261(5120):438–446

364. Issaeva I et al (2007) Knockdown of ALR (MLL2) reveals ALR target genes and leads to alterations in cell adhesion and growth. Mol Cell Biol 27(5):1889–1903
365. Cho YW et al (2007) PTIP associates with MLL3- and MLL4-containing histone H3 lysine 4 methyltransferase complex. J Biol Chem 282(28):20395–20406
366. Burchfield JS et al (2015) JMJD3 as an epigenetic regulator in development and disease. Int J Biochem Cell Biol 67:148–157
367. Manna S et al (2015) Histone H3 lysine 27 demethylases Jmjd3 and Utx are required for T-cell differentiation. Nat Commun 6:8152
368. Park SY, Park JW, Chun YS (2016) Jumonji histone demethylases as emerging therapeutic targets. Pharmacol Res 105:146–151
369. Horton JR et al (2011) Structural basis for human PHF2 Jumonji domain interaction with metal ions. J Mol Biol 406(1):1–8
370. Baba A et al (2011) PKA-dependent regulation of the histone lysine demethylase complex PHF2-ARID5B. Nat Cell Biol 13(6):668–675
371. Hata K et al (2013) Arid5b facilitates chondrogenesis by recruiting the histone demethylase Phf2 to Sox9-regulated genes. Nat Commun 4:2850
372. Osawa T et al (2011) Increased expression of histone demethylase JHDM1D under nutrient starvation suppresses tumor growth via down-regulating angiogenesis. Proc Natl Acad Sci U S A 108(51):20725–20729
373. Ma Q et al (2015) The histone demethylase PHF8 promotes prostate cancer cell growth by activating the oncomiR miR-125b. Onco Targets Ther 8:1979–1988
374. Wang Q et al (2016) Stabilization of histone demethylase PHF8 by USP7 promotes breast carcinogenesis. J Clin Invest 126(6):2205–2220
375. Zhu G et al (2015) Elevated expression of histone demethylase PHF8 associates with adverse prognosis in patients of laryngeal and hypopharyngeal squamous cell carcinoma. Epigenomics 7(2):143–153
376. Shen Y, Pan X, Zhao H (2014) The histone demethylase PHF8 is an oncogenic protein in human non-small cell lung cancer. Biochem Biophys Res Commun 451(1):119–125
377. Sun X et al (2013) Oncogenic features of PHF8 histone demethylase in esophageal squamous cell carcinoma. PLoS One 8(10):e77353
378. Arteaga MF et al (2013) The histone demethylase PHF8 governs retinoic acid response in acute promyelocytic leukemia. Cancer Cell 23(3):376–389
379. Sun LL et al (2013) Overexpression of Jumonji AT-rich interactive domain 1B and PHD finger protein 2 is involved in the progression of esophageal squamous cell carcinoma. Acta Histochem 115(1):56–62
380. Sinha S et al (2008) Alterations in candidate genes PHF2, FANCC, PTCH1 and XPA at chromosomal 9q22.3 region: pathological significance in early- and late-onset breast carcinoma. Mol Cancer 7:84
381. Ghosh A et al (2012) Association of FANCC and PTCH1 with the development of early dysplastic lesions of the head and neck. Ann Surg Oncol 19(Suppl 3):S528–S538
382. Lee KH et al (2015) PHF2 histone demethylase acts as a tumor suppressor in association with p53 in cancer. Oncogene 34(22):2897–2909
383. Pattabiraman DR et al (2016) Activation of PKA leads to mesenchymal-to-epithelial transition and loss of tumor-initiating ability. Science 351(6277):aad3680
384. Loenarz C et al (2010) PHF8, a gene associated with cleft lip/palate and mental retardation, encodes for an Nepsilon-dimethyl lysine demethylase. Hum Mol Genet 19(2):217–222
385. Abidi F et al (2007) A novel mutation in the PHF8 gene is associated with X-linked mental retardation with cleft lip/cleft palate. Clin Genet 72(1):19–22
386. Koivisto AM et al (2007) Screening of mutations in the PHF8 gene and identification of a novel mutation in a Finnish family with XLMR and cleft lip/cleft palate. Clin Genet 72(2):145–149
387. Laumonnier F et al (2005) Mutations in PHF8 are associated with X linked mental retardation and cleft lip/cleft palate. J Med Genet 42(10):780–786
388. Yang Y et al (2010) Structural insights into a dual-specificity histone demethylase ceKDM7A from *Caenorhabditis elegans*. Cell Res 20(8):886–898

389. Feng W et al (2010) PHF8 activates transcription of rRNA genes through H3K4me3 binding and H3K9me1/2 demethylation. Nat Struct Mol Biol 17(4):445–450
390. Kleine-Kohlbrecher D et al (2010) A functional link between the histone demethylase PHF8 and the transcription factor ZNF711 in X-linked mental retardation. Mol Cell 38(2):165–178
391. Fortschegger K et al (2010) PHF8 targets histone methylation and RNA polymerase II to activate transcription. Mol Cell Biol 30(13):3286–3298
392. Liu W et al (2010) PHF8 mediates histone H4 lysine 20 demethylation events involved in cell cycle progression. Nature 466(7305):508–512
393. Qi HH et al (2010) Histone H4K20/H3K9 demethylase PHF8 regulates zebrafish brain and craniofacial development. Nature 466(7305):503–507
394. Qiu J et al (2010) The X-linked mental retardation gene PHF8 is a histone demethylase involved in neuronal differentiation. Cell Res 20(8):908–918
395. Xu W et al (2011) Oncometabolite 2-hydroxyglutarate is a competitive inhibitor of alpha-ketoglutarate-dependent dioxygenases. Cancer Cell 19(1):17–30
396. Upadhyay AK et al (2012) An analog of BIX-01294 selectively inhibits a family of histone H3 lysine 9 Jumonji demethylases. J Mol Biol 416(3):319–327
397. Yu L et al (2010) Structural insights into a novel histone demethylase PHF8. Cell Res 20(2):166–173
398. Yue WW et al (2010) Crystal structure of the PHF8 Jumonji domain, an Nepsilon-methyl lysine demethylase. FEBS Lett 584(4):825–830
399. Wen H et al (2010) Recognition of histone H3K4 trimethylation by the plant homeodomain of PHF2 modulates histone demethylation. J Biol Chem 285(13):9322–9326
400. Ahuja N, Sharma AR, Baylin SB (2016) Epigenetic therapeutics: a new weapon in the war against cancer. Annu Rev Med 67:73–89
401. Baylin SB, Ohm JE (2006) Epigenetic gene silencing in cancer - a mechanism for early oncogenic pathway addiction? Nat Rev Cancer 6(2):107–116
402. Jones PA, Baylin SB (2007) The epigenomics of cancer. Cell 128(4):683–692
403. Hoffmann I et al (2012) The role of histone demethylases in cancer therapy. Mol Oncol 6(6):683–703
404. Gale M et al (2016) Screen-identified selective inhibitor of lysine demethylase 5A blocks cancer cell growth and drug resistance. Oncotarget 7(26):39931–39944
405. Seligson DB et al (2005) Global histone modification patterns predict risk of prostate cancer recurrence. Nature 435(7046):1262–1266
406. Lohse B et al (2011) Inhibitors of histone demethylases. Bioorg Med Chem 19(12):3625–3636
407. Bradshaw JM et al (2015) Prolonged and tunable residence time using reversible covalent kinase inhibitors. Nat Chem Biol 11(7):525–531
408. Mould DP et al (2015) Reversible inhibitors of LSD1 as therapeutic agents in acute myeloid leukemia: clinical significance and progress to date. Med Res Rev 35(3):586–618
409. Hojfeldt JW, Agger K, Helin K (2013) Histone lysine demethylases as targets for anticancer therapy. Nat Rev Drug Discov 12(12):917–930
410. Khan MN, Suzuki T, Miyata N (2013) An overview of phenylcyclopropylamine derivatives: biochemical and biological significance and recent developments. Med Res Rev 33(4):873–910
411. McGrath JP et al (2016) Pharmacological inhibition of the histone lysine demethylase KDM1A suppresses the growth of multiple acute myeloid leukemia subtypes. Cancer Res 76(7):1975–1988
412. Mohammad HP, Kruger RG (2016) Antitumor activity of LSD1 inhibitors in lung cancer. Mol Cell Oncol 3(2):e1117700
413. Mohammad HP et al (2015) A DNA hypomethylation signature predicts antitumor activity of LSD1 inhibitors in SCLC. Cancer Cell 28(1):57–69
414. McAllister TE et al (2016) Recent progress in histone demethylase inhibitors. J Med Chem 59(4):1308–1329
415. Chin YW, Han SY (2015) KDM4 histone demethylase inhibitors for anti-cancer agents: a patent review. Expert Opin Ther Pat 25(2):135–144

416. Thinnes CC et al (2014) Targeting histone lysine demethylases - progress, challenges, and the future. Biochim Biophys Acta 1839(12):1416–1432
417. Shih JC, Chen K, Ridd MJ (1999) Monoamine oxidase: from genes to behavior. Annu Rev Neurosci 22:197–217
418. Lee MG et al (2006) Histone H3 lysine 4 demethylation is a target of nonselective antidepressive medications. Chem Biol 13(6):563–567
419. Schmidt DM, McCafferty DG (2007) trans-2-Phenylcyclopropylamine is a mechanism-based inactivator of the histone demethylase LSD1. Biochemistry 46(14):4408–4416
420. Ueda R et al (2009) Identification of cell-active lysine specific demethylase 1-selective inhibitors. J Am Chem Soc 131(48):17536–17537
421. Culhane JC et al (2006) A mechanism-based inactivator for histone demethylase LSD1. J Am Chem Soc 128(14):4536–4537
422. Kumarasinghe IR, Woster PM (2014) Synthesis and evaluation of novel cyclic peptide inhibitors of lysine-specific demethylase 1. ACS Med Chem Lett 5(1):29–33
423. Suzuki T, Miyata N (2011) Lysine demethylases inhibitors. J Med Chem 54(24):8236–8250
424. Maes T et al (2015) Advances in the development of histone lysine demethylase inhibitors. Curr Opin Pharmacol 23:52–60
425. Martinez ED, Gazdar AF (2016) Inhibiting the Jumonji family: a potential new clinical approach to targeting aberrant epigenetic mechanisms. Epigenomics 8(3):313–316
426. Rotili D et al (2014) Pan-histone demethylase inhibitors simultaneously targeting Jumonji C and lysine-specific demethylases display high anticancer activities. J Med Chem 57(1):42–55
427. Opocher G, Schiavi F (2011) Functional consequences of succinate dehydrogenase mutations. Endocr Pract 17(Suppl 3):64–71
428. Dang L et al (2009) Cancer-associated IDH1 mutations produce 2-hydroxyglutarate. Nature 462(7274):739–744
429. Losman JA, Kaelin WG Jr (2013) What a difference a hydroxyl makes: mutant IDH, (R)-2-hydroxyglutarate, and cancer. Genes Dev 27(8):836–852
430. Losman JA et al (2013) (R)-2-hydroxyglutarate is sufficient to promote leukemogenesis and its effects are reversible. Science 339(6127):1621–1625
431. Zhao S et al (2009) Glioma-derived mutations in IDH1 dominantly inhibit IDH1 catalytic activity and induce HIF-1alpha. Science 324(5924):261–265
432. Dang CV et al (2011) Therapeutic targeting of cancer cell metabolism. J Mol Med (Berl) 89(3):205–212
433. Choi C et al (2012) 2-hydroxyglutarate detection by magnetic resonance spectroscopy in IDH-mutated patients with gliomas. Nat Med 18(4):624–629
434. Gross S et al (2010) Cancer-associated metabolite 2-hydroxyglutarate accumulates in acute myelogenous leukemia with isocitrate dehydrogenase 1 and 2 mutations. J Exp Med 207(2):339–344
435. Lu C et al (2012) IDH mutation impairs histone demethylation and results in a block to cell differentiation. Nature 483(7390):474–478
436. Xiao M et al (2012) Inhibition of alpha-KG-dependent histone and DNA demethylases by fumarate and succinate that are accumulated in mutations of FH and SDH tumor suppressors. Genes Dev 26(12):1326–1338
437. Hamada S et al (2009) Synthesis and activity of N-oxalylglycine and its derivatives as Jumonji C-domain-containing histone lysine demethylase inhibitors. Bioorg Med Chem Lett 19(10):2852–2855
438. Heinemann B et al (2014) Inhibition of demethylases by GSK-J1/J4. Nature 514(7520):E1–E2
439. Kruidenier L et al (2014) Kruidenier et al. reply. Nature 514(7520):E2
440. Wang L et al (2013) A small molecule modulates Jumonji histone demethylase activity and selectively inhibits cancer growth. Nat Commun 4:2035
441. Nielsen AL et al (2012) Identification of catechols as histone-lysine demethylase inhibitors. FEBS Lett 586(8):1190–1194

442. Liang J et al (2016) Lead optimization of a pyrazolo[1,5-a]pyrimidin-7(4H)-one scaffold to identify potent, selective and orally bioavailable KDM5 inhibitors suitable for in vivo biological studies. Bioorg Med Chem Lett 26(16):4036–4041
443. Luo X et al (2011) A selective inhibitor and probe of the cellular functions of Jumonji C domain-containing histone demethylases. J Am Chem Soc 133(24):9451–9456
444. Wagner EK et al (2012) Identification and characterization of small molecule inhibitors of a plant homeodomain finger. Biochemistry 51(41):8293–8306
445. Merk A et al (2016) Breaking Cryo-EM resolution barriers to facilitate drug discovery. Cell 165(7):1698–1707